NIEHS Report on the In Vivo Repeat Dose Biological Potency Study of 1,1,2,2-Tetrahydroperfluoro-1-dodecanol (CASRN 865-86-1) in Sprague Dawley (Hsd:Sprague Dawley® SD®) Rats (Gavage Studies)

NIEHS 08

March 2023

NIEHS Report on the
In Vivo Repeat Dose Biological Potency Study of 1,1,2,2-Tetrahydroperfluoro-1-dodecanol (CASRN 865-86-1) in Sprague Dawley (Hsd:Sprague Dawley® SD®) Rats (Gavage Studies)

NIEHS Report 08

March 2023

Foreword

The National Institute of Environmental Health Sciences (NIEHS) is one of 27 institutes and centers of the National Institutes of Health, which is part of the U.S. Department of Health and Human Services. The NIEHS mission is to discover how the environment affects people in order to promote healthier lives. NIEHS works to accomplish its mission by conducting and funding research on human health effects of environmental exposures; developing the next generation of environmental health scientists; and providing critical research, knowledge, and information to citizens and policymakers who are working to prevent hazardous exposures and reduce the risk of disease and disorders connected to the environment. NIEHS is a foundational leader in environmental health sciences and committed to ensuring that its research is directed toward a healthier environment and healthier lives for all people.

The NIEHS Report series began in 2022. The environmental health sciences research described in this series is conducted primarily by the Division of Translational Toxicology (DTT) at NIEHS. NIEHS/DTT scientists conduct innovative toxicology research that aligns with real-world public health needs and translates scientific evidence into knowledge that can inform individual and public health decision-making.

NIEHS reports are available free of charge on the NIEHS/DTT website and cataloged in PubMed, a free resource developed and maintained by the National Library of Medicine (part of the National Institutes of Health).

In Vivo Repeat Dose Biological Potency Study of
1,1,2,2-Tetrahydroperfluoro-1-dodecanol in Sprague Dawley Rats

Table of Contents

In Vivo Repeat Dose Biological Potency Study of
1,1,2,2-Tetrahydroperfluoro-1-dodecanol in Sprague Dawley Rats

Tables

In Vivo Repeat Dose Biological Potency Study of
1,1,2,2-Tetrahydroperfluoro-1-dodecanol in Sprague Dawley Rats

About This Report

Authors

Scott S. Auerbach[1], Jeff D. Ballin[2], James C. Blake[3], Donna B. Browning[3], Bradley J. Collins[1], Michelle C. Cora[1], Reshan A. Fernando[3], Jennifer M. Fostel[1], Ying F. Liu[4], Jeanne Luh[5], Nicholas J. Machesky[2], Georgia K. Roberts[1], Kelly A. Shipkowski[1], Melanie A.R. Silinski[3], Anthony J. Skowronek[2], Barney R. Sparrow[2], Heather Toy[6], Suramya Waidyanatha[1], AtLee T.D. Watson[1]

[1]Division of Translational Toxicology, National Institute of Environmental Health Sciences, Research Triangle Park, North Carolina, USA

[2]Battelle, Columbus, Ohio, USA

[3]RTI International, Research Triangle Park, North Carolina, USA

[4]ASRC Federal, Research Triangle Park, North Carolina, USA

[5]ICF, Reston, Virginia, USA

[6]AmplifyBio, West Jefferson, Ohio, USA

Division of Translational Toxicology, National Institute of Environmental Health Sciences, Research Triangle Park, North Carolina, USA
Evaluated and interpreted the results and reported findings; developed reporting framework
Scott S. Auerbach, Ph.D., Study Scientist
Michelle C. Cora, D.V.M.
Georgia K. Roberts, Ph.D.
Kelly A. Shipkowski, Ph.D.
AtLee T.D. Watson, Ph.D.

Coordinated data integration
Jennifer M. Fostel, Ph.D.

Analyzed and interpreted analytical chemistry data
Bradley J. Collins, M.S.P.H.
Suramya Waidyanatha, Ph.D.

Battelle, Columbus, Ohio, USA
Provided contract oversight
Barney R. Sparrow, Ph.D.

Conducted in-life studies
Anthony J. Skowronek, D.V.M., Ph.D.

Performed RNA isolation
Nicholas J. Machesky, Ph.D.

Conducted thyroid biomarker analysis
Jeff D. Ballin, Ph.D.

AmplifyBio, West Jefferson, Ohio, USA
Compiled results
Heather Toy, B.S., Study Director

RTI International, Research Triangle Park, North Carolina, USA
Conducted prestart chemistry activities, dose formulations, and biological sample chemistry analyses of total thyroid hormone levels
Reshan A. Fernando, Ph.D., Principal Investigator
James C. Blake, B.A., Deputy Principal Investigator
Donna B. Browning, B.S.
Melanie A.R. Silinski, Ph.D.

ICF, Reston, Virginia, USA
Contributed to technical writing and data integration and ensured report quality
Jeanne Luh, Ph.D.

ASRC Federal, Research Triangle Park, North Carolina, USA
Developed data tables and supplemental materials
Ying F. Liu, Ph.D.

Contributors

Division of Translational Toxicology, National Institute of Environmental Health Sciences, Research Triangle Park, North Carolina, USA
Critically reviewed report and results
John R. Bucher, Ph.D.
Fred M. Parham, Ph.D.
Nigel J. Walker, Ph.D.

Contributed to development and review of reporting framework
Michael J. DeVito, Ph.D.
William M. Gwinn, Ph.D.
Scott A. Masten, Ph.D.
Alison H. Harrill, Ph.D.
Matthew D. Stout, Ph.D.
Greg S. Travlos, D.V.M.
Mary S. Wolfe, Ph.D.

Developed and updated BMDS software package
Andrew J. Shapiro, M.S.P.H.

ASRC Federal, Research Triangle Park, North Carolina, USA
Developed data tables and supplemental materials
Julie Berke, B.S.

Shihan He, Ph.D.
Christina Myers, M.S.

CSS Corporation, Research Triangle Park, North Carolina, USA
Prepared quality assessment audits
Steven Brecher, Ph.D., Principal Investigator
Sudha Iyer, B.S.
Varghese S. Tharakan, D.V.M.

Sciome LLC, Research Triangle Park, North Carolina, USA
Provided bioinformatics analysis
Michele R. Balik-Meisner, Ph.D.
Dhiral P. Phadke, M.S.
Ruchir R. Shah, Ph.D.

ICF, Reston, Virginia, USA
Provided contract oversight
David F. Burch, M.E.M., Principal Investigator
Cary E. Haver, M.P.H.
Jessica A. Wignall, M.S.P.H.

Prepared and edited report
Lauren M. Browning, M.S.
Katherine S. Duke, Ph.D.
Tara Hamilton, M.S.
Pamela A. Hartman, M.E.M.
Lisa M. Prince, Ph.D.
Samantha J. Snow, Ph.D.
Jonathan R. Thompson, B.S.
Nkoli Ukpabi, M.S.

Peer Review

This report was modeled after the *NTP Research Report on In Vivo Repeat Dose Biological Potency Study of Triphenyl Phosphate (CAS No. 115-86-6) in Male Sprague Dawley (Hsd:Sprague Dawley® SD®) Rats (Gavage Studies)* (https://doi.org/10.22427/NTP-RR-8), which was reviewed internally at the National Institute of Environmental Health Sciences and peer reviewed by external experts. Importantly, these reports employ mathematical model-based approaches to identify and report potency of dose-responsive effects and do not attempt more subjective interpretation (i.e., make calls or reach conclusions on hazard). The peer reviewers of the initial 5-day research report determined that the study design, analysis methods, and results presentation were appropriate. The study design, analysis methods, and results presentation employed for this study are identical to those previously reviewed, approved, and reported; therefore, following internal review, the *NIEHS Report on the In Vivo Repeat Dose Biological Potency Study of 1,1,2,2-Tetrahydroperfluoro-1-dodecanol (CASRN 865-86-1) in Sprague Dawley (Hsd:Sprague Dawley® SD®) Rats (Gavage Studies)* was not subjected to further external peer review.

In Vivo Repeat Dose Biological Potency Study of
1,1,2,2-Tetrahydroperfluoro-1-dodecanol in Sprague Dawley Rats

Publication Details

Acknowledgments

In Vivo Repeat Dose Biological Potency Study of
1,1,2,2-Tetrahydroperfluoro-1-dodecanol in Sprague Dawley Rats

Abstract

Background: 1,1,2,2-Tetrahydroperfluoro-1-dodecanol (10:2 fluorotelomer alcohol) is a member of the per- and polyfluoroalkyl class of compounds to which humans are widely exposed. Toxicological information on this class of chemicals is sparse. A short-term, in vivo transcriptomic study was used to assess the biological potency of 1,1,2,2-tetrahydroperfluoro-1-dodecanol.

Methods: A short-term in vivo biological potency study on 1,1,2,2-tetrahydroperfluoro-1-dodecanol in adult male and female Sprague Dawley (Hsd:Sprague Dawley® SD®) rats was conducted. 1,1,2,2-Tetrahydroperfluoro-1-dodecanol was formulated in acetone:corn oil (1:99) and administered once daily for 5 consecutive days by gavage (study days 0–4). 1,1,2,2-Tetrahydroperfluoro-1-dodecanol was administered at 10 doses (0, 0.07, 0.2, 0.7, 2, 6, 18, 55, 160, and 475 mg/kg body weight [mg/kg]). Blood was collected from animals dedicated for internal dose assessment in the 2 and 18 mg/kg groups. On study day 5, the day after the final dose was administered, animals were euthanized, standard toxicological measures were assessed, and the liver and kidney were assayed in gene expression studies using the TempO-Seq assay. Modeling was conducted to identify the benchmark doses (BMDs) associated with apical toxicological endpoints and transcriptional changes in the liver and kidney. A benchmark response of one standard deviation was used to model all endpoints.

Results: Several clinical pathology and organ weight measurements showed dose-related changes from which BMD values were calculated. In male rats, the effects included significantly increased relative liver weight, increased absolute liver weight, decreased reticulocyte count, increased thyroid stimulating hormone concentration, and decreased free thyroxine concentration. The BMDs and benchmark dose lower confidence limits (BMD$_L$s) were 8.087 (4.336), 21.893 (10.337), 54.227 (30.205), 138.723 (20.376), and 142.469 (57.746) mg/kg, respectively. In female rats, the effects included significantly increased relative liver weight, increased alkaline phosphatase activity, increased absolute liver weight, decreased platelet count, increased monocyte count, increased absolute left kidney weight, increased large unstained cell count, increased absolute right kidney weight, and increased relative left kidney weight. The BMDs (BMD$_L$s) were 5.372 (2.294), 6.461 (6.003), 8.801 (3.465), 16.335 (9.571), 20.731 (4.642), 56.634 (10.508), 58.894 (25.959), 72.145 (18.001), and 85.629 (17.286) mg/kg, respectively. Average 1,1,2,2-tetrahydroperfluoro-1-dodecanol plasma concentrations at 2 hours postdose were similar in male and female rats. At 24 hours postdose, the concentration decreased and fell below the limit of detection of the analytical method in the 2 mg/kg female rats. Half-lives estimated using the two time points were 6.65 and 8.96 hours for the 2 and 18 mg/kg male rats, respectively, and 6.12 hours for the 18 mg/kg female rats.

In the liver of male and female rats, no Gene Ontology biological process or individual genes had BMD median values below the lower limit of extrapolation (<0.023 mg/kg). The most sensitive gene sets in male rats for which a reliable estimate of the BMD could be made were nucleotide biosynthetic process and organic hydroxy compound transport with median BMDs of 5.235 and 5.978 mg/kg and median BMD$_L$s of 2.666 and 3.303 mg/kg, respectively. The most sensitive gene sets in female rats for which a reliable estimate of the BMD could be made were internal protein amino acid acetylation and glutamine family amino acid metabolic process with median BMDs of 5.355 and 8.071 mg/kg and median BMD$_L$s of 3.108 and 3.552 mg/kg, respectively. The most sensitive upregulated genes in male rats with reliable BMD estimates

included *Akr7a3*, *Ephx1*, *Me1*, *Cyp4a1*, *Anxa7*, and *Slc17a3* with BMDs (BMD$_L$s) of 2.192 (1.593), 2.467 (1.828), 3.531 (2.076), 4.588 (2.345), 4.660 (2.970), and 5.147 (3.485) mg/kg, respectively. The most sensitive downregulated genes in male rats with reliable BMD estimates were *Pck1*, *A2m*, *Loc100911545/A2m*, and *Zfp354a* with BMDs (BMD$_L$s) of 1.149 (0.548), 1.733 (0.972), 1.733 (0.972), and 1.785 (0.579) mg/kg, respectively. In female rats, the top 10 most sensitive individual genes were upregulated. These genes were *Abcc3*, *Gsta2*, *Gsta5*, *Ephx1*, *Akr7a3*, *Ehhadh*, *Pir*, *Gclm*, *Dao*, and *Me1* with BMDs (BMD$_L$s) of 5.019 (2.945), 5.153 (2.796), 5.153 (2.796), 5.233 (3.072), 5.348 (3.082), 5.355 (3.108), 6.124 (2.642), 8.034 (3.552), 8.071 (2.669), and 8.192 (2.618) mg/kg, respectively.

In the kidney of male and female rats, no Gene Ontology biological process had BMD median values below the lower limit of extrapolation (<0.023 mg/kg). The most sensitive gene sets in male rats for which a reliable estimate of the BMD could be made were regulation of myeloid leukocyte mediated immunity and response to progesterone with median BMDs of 144.319 and 145.437 mg/kg and median BMD$_L$s of 57.694 and 104.718 mg/kg, respectively. The most sensitive gene sets in female rats for which a reliable estimate of the BMD could be made were innate immune response and activation of immune response with median BMDs of 57.313 and 78.645 mg/kg and median BMD$_L$s of 37.882 and 45.596 mg/kg, respectively. No individual kidney genes in male rats had median BMD values <0.023 mg/kg. The most sensitive upregulated genes in male rats with reliable BMD estimates included *Ugt2b7*, *Ephx1*, *Adgre1*, *Map2*, *Slc6a1*, *Naaa*, *Il1b*, *Cyp24a1*, and *Nsg1* with BMDs (BMD$_L$s) of 4.139 (1.398), 12.509 (3.282), 119.065 (89.170), 145.437 (104.718), 145.445 (104.722), 151.002 (107.821), 153.991 (109.464), 189.111 (127.579), and 216.472 (166.237) mg/kg, respectively. One gene, *Top2a*, was downregulated with a BMD (BMD$_L$) of 203.468 (108.442) mg/kg. In female rats, one individual gene, *Mrc1*, was downregulated and had a BMD value <0.023 mg/kg. The most sensitive genes with reliable BMD estimates were upregulated and included *Ckap2*, *Ugt2b37*, *Slc51a*, *Ugt2b7*, *Bbox1*, *Adgre1*, *Clec4a*, *Cyp26b1*, and *Lilrb4* with BMDs (BMD$_L$s) of 2.608 (0.997), 32.501 (7.520), 37.134 (11.007), 54.314 (15.595), 61.319 (39.473), 61.524 (39.671), 82.466 (47.872), 238.250 (181.323), and 350.991 (212.248) mg/kg, respectively.

Summary: Taken together, in male rats, the most sensitive gene set BMD (BMD$_L$) median, individual gene BMD (BMD$_L$), and apical endpoint BMD (BMD$_L$) values that could be reliably determined occurred at 5.235 (2.666), 1.149 (0.548), and 8.087 (4.336) mg/kg, respectively. In female rats, the most sensitive gene set BMD (BMD$_L$) median, individual gene BMD (BMD$_L$), and apical endpoint BMD (BMD$_L$) values that could be reliably determined occurred at 5.355 (3.108), 2.608 (0.997), and 5.372 (2.294) mg/kg, respectively. The BMD (BMD$_L$) could not be determined for one individual gene and was estimated to be <0.023 mg/kg.

Background

1,1,2,2-Tetrahydroperfluoro-1-dodecanol (10:2 fluorotelomer alcohol) (CASRN: 865-86-1, U.S. Environmental Protection Agency [EPA] Chemical Dashboard: DTXSID2029905,[1] PubChem CID: 70083,[2] European Committee Number: 212-748-7[3]) is a member of the per- and polyfluoroalkyl class of compounds that are associated with numerous toxicological effects.[4] There is widespread human exposure to this class of compounds.[5; 6] The predicted upper 95th percentile human exposure to 1,1,2,2-tetrahydroperfluoro-1-dodecanol is 0.00112 mg/kg body weight/day.[7] This dose level is within 100-fold of the lowest dose tested in this study. A review of the existing literature failed to identify any in vivo toxicological information on 1,1,2,2-tetrahydroperfluoro-1-dodecanol, and according to the EPA Chemical Dashboard, no quantitative risk assessment values or quantitative hazard values exist for this test article.[8] Publicly available information on 1,1,2,2-tetrahydroperfluoro-1-dodecanol can be found in PubChem[2] and the EPA Chemical Dashboard.[1]

Recent studies have demonstrated that short-term in vivo gavage studies coupled with transcriptomics on select target organs can be used to estimate a biological potency that provides a reasonable approximation of toxicological potency in long-term guideline toxicological assessments.[9] To estimate biological potency and gain insight into the nature of biological changes elicited by 1,1,2,2-tetrahydroperfluoro-1-dodecanol, the National Institute of Environmental Health Sciences performed a short-term in vivo biological potency study of male and female Sprague Dawley (Hsd:Sprague Dawley® SD®) rats. The results of this study are presented in this report.

Materials and Methods

Study Design

Male and female Sprague Dawley (Hsd:Sprague Dawley® SD®) rats were obtained from Envigo (Haslett, MI). On receipt, the rats were 6–7 weeks of age. Animals were quarantined for a minimum of 10 days and then randomly assigned to 1 of 10 dose groups. The rats in each dose group were then administered 1,1,2,2-tetrahydroperfluoro-1-dodecanol (10:2 fluorotelomer alcohol) in acetone:corn oil (1:99) by gavage for 5 consecutive days (study days 0–4) at a dose level of 0, 0.07, 0.2, 0.7, 2, 6, 18, 55, 160, or 475 mg/kg body weight (mg/kg). There were 5 rats per sex in each dosed group and 10 per sex in the vehicle control group; an additional 3 rats per sex were added to the 2 and 18 mg/kg groups for internal dose assessment. Dosage volume was 5 mL/kg body weight and was based on each animal's most recent body weight. Euthanasia, blood/serum collection, and tissue sample collection were completed on study day 5, the day following the final administration of the test article. Blood was also collected from animals dedicated for internal dose assessment at 2 and 24 hours following the last dose administered on study day 4. Animal identification numbers and FASTQ data file names for each animal are presented in Appendix B.

Dose Selection Rationale

Dose selection was informed by a median lethal dose (LD$_{50}$) prediction from the OPEn structure-activity/property Relationship App (OPERA),[10; 11] which estimated 636 mg/kg/day with an uncertainty range of 319–1,270 mg/kg/day. Further, an estimated point of departure of 18 mg/kg/day with an uncertainty range of 0.3–197 mg/kg/day was provided by the U.S. Environmental Protection Agency (EPA).[12] To be certain that a 5-day maximum tolerated dose was achieved, to manage challenges with solubility, and to identify a minimum biological effect level dose, a top dose of 475 mg/kg was chosen, and approximately half-log dose spacing of nine lower dose levels, including a vehicle control, was selected to carry out the study.

Chemistry

1,1,2,2-Tetrahydroperfluoro-1-dodecanol was obtained from SynQuest Laboratories, Inc. (Alachua, FL; lot 604301). The identity of the chemical was confirmed by fluorine nuclear magnetic resonance (^{19}F NMR) spectroscopy and by gas chromatography with mass spectrometry (GC/MS), and purity (97.8%; six impurities) of the chemical was assessed by GC/MS. Bulk chemical was stored at room temperature.

Dose formulations were prepared in 1% acetone in corn oil at 0 (vehicle control), 0.014, 0.04, 0.14, 0.40, 1.2, 3.6, 11, 32, and 95 mg/mL. The preadministration concentration of test article in the vehicle was analyzed using GC with flame ionization detection. The 0.40, 11, and 32 mg/mL formulations were 15.1%, 12.9%, and 10.2% below their target concentrations, respectively. All other formulations were within 10% of the target concentration. Formulation stability was confirmed using a 0.014 mg/mL formulation for up to 44 days at room temperature. Homogeneity was confirmed using a 95 mg/mL formulation. All chemistry activities were conducted by RTI International (Research Triangle Park, NC).

Clinical Examinations and Sample Collection

Clinical Observations

All rats were observed twice daily for signs of mortality or moribundity. Formal (out of cage) clinical observations were performed daily.

Body and Organ Weights

Animals were weighed during quarantine for randomization on the first day of dosing (study day 0) and on the day of necropsy (study day 5). A gross necropsy was performed on all rats that died spontaneously or were humanely euthanized due to moribund condition. During necropsy for all animals, the heart, liver, and kidneys were removed, and organ weights were recorded; bilateral organs were weighed separately.

Clinical Pathology

Animals were euthanized in random order by CO_2/O_2 (70%/30%) anesthesia 1 day after the final day of dosing. Blood samples were collected from each sex within a 1-hour window and were taken via vena cava or aorta. Blood was collected into tubes containing K_3 EDTA (tripotassium ethylenediaminetetraacetic acid) for hematology analysis and into tubes void of anticoagulant for serum chemistry and thyroid hormone measurements. The following hematology parameters were measured on an Advia® 120 Hematology Analyzer (Siemens Medical Solutions USA, Inc., Malvern, PA): erythrocyte count, hemoglobin, hematocrit, mean cell volume, mean cell hemoglobin, mean cell hemoglobin concentration, white blood cell count and differential, reticulocyte count, platelet count, and nucleated erythrocyte count. Manual hematocrit was determined using a microcentrifuge and capillary reader. Blood smears were prepared, and qualitative evaluation of cellular morphology was performed per study protocol. The following clinical chemistry parameters were measured on a Roche cobas® c501 Chemistry Analyzer (Roche Diagnostics, Indianapolis, IN): alanine aminotransferase (ALT), albumin, alkaline phosphatase (ALP), aspartate aminotransferase (AST), total bile acids, total bilirubin, direct bilirubin, cholesterol, creatine kinase, creatinine, glucose, sorbitol dehydrogenase (SDH), total protein, triglycerides, and urea nitrogen. Globulin, albumin/globulin (A/G) ratio, and indirect bilirubin were calculated based on direct measurements (e.g., indirect bilirubin = total bilirubin − direct bilirubin). Serum concentrations for thyroid stimulating hormone (TSH) and free thyroxine (fT4) were determined by immunoassay using commercially available immunoassay kits from EMD Millipore Corporation (Billerica, MA) for TSH and Biomatik Corporation (Kitchener, Ontario, Canada) for fT4. Serum concentrations of total thyroxine (total T4) and total triiodothyronine (total T3) were determined using a validated method described elsewhere.[13] Individual animal and summary clinical chemistry, hematology, and hormonal data are available in Appendix F.

Internal Dose Assessment

A screening level assessment of the internal dose was performed to determine whether the test chemical had bioaccumulative properties (i.e., if the half-life was >24 hours). Blood was collected from animals dedicated for internal dose assessment in the 2 and 18 mg/kg groups at 2 and 24 hours following the last dose administered on study day 4. At 2 hours postdose, blood was collected from the jugular vein of unanesthetized animals. At 24 hours postdose (study

day 5), blood was collected from all study animals and dedicated internal dose assessment animals from the vena cava or abdominal aorta while animals were anesthetized with CO_2/O_2 (70%/30%). Blood was collected into tubes containing K_3 EDTA and kept on wet ice until plasma isolation, within 2 hours of collection. Samples were stored frozen (−85°C to −60°C) until analysis as described in Appendix A.

Transcriptomics

Sample Collection for Transcriptomics

Within 5 minutes of euthanasia, samples from the left liver lobe and right kidney were collected from all study animals for transcriptomic analysis. Half of the left liver lobe and half of the right kidney were processed for RNA isolation. Approximately 250 mg of each tissue was cut into small pieces (approximately 5 mm^3) and placed into cryotubes containing RNA*later™*. The tissue samples were stored at 2°C to 8°C overnight. The RNA*later™* was then removed and the samples were stored in a −85°C to −60°C freezer until processed for RNA isolation.

RNA Isolation, Library Creation, and Sequencing

RNA isolation was performed on tissue samples preserved in RNA*later™*. Tissues were homogenized in QIAzol buffer (Qiagen Inc., Valencia, CA) using the TissueLyser II bead-beating system followed by RNA extraction using the RNeasy 96 QIAcube HT kits (Cat# 74171, Qiagen Inc., Valencia, CA) with a DNA digestion step. The concentration and purity of all isolated samples were determined from absorbency readings taken at 260 and 280 nm using a NanoDrop ND-8000 Spectrophotometer (NanoDrop Technologies, Wilmington, DE). The readings accurately determined the concentration of each sample while ensuring that an acceptable purity (A_{260}/A_{280} ratio) between 1.80 and 2.20 was achieved. After quantification, RNA was stored at −70°C ± 10°C until further processing.

One microliter of each RNA sample (500–660 ng/µL) was hybridized with the S1500+ beta detector oligo pool mix (2 µL per sample) using the following thermocycler settings: 10 minutes at 70°C, followed by a gradual decrease to 45°C over 49 minutes, and ending with a 45°C hold for 1 minute. Hybridization was followed by nuclease digestion (24 µL nuclease mix addition followed by 90 minutes at 37°C), ligation (24 µL ligation mix addition followed by 60 minutes at 37°C), and heat denaturation (at 80°C for 15 minutes). Ten microliters of each ligation product were then transferred to a 96-well polymerase chain reaction (PCR) amplification microplate with 10 µL of PCR mix per well. Through 25 cycles of amplification, well-specific "barcoded" primer pairs were introduced to templates. Five microliters of the PCR amplification products from each well were then pooled into a single sequencing library. The TempO-Seq library was then processed with a PCR clean-up kit (Machery-Nagel, Mountain View, CA) prior to sequencing. Sequencing was performed using a 50-cycle single-end read flow cell on a HiSeq 2500 Sequencing System (Illumina, San Diego, CA). Processing of sequencing data was conducted using Illumina's BCL2FASTQ software employing default parameter settings.

Sequence Data Processing

FASTQ files of TempO-Seq reads were aligned to the probe sequences from the target platform using Bowtie version 1.2.2[14] with the following parameters: -v 3 -k 1 -m 1 --best --strata. This configuration allows up to three mismatches and reports the single best alignment. After

alignment, the total sequenced reads, the percentage of reads aligning to the platform manifest, the alignment rate, and the percentage of expressed probes (≥ 5 reads per probe) were calculated for each sample.

Sequencing Quality Checks and Outlier Removal

Samples were flagged for values below the following thresholds: sequencing depth <300 K, total alignment rate <40%, unique alignment rate <30%, number of aligned reads <300 K, or percentage of probes with at least five reads <50%. Filtering on the percentage of expressed probes eliminates biased samples for which the sequenced reads only reflect a small portion of the measured transcriptome. In addition, FastQC was run on all samples to ensure adequate per base quality and per base N content, where N represents bases that could not be identified. All 1,1,2,2-tetrahydroperfluoro-1-dodecanol samples passed the criteria mentioned above.

Principal component (PCA), hierarchical cluster, and inter-replicate correlation analyses were performed. These analyses highlighted one outlier liver sample, which was removed before downstream analysis.

The processing of samples from the study of 1,1,2,2-tetrahydroperfluoro-1-dodecanol was done in parallel with three other chemicals that were studied under a similar protocol, therefore allowing for a more powerful collective assessment of the data. Specifically, the samples from all four studies were distributed over twelve 96-well plates (i.e., one plate per chemical per tissue and four additional plates with overflow samples for three of the chemicals, with nine doses plus vehicle control). For kidney samples, average read depth per chemical varied across plates. Kidney samples on one of the overflow plates also clustered separately (in the PCA and hierarchical cluster analysis) from the other kidney samples for a given chemical. Therefore, kidney samples on that overflow plate were removed, resulting in one plate of data per chemical for the downstream analysis of kidney samples. The exclusion of these data had limited impact on the analysis as the samples from each dose group were randomly sorted into the overflow plates. The final sample counts that were used for benchmark dose (BMD) analysis of the transcriptomics data are shown in Table 1.

Table 1. Final Sample Counts for Benchmark Dose Analysis of the Transcriptomics Data

	0 mg/kg	0.07 mg/kg	0.2 mg/kg	0.7 mg/kg	2 mg/kg	6 mg/kg	18 mg/kg	55 mg/kg	160 mg/kg	475 mg/kg
Male										
Liver	10	5	5	5	5	5	5	5	5	5
Kidney	9	5	5	4	4	4	3	2	4	2
Female										
Liver	10	5	4	5	5	5	5	5	5	5
Kidney	10	3	5	4	5	5	4	5	3	4

Data Normalization

The aligned read counts for attenuated probes were properly readjusted to calculate unattenuated equivalent counts using the attenuation factors provided in the platform manifest. To account for between-sample sequencing depth variation, unattenuated read counts were normalized at the probe level by applying reads per million normalization. A pseudo-read-count of 1.0 was added

to each normalized expression value, and then the values were log2 transformed to complete the normalization. Principal component-based visualizations of the final expression data set used from modeling are available in Appendix C.

Data Analysis

Statistical Analysis of Body Weights, Organ Weights, and Clinical Pathology

Two approaches were employed to assess the significance of pairwise comparisons between dosed and vehicle control groups in the analysis of continuous variables. Organ and body weight data, which have approximately normal distributions, were analyzed using the parametric multiple comparison procedures of Williams[15; 16] and Dunnett.[17] Clinical pathology data, which typically have skewed distributions, were analyzed using the nonparametric multiple comparison methods of Shirley[18] and Dunn.[19] The Jonckheere test[20] was used to assess the significance of dose-response trends and to determine whether a trend-sensitive test (Williams or Shirley test) was more appropriate for pairwise comparisons than a test that assumes no monotonic dose response (Dunnett or Dunn test). Trend-sensitive tests were used when the Jonckheere test was significant at $p \leq 0.01$.

Prior to analysis, values identified by the outlier test of Dixon and Massey[21] were examined by National Institute of Environmental Health Sciences (NIEHS) staff. Values from animals suspected of illness due to causes other than experimental exposure and values that the laboratory indicated as inadequate due to measurement problems were eliminated from the analysis.

A no-observed-effect level (NOEL) was identified as the highest dose not showing a significant ($p \leq 0.05$) pairwise difference relative to the vehicle control group. A lowest-observed-effect level (LOEL) was identified as the lowest dose demonstrating a significant ($p \leq 0.05$) pairwise difference relative to the vehicle control group. Throughout the results section for apical endpoints, interpretation of BMDs is made in relationship to NOEL and LOEL values for specific endpoints, as defined here, and are not meant to reflect an overall study NOEL or LOEL.

Benchmark Dose Analysis of Body Weights, Organ Weights, and Clinical Pathology

Clinical pathology, body weight, and organ weight endpoints that exhibited a significant trend and pairwise test were submitted in batch for automated BMD modeling analysis. For body weight, the BMD and benchmark dose lower confidence limit (BMD$_L$) were presented as not determined when there were no significant results. BMD modeling and analysis was conducted using a modification of Benchmark Dose Modeling Software (BMDS) version 2.7.0. Data sets were executed using the Python BMDS interface (https://pypi.python.org/pypi/bmds; version 0.11), which allows for batch processing of multiple data sets. Data for all endpoints submitted were continuous. A default benchmark response (BMR) of one standard deviation (relative to control) was used for all data sets. The following BMDS 2.7.0 models were used to model the means of the data sets:

- Linear

- Polynomial 2°, 3°, 4°, 5°, 6°, 7°, 8°
- Power
- Hill
- Exponential M2, M3, M4, M5

Multiple versions of the polynomial model were executed, from a polynomial of degree 2 to a polynomial of degree equal to the number of dose groups minus 1 (e.g., if a data set had five dose groups, a 2°, 3°, and 4° polynomial model would be executed). Models were initialized using BMDS 2.7.0 model defaults, including restricting the power parameter of the power model and n-parameter of the Hill model to >1 and the beta parameters of the polynomial model to positive or negative, depending on the mean response direction of the data set. For all models, either a constant or nonconstant variance model was selected as outlined in the EPA BMD technical guidance[22] and was implemented in the BMDS 2.7.0 software.

After model execution, BMDs were selected using the model recommendation procedures generally described in the EPA BMD technical guidance[22] and the automated decision logic described in Wignall et al.[23] and summarized in Appendix D, Table D-1. Models were placed into one of four possible bins, depending on the results and the bin recommendation logic:

(1) **Failure:** model did not successfully complete

(2) **Nonviable model (NVM):** model successfully completed but failed acceptability criteria

(3) **Not reportable (NR):** model is identified and meets all acceptability criteria with the exception of the estimated BMD being below the lower limit of extrapolation (<1/3 the lowest nonzero dose tested); BMD reported as <1/3 the lowest nonzero dose tested and BMD$_L$ is not reportable

(4) **Viable model:** candidate for recommended model without warning

If only one model was in the viable model bin, it was selected as the best-fitting model. If the viable bin had more than one model, consistent with EPA guidance,[22] either the model with the lowest Akaike information criterion (AIC) or lowest BMD$_L$ was selected. If the range of BMD$_L$ values was sufficiently close (less than threefold difference), the AIC value was used; otherwise, the BMD$_L$ value was used. If no model was recommended, no BMD was presented in the results. Details on the analysis criteria and decision tree are provided in Table D-1 and Figure D-1, respectively. To avoid effects of model extrapolation, BMD values derived from viable models that were threefold lower than the lowest nonzero dose tested were reported as <1/3 the lowest nonzero dose tested, and corresponding BMD$_L$ values were not reported. Finally, all modeling results from apical data yielding a BMD were reviewed by a subject matter expert to determine the validity of the modeling results and potency estimates.

Benchmark Dose Analysis of Transcriptomics Data

The BMD analysis of the transcriptomic data was performed in accordance with the National Toxicology Program (NTP) best practices for genomic dose-response modeling as reviewed by an independent panel of experts in October 2017. These recommendations are described in the 2018 publication, *National Toxicology Program Approach to Genomic Dose Response Modeling*.[24]

In Vivo Repeat Dose Biological Potency Study of
1,1,2,2-Tetrahydroperfluoro-1-dodecanol in Sprague Dawley Rats

Dose-response analyses of normalized gene expression data were performed using BMDExpress 2.30.0507 BETA (https://github.com/auerbachs/BMDExpress-2/releases). A trend test (the Williams trend test[15; 16] p ≤ 0.05, 10,000 permutations) and fold change filter (1.5-fold change up or down relative to the vehicle control group for probe sets) were applied to the data set to remove probe sets demonstrating no response to chemical exposure from subsequent analysis. These filter criteria were empirically determined with the goal of balancing false discovery with reproducibility. The criteria are consistent with the MicroArray Quality Control recommendations to combine the nominal p value threshold with a fold change filter to maximize replicability of transcriptomic findings across labs.[25] The following dose-response models were fit to the probe sets that passed the trend test and fold change filter:

- Hill
- Power
- Linear
- Polynomial 2°
- Exponential M2, M3, M4, M5

All gene expression data analyzed in BMDExpress were log2 transformed, and thus nearly all probes (also known as detection oligos or DO) were assumed to exhibit constant variance across the doses. For this reason and for efficiency purposes, each model was run assuming constant variance. Lacking any broadly applicable guidance regarding the level of change in gene expression considered biologically significant, a BMR of one standard deviation (relative to the fit at control) was used in this study. This approach enables standardization of the BMR between apical endpoints and transcriptomic endpoints and provides a standard for use across multiple chemicals tested in this rapid screening paradigm. The expression direction (upregulated or downregulated) for each probe was determined by a trend test intrinsic to the model executables (provided by EPA) contained in BMDExpress.

To identify the best-fit model for each fitted probe, the AIC values for each fitted model were compared and the model with the lowest AIC was selected. The best model for each probe was used to calculate the BMD, BMD_L, and BMD upper confidence limit (BMD_U). The specific parameter settings, selected from the BMDExpress software when performing probe-level BMD analysis, were as follows: maximum iterations – 250, confidence level – 0.95, BMR factor – 1 (the multiplier of the standard deviation that defined the BMD), restrict power – no restriction, and constant variance – selected. The specific model selection setting in the BMDExpress software when performing probe set-level BMD analysis was as follows: best poly model test – lowest AIC, flag Hill model with "k" parameters – <1/3 the lowest nonzero dose tested, and best model selection with flagged Hill model – include flagged Hill model. The inclusion of the flagged models is a deviation from EPA BMD analysis guidance.[22] The justification for this deviation relates to subsequent use of the data in which the probe BMD values are grouped into gene sets from which a median BMD is derived. If the probes were removed from the analysis or forced to another model, the probe might not be counted in the gene set analysis and could lead to loss of "active" gene sets. Importantly, most of the probes that produce flagged Hill models show highly potent responses and should therefore be counted in the analysis.

To perform Gene Ontology (GO; annotation accession date: 07/15/2020) gene set analysis, only GO terms with ≥10 and ≤250 annotated genes measured on the gene expression platform were

considered. Before sorting genes into the GO terms, the best-fit model for each probe was subjected to a filtering process to remove those probes (1) with a BMD greater than the highest dose tested, (2) that mapped to more than one gene, (3) that had a global goodness-of-fit p value ≤0.1, and (4) with a BMD_U/BMD_L ratio >40. GO terms that were at least 5% populated and contained three genes that passed the criteria mentioned above were considered "active" (i.e., responsive to chemical exposure). For this report, GO terms populated with identical sets of differentially expressed genes were filtered to limit redundancy in reporting based on the following selection criteria: (1) highest percentage populated and (2) most specific/highest GO level. Redundant GO terms failing to differentiate on the basis of these criteria were retained and reported. A complete list of "active" GO terms can be found in Appendix F. To avoid effects of model extrapolation, GO terms exhibiting BMD values below the lower limit of extrapolation (<1/3 the lowest nonzero dose tested) were reported as <1/3 the lowest nonzero dose tested and corresponding BMD_L and BMD_U values were not reported.

To perform Individual Gene Analysis, the best-fit model for each probe was subjected to a filtering process to remove those probes (1) with a BMD greater than the highest dose tested, (2) that mapped to more than one gene, (3) that had a global goodness-of-fit p value ≤0.1, or (4) with a BMD_U/BMD_L ratio >40. For genes that had more than one probe represented on the platform and passed this filtering process, a median BMD was used to estimate the BMD, BMD_L, and BMD_U values. To ensure only genes with a robust response were assessed for potency, genes with probes that had a median fold change <|2| were removed prior to reporting. A complete list of genes and their corresponding metrics can be found in Appendix F. To avoid effects of model extrapolation, genes exhibiting BMD values below the lower limit of extrapolation (<1/3 the lowest nonzero dose tested) were reported as <1/3 the lowest nonzero dose tested and corresponding BMD_L and BMD_U values were not reported.

A summary of the BMDExpress gene expression analysis pipeline used in this study is shown in Figure D-2.

Empirical False Discovery Rate Determination for Genomic Dose-response Modeling

The genomic dose-response analysis pipeline is a complex multistep process with multiple modeling steps and parameter variables. Because of this complexity, traditional statistical models for determining false discovery rates for the genes and pathways are not straightforward to apply. To overcome this issue, an empirical false discovery rate was determined on the basis of the totality of the analysis pipeline. This was done through the evaluation of synthetic null data sets derived from vehicle control data from four short-term repeat dose toxicogenomic studies including 1,1,2,2-tetrahydroperfluoro-1-dodecanol (each with 10 vehicle control samples). The other toxicogenomic studies, which are reported in separate NIEHS reports, are of perfluorohexanesulfonamide,[26] 6:1 fluorotelomer alcohol,[27] and 2,3-benzofluorene.[28] Samples from all four studies were processed as a group and subjected to sequencing at the same time and were visually inspected to ensure there was no batch effect between the different studies.

To create synthetic null data for a given group (tissue per sex combination), up to 40 vehicle control samples from the original studies (10 replicates × 4 chemicals) were used to generate the data sets, with outliers excluded from the analysis. Each computationally generated sample was created by mixing two randomly selected vehicle control samples via a weighted average

approach through which weights were obtained from random uniform (0,1) distribution. A total of 55 samples (10 vehicle control samples + 45 dosed samples [9 doses × 5 replicates]) were computationally generated per data set and assigned doses spaced by approximately half-log. A total of 20 data sets were generated per group (i.e., 20 data sets each for female kidney, male kidney, female liver, and male liver) and analyzed using both the individual gene-level and GO biological process (gene set) analysis pipeline employed to analyze the data from each study. The median empirical false discovery rates across the 20 null sets in each group for gene-level analysis across each group were 0.037%, 0.037%, 0%, and 0% (female kidney, male kidney, female liver, and male liver, respectively). The median empirical false discovery rate for each of the 20 null data sets in each group using the GO biological process (gene set) level analysis was 0%. Details of the empirical false discovery rate analysis are available in Appendix C. The associated bm2 analysis file that is the basis of the empirical false discovery rate can be found in Appendix F.

Data Accessibility

Primary and analyzed data used in this study are available to the public at
https://doi.org/10.22427/NIEHS-DATA-NIEHS-08.[29]

Results

Animal Condition, Body Weights, and Organ Weights

All male and female rats administered 1,1,2,2-tetrahydroperfluoro-1-dodecanol
(10:2 fluorotelomer alcohol) survived to the end of the study with no adverse clinical
observations noted (Appendix F). There were no significant changes in terminal body weight for
male or female rats administered 1,1,2,2-tetrahydroperfluoro-1-dodecanol (Table 2).

In male rats at study termination, a significant increase in absolute and relative liver weights
occurred in dose groups ≥55 and ≥18 mg/kg body weight (mg/kg), respectively; both endpoints
had positive trends (Table 3). The benchmark doses (benchmark dose lower confidence limits)—
BMDs (BMD_Ls)—for increased absolute and relative liver weights were 21.893 (10.337) and
8.087 (4.336) mg/kg, respectively. The BMDs for all organ weights were reviewed by a subject
matter expert for anomalous modeling results (i.e., when the traditional statistics are notably
different from the estimated BMD values). Significant trend and pairwise comparisons were not
observed in absolute or relative heart, right kidney, or left kidney weights (Appendix F).

In female rats at study termination, a significant increase in absolute and relative liver weights
occurred in dose groups ≥6 and ≥18 mg/kg, respectively, with BMDs (BMD_Ls) of 8.801 (3.465)
and 5.372 (2.294) mg/kg, respectively (Table 3). Absolute right and left kidney weights were
significantly increased in the ≥55 mg/kg groups with BMDs (BMD_Ls) of 72.145 (18.001) and
56.634 (10.508) mg/kg, respectively. Relative right and left kidney weights were significantly
increased in the ≥160 mg/kg female rats. The BMD (BMD_L) for increased relative left kidney
weight was 85.629 (17.286) mg/kg; a BMD (BMD_L) was not determined for increased relative
right kidney weight because no viable model was available. The organ weights mentioned above
all exhibited positive trends. Significant trend and pairwise comparisons were not observed in
absolute or relative heart weights (Appendix F).

In Vivo Repeat Dose Biological Potency Study of
1,1,2,2-Tetrahydroperfluoro-1-dodecanol in Sprague Dawley Rats

Table 2. Summary of Body Weights of Male and Female Rats Administered 1,1,2,2-Tetrahydroperfluoro-1-dodecanol for Five Days

Study Day[a,b]	0 mg/kg	0.07 mg/kg	0.2 mg/kg	0.7 mg/kg	2 mg/kg	6 mg/kg	18 mg/kg	55 mg/kg	160 mg/kg	475 mg/kg	BMD_{1Std} (mg/kg)	BMD_{L1Std} (mg/kg)
Male												
n	10	5	5	5	5	5	5	5	5	5	NA	NA
0	316.7 ± 6.2	311.2 ± 4.6	317.9 ± 5.8	318.5 ± 5.8	312.4 ± 8.8	317.0 ± 6.3	313.0 ± 9.4	319.1 ± 8.3	317.2 ± 3.8	317.5 ± 5.2	ND	ND
5	333.9 ± 7.5	326.2 ± 9.9	333.0 ± 7.0	336.4 ± 7.3	328.0 ± 9.0	334.3 ± 8.8	325.3 ± 8.8	338.2 ± 9.5	334.6 ± 4.7	333.8 ± 7.4	ND	ND
Female												
n	10	5	5	5	5	5	5	5	5	5	NA	NA
0	214.3 ± 2.8	216.0 ± 1.7	216.0 ± 1.8	216.6 ± 2.9	210.3 ± 4.2	218.4 ± 2.2	216.1 ± 4.9	217.6 ± 3.5	216.4 ± 3.9	217.6 ± 3.9	ND	ND
5	222.6 ± 3.1	223.6 ± 1.6	222.3 ± 1.9	223.4 ± 3.2	221.0 ± 5.1	227.8 ± 3.1	224.4 ± 6.2	226.9 ± 2.5	225.6 ± 2.5	226.2 ± 4.3	ND	ND

BMD_{1Std} = benchmark dose corresponding to a benchmark response set to one standard deviation from the mean; BMD_{L1Std} = benchmark dose lower confidence limit corresponding to a benchmark response set to one standard deviation from the mean; NA = not applicable; ND = not determined.
[a]Data are displayed as mean ± standard error of the mean; body weight data are presented in grams.
[b]Statistical analysis performed by the Jonckheere (trend) and Williams or Dunnett (pairwise) tests.

Table 3. Summary of Select Organ Weights of Male and Female Rats Administered 1,1,2,2-Tetrahydroperfluoro-1-dodecanol for Five Days

Endpoint[a,b,c]	0 mg/kg	0.07 mg/kg	0.2 mg/kg	0.7 mg/kg	2 mg/kg	6 mg/kg	18 mg/kg	55 mg/kg	160 mg/kg	475 mg/kg	BMD$_{1Std}$ (mg/kg)	BMD$_{L1Std}$ (mg/kg)
Male												
n	10	5	5	5	5	5	5	5	5	5	NA	NA
Terminal Body Wt. (g)	333.9 ± 7.5	326.2 ± 9.9	333.0 ± 7.0	336.4 ± 7.3	328.0 ± 9.0	334.3 ± 8.8	325.3 ± 8.8	338.2 ± 9.5	334.6 ± 4.7	333.8 ± 7.4	ND	ND
Liver												
Absolute (g)	12.52 ± 0.44**	11.81 ± 0.75	12.57 ± 0.54	12.61 ± 0.55	12.05 ± 0.29	13.14 ± 0.52	13.48 ± 0.63	14.30 ± 0.40*	15.69 ± 0.54**	15.34 ± 0.53**	21.893	10.337
Relative (mg/g)[d]	37.41 ± 0.66**	36.07 ± 1.30	37.70 ± 0.96	37.42 ± 0.94	36.77 ± 0.42	39.29 ± 0.88	41.44 ± 1.47**	42.31 ± 0.83**	46.85 ± 1.16**	45.93 ± 0.91**	8.087	4.336
Female												
n	10	5	5	5	5	5	5	5	5	5	NA	NA
Terminal Body Wt. (g)	222.6 ± 3.1	223.6 ± 1.6	222.3 ± 1.9	223.4 ± 3.2	221.0 ± 5.1	227.8 ± 3.1	224.4 ± 6.2	226.9 ± 2.5	225.6 ± 2.5	226.2 ± 4.3	ND	ND
Right Kidney												
Absolute (g)	0.66 ± 0.01**	0.70 ± 0.01	0.68 ± 0.03	0.67 ± 0.02	0.68 ± 0.02	0.67 ± 0.01	0.70 ± 0.03	0.71 ± 0.01*	0.72 ± 0.03*	0.76 ± 0.02**	72.145	18.001
Relative (mg/g)	2.97 ± 0.06**	3.15 ± 0.03	3.04 ± 0.10	3.00 ± 0.04	3.08 ± 0.09	2.94 ± 0.04	3.11 ± 0.07	3.15 ± 0.06	3.21 ± 0.10*	3.34 ± 0.04**	NVM	NVM
Left Kidney												
Absolute (g)	0.64 ± 0.02**	0.69 ± 0.02	0.66 ± 0.03	0.67 ± 0.01	0.68 ± 0.01	0.67 ± 0.01	0.69 ± 0.02	0.70 ± 0.01*	0.72 ± 0.03**	0.72 ± 0.02**	56.634	10.508
Relative (mg/g)	2.89 ± 0.06**	3.10 ± 0.10	2.97 ± 0.10	3.01 ± 0.04	3.06 ± 0.07	2.92 ± 0.05	3.07 ± 0.07	3.08 ± 0.04	3.21 ± 0.09**	3.17 ± 0.05**	85.629	17.286
Liver												
Absolute (g)	8.16 ± 0.24**	8.31 ± 0.30	7.69 ± 0.31	8.16 ± 0.21	8.12 ± 0.20	9.10 ± 0.49*	9.07 ± 0.39*	9.86 ± 0.41**	9.92 ± 0.48**	10.02 ± 0.34**	8.801	3.465
Relative (mg/g)	36.65 ± 0.85**	37.16 ± 1.11	34.56 ± 1.12	36.52 ± 0.61	36.73 ± 0.38	39.90 ± 1.78	40.46 ± 1.61*	43.48 ± 1.96**	43.90 ± 1.75**	44.27 ± 0.82**	5.372	2.294

Statistical significance for a dosed group indicates a significant pairwise test compared to the vehicle control group. Statistical significance for the vehicle control group indicates a significant trend test.
*Statistically significant at $p \leq 0.05$; **$p \leq 0.01$.
BMD$_{1Std}$ = benchmark dose corresponding to a benchmark response set to one standard deviation from the mean; BMD$_{L1Std}$ = benchmark dose lower confidence limit corresponding to a benchmark response set to one standard deviation from the mean; NA = not applicable; ND = not determined; NVM = nonviable model.
[a]Descriptions of organ weight endpoints and changes are provided in Appendix E.
[b]Data are displayed as mean ± standard error of the mean.
[c]Statistical analysis performed by the Jonckheere (trend) and Williams or Dunnett (pairwise) tests.
[d]Relative organ weights (organ weight-to-body weight ratios) are given as mg organ weight/g body weight.

Clinical Pathology

In male rats, alkaline phosphatase (ALP) activity had a positive trend with significant pairwise comparisons in the 160 and 475 mg/kg groups; a BMD (BMD_L) was not determined because no viable model was available (Table 4). In female rats, aspartate aminotransferase (AST) activity had a positive trend with a significant pairwise comparison in the 55 mg/kg group; a BMD (BMD_L) was not determined because no viable model was available. ALP activity in female rats had a positive trend and a significant pairwise comparison in the 475 mg/kg group with a BMD (BMD_L) of 6.461 (6.003) mg/kg. In male rats, cholesterol concentration had significant trend and pairwise comparisons. Although a BMD was estimated for cholesterol concentration, its value was much lower (approximately 10- to 25-fold) than would be expected given the endpoint-specific no-observed-effect level (NOEL) and lowest-observed-effect level (LOEL) values, suggesting that the BMD estimate did not accurately reflect the true potency of the effect and was likely an anomalous product of the BMD modeling approach. The BMDs for all clinical pathology endpoints were reviewed by a subject matter expert for anomalous modeling results (i.e., when the traditional statistics are notably different from the estimated BMD values).

In male rats, the reticulocyte count exhibited a negative trend with a significant pairwise comparison at the 475 mg/kg group; the BMD (BMD_L) was 54.227 (30.205) mg/kg (Table 5). In female rats, platelet count had a negative trend and significant pairwise comparisons in the ≥ 160 mg/kg groups with a BMD (BMD_L) of 16.335 (9.571) mg/kg. In addition, the monocyte and large unstained cell counts in the female rats had a positive trend and significant pairwise comparisons in dose groups ≥ 160 mg/kg with BMDs (BMD_Ls) of 20.731 (4.642) and 58.894 (25.959) mg/kg, respectively. The neutrophil count in female rats had significant trend and pairwise comparisons. Although a BMD was estimated, its value was much lower (approximately 250- to 770-fold) than would be expected given the endpoint-specific NOEL and LOEL values, suggesting that the BMD estimate did not accurately reflect the true potency of the effect and was likely an anomalous product of the BMD modeling approach.

In male rats, free thyroxine (fT4) concentration had a negative trend and a significant pairwise comparison in the 160 mg/kg group with a BMD (BMD_L) of 142.469 (57.746) mg/kg (Table 6). Additionally, thyroid stimulating hormone (TSH) concentration had a positive trend and a significant pairwise comparison in the 475 mg/kg male rats with a BMD (BMD_L) of 138.723 (20.376) mg/kg. In female rats, there were no thyroid hormone parameters that exhibited significant trend and pairwise comparisons (Appendix F).

In Vivo Repeat Dose Biological Potency Study of
1,1,2,2-Tetrahydroperfluoro-1-dodecanol in Sprague Dawley Rats

Table 4. Summary of Select Clinical Chemistry Data for Male and Female Rats Administered 1,1,2,2-Tetrahydroperfluoro-1-dodecanol for Five Days

Endpoint[a,b]	0 mg/kg	0.07 mg/kg	0.2 mg/kg	0.7 mg/kg	2 mg/kg	6 mg/kg	18 mg/kg	55 mg/kg	160 mg/kg	475 mg/kg	BMD$_{1Std}$ (mg/kg)	BMD$_{L1Std}$ (mg/kg)
Male												
n	9[c]	5	5	5	5	5	5	5	5	4[c]	NA	NA
Cholesterol (mg/dL)	118.1 ± 3.7*	117.0 ± 5.1	110.0 ± 2.8	114.8 ± 2.5	113.8 ± 2.8	118.6 ± 3.7	104.6 ± 6.5	115.6 ± 5.5	107.6 ± 5.7	100.8 ± 1.4*	17.539[d]	14.31[d]
Alkaline Phosphatase (IU/L)	267.8 ± 8.0**	253.4 ± 24.6	252.8 ± 8.7	277.0 ± 18.2	269.5 ± 8.2[e]	263.8 ± 10.7	285.0 ± 4.5	284.8 ± 20.5	326.0 ± 23.7*	351.0 ± 12.8**	NVM	NVM
Female												
n	10	5	5	5	5	5	5	5	5	5	NA	NA
Alkaline Phosphatase (IU/L)	200.1 ± 9.7**	195.6 ± 10.5	176.8 ± 8.3	191.4 ± 13.6	207.0 ± 17.8	210.2 ± 9.6	235.4 ± 3.8	234.2 ± 6.4	235.6 ± 14.2	247.8 ± 8.0**	6.461	6.003
Aspartate Aminotransferase (U/L)	78.50 ± 2.13*	81.40 ± 4.21	79.40 ± 2.25	84.00 ± 5.55	80.80 ± 1.66	75.80 ± 1.53	77.40 ± 1.66	92.80 ± 3.29*	89.20 ± 3.15	82.60 ± 0.60	NVM	NVM

Statistical significance for a dosed group indicates a significant pairwise test compared to the vehicle control group. Statistical significance for the vehicle control group indicates a significant trend test.
*Statistically significant at $p \le 0.05$; **$p \le 0.01$.
BMD$_{1Std}$ = benchmark dose corresponding to a benchmark response set to one standard deviation from the mean; BMD$_{L1Std}$ = benchmark dose lower confidence limit corresponding to a benchmark response set to one standard deviation from the mean; NA = not applicable; NVM = nonviable model.
[a]Data are displayed as mean ± standard error of the mean.
[b]Statistical analysis performed by the Jonckheere (trend) and Shirley or Dunn (pairwise) tests.
[c]One sample in the indicated dose groups was not received.
[d]BMD values are much lower than would be expected given the lowest-observed-effect level and no-observed-effect level values, suggesting that the BMD estimates do not accurately reflect the true potency of the effect of these endpoints and are likely an anomalous product of the BMD modeling approach.
[e]One value for alkaline phosphatase in the 2 mg/kg group was excluded due to analysis concerns.

Table 5. Summary of Select Hematology Data for Male and Female Rats Administered 1,1,2,2-Tetrahydroperfluoro-1-dodecanol for Five Days

Endpoint[a,b]	0 mg/kg	0.07 mg/kg	0.2 mg/kg	0.7 mg/kg	2 mg/kg	6 mg/kg	18 mg/kg	55 mg/kg	160 mg/kg	475 mg/kg	BMD$_{1Std}$ (mg/kg)	BMD$_{L1Std}$ (mg/kg)
Male												
n	10	5	5	5	5	5	5	5	5	4[c]	NA	NA
Reticulocytes ($10^3/\mu$L)	227.4 ± 9.7**	226.4 ± 9.3	264.3 ± 16.1	258.4 ± 19.0	234.7 ± 15.1	241.2 ± 11.9	216.7 ± 17.7	210.6 ± 3.9	226.6 ± 24.3	174.5 ± 7.3*	54.227	30.205
Female												
n	10	5	5	4[d]	4[d]	5	5	5	5	5	NA	NA
Platelets ($10^3/\mu$L)	1,041 ± 37**	1,067 ± 52	997 ± 34	971 ± 26	997 ± 19	966 ± 28	926 ± 31	1,011 ± 21	916 ± 34*	823 ± 55**	16.335	9.571
Neutrophils ($10^3/\mu$L)	0.42 ± 0.03**	0.53 ± 0.03	0.62 ± 0.06	0.49 ± 0.03	0.53 ± 0.08	0.57 ± 0.09	0.53 ± 0.08	0.61 ± 0.05**	0.60 ± 0.12*	0.72 ± 0.11**	0.071[e]	0.013[e]
Monocytes ($10^3/\mu$L)	0.18 ± 0.02**	0.20 ± 0.03	0.22 ± 0.05	0.17 ± 0.02	0.19 ± 0.04	0.29 ± 0.04	0.24 ± 0.03	0.28 ± 0.04	0.38 ± 0.07**	0.30 ± 0.09*	20.731	4.642
Large Unstained Cells ($10^3/\mu$L)	0.04 ± 0.00**	0.05 ± 0.01	0.04 ± 0.01	0.04 ± 0.01	0.04 ± 0.01	0.05 ± 0.01	0.04 ± 0.01	0.05 ± 0.01	0.06 ± 0.01*	0.07 ± 0.02*	58.894	25.959

Statistical significance for a dosed group indicates a significant pairwise test compared to the vehicle control group. Statistical significance for the vehicle control group indicates a significant trend test.

*Statistically significant at $p \le 0.05$; **$p \le 0.01$.

BMD$_{1Std}$ = benchmark dose corresponding to a benchmark response set to one standard deviation from the mean; BMD$_{L1Std}$ = benchmark dose lower confidence limit corresponding to a benchmark response set to one standard deviation from the mean; NA = not applicable.

[a]Data are displayed as mean ± standard error of the mean.

[b]Statistical analysis performed by the Jonckheere (trend) and Shirley or Dunn (pairwise) tests.

[c]One sample in the indicated dose group was not received.

[d]One sample from each of the indicated dose groups had a clot present and was not analyzed.

[e]BMD values are much lower than would be expected given the lowest-observed-effect level and no-observed-effect level values, suggesting that the BMD estimates do not accurately reflect the true potency of the effect of these endpoints and are likely an anomalous product of the BMD modeling approach.

In Vivo Repeat Dose Biological Potency Study of
1,1,2,2-Tetrahydroperfluoro-1-dodecanol in Sprague Dawley Rats

Table 6. Summary of Select Hormone Data for Male Rats Administered 1,1,2,2-Tetrahydroperfluoro-1-dodecanol for Five Days

Endpoint[a,b]	0 mg/kg	0.07 mg/kg	0.2 mg/kg	0.7 mg/kg	2 mg/kg	6 mg/kg	18 mg/kg	55 mg/kg	160 mg/kg	475 mg/kg	BMD_{1Std} (mg/kg)	BMD_{L1Std} (mg/kg)
n	9[c]	4[c]	4[c]	4[c]	4[c]	4[c]	4[c]	5	5	5	NA	NA
TSH (ng/mL)	4.500 ± 0.667**	3.275 ± 0.867	2.725 ± 0.602	4.050 ± 1.005	3.425 ± 0.807	5.400 ± 1.158	6.800 ± 1.529	12.480 ± 2.168	5.760 ± 0.865	11.560 ± 2.285*	138.723	20.376
fT4 (ng/dL)	7.260 ± 0.292*	7.205 ± 0.237	6.785 ± 0.199	5.980 ± 0.367	6.840 ± 0.685	6.485 ± 0.583	6.980 ± 0.472	7.042 ± 0.249	5.604 ± 0.354*	6.232 ± 0.531	142.469	57.746

Statistical significance for a dosed group indicates a significant pairwise test compared to the vehicle control group. Statistical significance for the vehicle control group indicates a significant trend test.
*Statistically significant at $p \leq 0.05$; **$p \leq 0.01$.
BMD_{1Std} = benchmark dose corresponding to a benchmark response set to one standard deviation from the mean; BMD_{L1Std} = benchmark dose lower confidence limit corresponding to a benchmark response set to one standard deviation from the mean; NA = not applicable; TSH = thyroid stimulating hormone; fT4 = free thyroxine.
[a]Data are displayed as mean ± standard error of the mean.
[b]Statistical analysis performed by the Jonckheere (trend) and Shirley or Dunn (pairwise) tests.
[c]One sample in the indicated dose groups did not have sufficient specimen volume available for analysis.

Internal Dose Assessment

For the 2 and 18 mg/kg groups, 1,1,2,2-tetrahydroperfluoro-1-dodecanol plasma concentrations were determined at 2 and 24 hours following the last dose administered on study day 4 to male and female rats. Average 1,1,2,2-tetrahydroperfluoro-1-dodecanol concentrations are given in Table 7. At 2 hours following administration, the average concentrations of 1,1,2,2-tetrahydroperfluoro-1-dodecanol in male and female rats in each dosed group were similar; as the administered dose increased from 2 to 18 mg/kg (a ninefold increase), there was a less-than-proportional increase (approximately four- to fivefold) in the average 1,1,2,2-tetrahydroperfluoro-1-dodecanol plasma concentration, suggesting changes in the absorption, distribution, metabolism, and excretion processes (e.g., lower absorption and/or induction of metabolism and clearance pathways) as the dose increased. At 24 hours postdose, the concentration decreased across each dosed group; in the 2 mg/kg group, the concentration was below the limit of quantitation (LOQ = 10 ng/mL) of the analytical method in female rats and close to the LOQ in male rats (average of 8 ng/mL), while in the 18 mg/kg group the concentration was approximately 5- and 12-fold lower in male and female rats, respectively. Half-lives estimated using the data from these two time points were similar between dosed groups and sexes (6.65 and 8.96 hours for the 2 and 18 mg/kg male rats, respectively, and 6.12 hours for the 18 mg/kg female rats); a value could not be estimated for the 2 mg/kg female rats due to concentrations falling below the LOQ at 24 hours.

Table 7. Summary of Plasma Concentration Data for Male and Female Rats Administered 1,1,2,2-Tetrahydroperfluoro-1-dodecanol for Five Days[a]

	2 mg/kg	18 mg/kg
n	3	3
Male		
2 Hours Postdose (ng/mL)	80.2 ± 9.75	395 ± 60.1
24 Hours Postdose (ng/mL)	8.1 ± 3.1	72.1 ± 5.52
Female		
2 Hours Postdose (ng/mL)	91.0 ± 16.9	386 ± 79.5
24 Hours Postdose (ng/mL)	BD	31.9 ± 3.09

If over 20% of the animals in a group are above the limit of detection, then half the limit of detection value is substituted for values that are below it.
BD = below detection; group did not have over 20% of its values above the limit of detection so mean and standard error were not calculated.
[a]Data are displayed as mean ± standard error of the mean.

Apical Endpoint Benchmark Dose Summary

A summary of the calculated BMDs for each toxicological endpoint is provided in Table 8. The endpoint-specific LOEL and NOEL are included and could be informative for endpoints that lack a calculated BMD either because no viable model was available or because the estimated BMD was below the lower limit of extrapolation (<0.023 mg/kg).

Table 8. BMD, BMD$_L$, LOEL, and NOEL Summary for Apical Endpoints, Sorted by BMD or LOEL from Low to High

Endpoint	BMD$_{1Std}$ (mg/kg)	BMD$_{L1Std}$ (mg/kg)	LOEL (mg/kg)[a]	NOEL (mg/kg)	Direction of Change
Male					
Relative Liver Weight	8.087	4.336	18	6	UP
Absolute Liver Weight	21.893	10.337	55	18	UP
Reticulocytes	54.227	30.205	475	160	DOWN
Thyroid Stimulating Hormone	138.723	20.376	475	160	UP
Free Thyroxine	142.469	57.746	160	55	DOWN
Alkaline Phosphatase	NVM	NVM	**160**	55	UP
Cholesterol	UREP[b]	UREP[b]	**475**	160	—[b]
Female					
Relative Liver Weight	5.372	2.294	18	6	UP
Alkaline Phosphatase	6.461	6.003	475	160	UP
Absolute Liver Weight	8.801	3.465	6	2	UP
Platelets	16.335	9.571	160	55	DOWN
Monocytes	20.731	4.642	160	55	UP
Absolute Left Kidney Weight	56.634	10.508	55	18	UP
Large Unstained Cells	58.894	25.959	160	55	UP
Absolute Right Kidney Weight	72.145	18.001	55	18	UP
Relative Left Kidney Weight	85.629	17.286	160	55	UP
Aspartate Aminotransferase	NVM	NVM	**55**	18	UP
Neutrophils	UREP	UREP	**55**	18	—
Relative Right Kidney Weight	NVM	NVM	**160**	55	UP

BMD$_{1Std}$ = benchmark dose corresponding to a benchmark response set to one standard deviation from the mean; BMD$_{L1Std}$ = benchmark dose lower confidence limit corresponding to a benchmark response set to one standard deviation from the mean; LOEL = lowest-observed-effect level; NOEL = no-observed-effect level; NVM = nonviable model, defined as a modeling result that does not meet prespecified fit criteria and hence is deemed unreliable; UREP = unreliable estimate of potency is a label based on review by a subject matter expert and rejection of BMD modeling results.
[a]Values in bold text indicate the LOEL of endpoints for which a BMD could not be calculated.
[b]BMD values are much lower than would be expected given the endpoint-specific LOEL and NOEL values, suggesting that the BMD estimates do not accurately reflect the true potency of the effect of these endpoints and are likely an anomalous product of the BMD modeling approach.

Gene Set Benchmark Dose Analysis

Chemical-induced alterations in liver and kidney gene transcript expression were examined to determine those gene sets most sensitive to 1,1,2,2-tetrahydroperfluoro-1-dodecanol exposure. To that end, BMD analysis of transcripts and gene sets (Gene Ontology [GO] biological process) was conducted to determine the potency of the chemical to elicit gene expression changes in the liver and kidney. This analysis used transcript-level BMD data to assess an aggregate score of gene set potency (median transcript BMD) and enrichment.

The "active" gene sets in the liver and kidney with the lowest BMD median values are shown in Table 9 and Table 10, respectively. The gene sets in Table 9 and Table 10 should be interpreted with caution from the standpoint of the underlying biological mechanism and any relationship to toxicity or toxic agents referenced in the GO term definitions. The data primarily should be considered a metric of potency for chemical-induced transcriptional changes (i.e., a concerted biological change) that could serve as a surrogate of estimated biological potency and, by extension, toxicological potency when more definitive toxicological data are unavailable.

No gene sets in the liver of male or female rats had estimated BMD median values <0.023 mg/kg. In male rats, the most sensitive GO biological processes for which a BMD value could be reliably calculated were nucleotide biosynthetic process (GO:0009165) and organic hydroxy compound transport (GO:0015850) with median BMDs (BMD_{LS}) of 5.235 (2.666) and 5.978 (3.303) mg/kg, respectively. In female rats, the most sensitive GO biological processes for which a BMD value could be reliably calculated were internal protein amino acid acetylation (GO:0006475) and glutamine family amino acid metabolic process (GO:0009064) with median BMDs (BMD_{LS}) of 5.355 (3.108) and 8.071 (3.552) mg/kg, respectively.

No gene sets in the kidney of male or female rats had estimated BMD median values <0.023 mg/kg. In male rats, the most sensitive GO biological processes for which a BMD value could be reliably calculated were regulation of myeloid leukocyte mediated immunity (GO:0002886) and response to progesterone (GO:0032570) with median BMDs (BMD_{LS}) of 144.319 (57.694) and 145.437 (104.718) mg/kg, respectively. In female rats, the most sensitive GO biological processes for which a BMD value could be reliably calculated were innate immune response (GO:0045087) and activation of immune response (GO:0002253) with median BMDs (BMD_{LS}) of 57.313 (37.882) and 78.645 (45.596) mg/kg, respectively. The full list of affected gene sets in the liver and kidney of male and female rats can be found in Appendix F.

Table 9. Top 10 Liver Gene Ontology Biological Process Gene Sets Ranked by Potency of Perturbation, Sorted by Benchmark Dose Median[a]

Category Name	No. of Active Genes/Platform Genes in Gene Set	% Gene Set Coverage	Active Genes	BMD_{1std} Median of Gene Set Transcripts (mg/kg)	Median BMD_{L1Std}–BMD_{U1Std} (mg/kg)	Genes with Changed Direction Up	Genes with Changed Direction Down
Male							
GO:0009165 nucleotide biosynthetic process	3/55	5%	*Rrm2b*; *Gcdh*; *Aldoa*	5.235	2.666–10.897	3	0
GO:0015850 organic hydroxy compound transport	3/50	6%	*Aqp9*; *Apoa1*; *Abcc3*	5.978	3.303–16.491	1	2

In Vivo Repeat Dose Biological Potency Study of 1,1,2,2-Tetrahydroperfluoro-1-dodecanol in Sprague Dawley Rats

Category Name	No. of Active Genes/Platform Genes in Gene Set	% Gene Set Coverage	Active Genes	BMD_{1std} Median of Gene Set Transcripts (mg/kg)	Median BMD_{L1Std}– BMD_{U1Std} (mg/kg)	Genes with Changed Direction Up	Genes with Changed Direction Down
GO:0051496 positive regulation of stress fiber assembly	3/21	14%	*Rhoc*; *Pak1*; *Apoa1*	6.710	2.595–19.237	2	1
GO:0042908 xenobiotic transport	4/11	36%	*Slc17a3*; *Abcg2*; *Abcc4*; *Abcc3*	6.716	3.394–26.223	4	0
GO:0032273 positive regulation of protein polymerization	3/30	10%	*Pak1*; *Icam1*; *Hspa1a*	7.304	2.595–23.878	3	0
GO:0032535 regulation of cellular component size	3/60	5%	*Sptan1*; *Icam1*; *Anxa7*	7.304	2.970–23.878	3	0
GO:1903426 regulation of reactive oxygen species biosynthetic process	5/48	10%	*Rgn*; *Ptgs2*; *Icam1*; *Hspd1*; *Foxo3*	7.304	3.587–23.878	3	2
GO:2000351 regulation of endothelial cell apoptotic process	3/28	11%	*Icam1*; *Foxo3*; *Ccl2*	7.304	2.250–23.878	2	1
GO:0070741 response to interleukin-6	3/14	21%	*Pck1*; *Icam1*; *Ccl2*	7.304	2.250–23.878	2	1
GO:1903428 positive regulation of reactive oxygen species biosynthetic process	3/33	9%	*Ptgs2*; *Icam1*; *Foxo3*	7.304	2.250–23.878	2	1
Female							
GO:0006475 internal protein amino acid acetylation	3/15	20%	*Pck1*; *Ncoa1*; *Ehhadh*	5.355	3.108–9.861	3	0

In Vivo Repeat Dose Biological Potency Study of 1,1,2,2-Tetrahydroperfluoro-1-dodecanol in Sprague Dawley Rats

Category Name	No. of Active Genes/Platform Genes in Gene Set	% Gene Set Coverage	Active Genes	BMD$_{1std}$ Median of Gene Set Transcripts (mg/kg)	Median BMD$_{L1Std}$– BMD$_{U1Std}$ (mg/kg)	Genes with Changed Direction Up	Genes with Changed Direction Down
GO:0009064 glutamine family amino acid metabolic process	3/24	13%	*Gclm*; *Gclc*; *Dao*	8.071	3.552–26.141	3	0
GO:0046700 heterocycle catabolic process	4/63	6%	*Hmox1*; *Dao*; *Aldh1l1*; *Akr7a3*	8.437	2.875–33.533	4	0
GO:1901361 organic cyclic compound catabolic process	5/89	6%	*Hmox1*; *Dao*; *Cyp1a2*; *Aldh1l1*; *Akr7a3*	8.803	3.082–26.141	4	1
GO:0009069 serine family amino acid metabolic process	4/13	31%	*Txnrd1*; *Gclm*; *Gclc*; *Dao*	9.286	4.360–24.515	4	0
GO:0055093 response to hyperoxia	3/24	13%	*Txnrd1*; *Cdkn1a*; *Cav1*	10.500	5.321–22.888	2	1
GO:1901605 alpha-amino acid metabolic process	5/72	7%	*Txnrd1*; *Plod2*; *Gclm*; *Gclc*; *Dao*	10.500	5.167–26.141	5	0
GO:0007093 mitotic cell cycle checkpoint	3/38	8%	*Zwint*; *Kntc1*; *Cdkn1a*	11.920	4.772–41.705	2	1
GO:0010823 negative regulation of mitochondrion organization	3/22	14%	*Hgf*; *Gclc*; *Acaa2*	11.956	5.167–23.735	2	1
GO:0035729 cellular response to hepatocyte growth factor stimulus	3/14	21%	*Hgf*; *Gclm*; *Gclc*	11.956	5.167–23.735	2	1

BMD$_{1Std}$ = benchmark dose corresponding to a benchmark response set to one standard deviation from the mean; BMD$_{L1Std}$ = benchmark dose lower confidence limit corresponding to a benchmark response set to one standard deviation from the mean; BMD$_{U1Std}$ = benchmark dose upper confidence limit corresponding to a benchmark response set to one standard deviation from the mean; GO = Gene Ontology.

[a]Definitions of GO terms were adapted from the Gene Ontology Resource.[30] Official gene symbols from the Rat Genome Database[31] are shown in the "Active Genes" column.

GO process description version: https://doi.org/10.22427/NTP-DATA-002-00600-0002-000-0.

GO:0009165 nucleotide biosynthetic process: The chemical reactions and pathways resulting in the formation of nucleotides, any nucleoside that is esterified with (ortho)phosphate or an oligophosphate at any hydroxyl group on the glycose moiety; may be mono-, di- or triphosphate; this definition includes cyclic-nucleotides (nucleoside cyclic phosphates).

GO:0015850 organic hydroxy compound transport: The directed movement of an organic hydroxy compound (organic alcohol) into, out of, or within a cell, or between cells, by means of some agent such as a transporter or pore. An organic hydroxy compound is an organic compound having at least one hydroxy group attached to a carbon atom.

GO:0051496 positive regulation of stress fiber assembly: Any process that activates or increases the frequency, rate, or extent of the assembly of a stress fiber, a bundle of microfilaments and other proteins found in fibroblasts.

GO:0042908 xenobiotic transport: The directed movement of a xenobiotic into, out of or within a cell, or between cells, by means of some agent such as a transporter or pore. A xenobiotic is a compound foreign to the organism exposed to it. It may be synthesized by another organism (like ampicillin) or it can be a synthetic chemical.

GO:0032273 positive regulation of protein polymerization: Any process that activates or increases the frequency, rate or extent of the process of creating protein polymers.

GO:0032535 regulation of cellular component size: A process that modulates the size of a cellular component.

GO:1903426 regulation of reactive oxygen species biosynthetic process: Any process that modulates the frequency, rate, or extent of reactive oxygen species biosynthetic process.

GO:2000351 regulation of endothelial cell apoptotic process: Any process that modulates the frequency, rate, or extent of endothelial cell apoptotic process.

GO:0070741 response to interleukin-6: Any process that results in a change in state or activity of a cell or an organism (in terms of movement, secretion, enzyme production, gene expression, etc.) as a result of an interleukin-6 stimulus.

GO:1903428 positive regulation of reactive oxygen species biosynthetic process: Any process that activates or increases the frequency, rate, or extent of reactive oxygen species biosynthetic process.

GO:0006475 internal protein amino acid acetylation: The addition of an acetyl group to a nonterminal amino acid in a protein.

GO:0009064 glutamine family amino acid metabolic process: The chemical reactions and pathways involving amino acids of the glutamine family, comprising arginine, glutamate, glutamine, and proline.

GO:0046700 heterocycle catabolic process: The chemical reactions and pathways resulting in the breakdown of heterocyclic compounds, those with a cyclic molecular structure, and at least two different atoms in the ring (or rings).

GO:1901361 organic cyclic compound catabolic process: The chemical reactions and pathways resulting in the breakdown of organic cyclic compound.

GO:0009069 serine family amino acid metabolic process: The chemical reactions and pathways involving amino acids of the serine family, comprising cysteine, glycine, homoserine, selenocysteine, and serine.

GO:0055093 response to hyperoxia: Any process that results in a change in state or activity of a cell or an organism (in terms of movement, secretion, enzyme production, gene expression, etc.) as a result of a stimulus indicating increased oxygen tension.

GO:1901605 alpha-amino acid metabolic process: The chemical reactions and pathways involving an alpha-amino acid.

GO:0007093 mitotic cell cycle checkpoint: A signaling process that ensures accurate chromosome replication and segregation by preventing progression through a mitotic cell cycle until conditions are suitable for the cell to proceed to the next stage.

GO:0010823 negative regulation of mitochondrion organization: Any process that decreases the frequency, rate, or extent of a process involved in the formation, arrangement of constituent parts, or disassembly of a mitochondrion.

GO:0035729 cellular response to hepatocyte growth factor stimulus: Any process that results in a change in state or activity of a cell (in terms of movement, secretion, enzyme production, gene expression, etc.) as a result of a hepatocyte growth factor stimulus.

Table 10. Top 10 Kidney Gene Ontology Biological Process Gene Sets Ranked by Potency of Perturbation, Sorted by Benchmark Dose Median[a]

Category Name	No. of Active Genes/Platform Genes in Gene Set	% Gene Set Coverage	Active Genes	BMD$_{1std}$ Median of Gene Set Transcripts (mg/kg)	Median BMD$_{L1Std}$– BMD$_{U1Std}$ (mg/kg)	Genes with Changed Direction Up	Genes with Changed Direction Down
Male							
GO:0002886 regulation of myeloid leukocyte mediated immunity	3/28	11%	*Rt1-S3*; *Hmox1*; *C3*	144.319	57.694– 153.260	2	1
GO:0032570 response to progesterone	3/40	8%	*Srebf1*; *Map2*; *C3*	145.437	104.718– 237.081	2	1
GO:0002703 regulation of leukocyte mediated immunity	4/79	5%	*Rt1-S3*; *Il1b*; *Hmox1*; *C3*	149.155	83.579– 205.964	3	1
GO:0002675 positive regulation of acute inflammatory response	3/17	18%	*Rt1-S3*; *Il1b*; *C3*	153.991	109.464– 258.668	2	1
GO:0072347 response to anesthetic	3/44	7%	*Slc6a1*; *Il1b*; *Grin1*	153.991	109.464– 258.668	3	0
GO:1903531 negative regulation of secretion by cell	3/60	5%	*Srebf1*; *Il1b*; *Hmox1*	153.991	109.464– 258.668	2	1
GO:0009408 response to heat	3/59	5%	*Il1b*; *Hmox1*; *Cxcl10*	153.991	109.464– 258.668	2	1
GO:0050766 positive regulation of phagocytosis	3/35	9%	*Il1b*; *Clec7a*; *C3*	153.991	109.464– 258.668	3	0
GO:0002718 regulation of cytokine production involved in immune response	3/36	8%	*Rt1-S3*; *Il1b*; *Hmox1*	153.991	109.464– 258.668	2	1

Category Name	No. of Active Genes/Platform Genes in Gene Set	% Gene Set Coverage	Active Genes	BMD_{1std} Median of Gene Set Transcripts (mg/kg)	Median BMD_{L1Std}–BMD_{U1Std} (mg/kg)	Genes with Changed Direction Up	Genes with Changed Direction Down
GO:0045665 negative regulation of neuron differentiation	3/54	6%	*Map2*; *Il1b*; *Fgf13*	153.991	109.464–258.668	2	1
Female							
GO:0045087 innate immune response	5/87	6%	*Vnn1*; *Fcer1g*; *Col12a1*; *Clec4a*; *C3*	57.313	37.882–112.773	4	1
GO:0002253 activation of immune response	4/69	6%	*Fyb1*; *Fcer1g*; *Col12a1*; *C3*	78.645	45.596–480.937	3	1
GO:0002250 adaptive immune response	3/57	5%	*Fcer1g*; *Adgre1*; *Clec4a*	82.466	47.872–265.955	3	0
GO:0050729 positive regulation of inflammatory response	3/52	6%	*Tslp*; *Fcer1g*; *C3*	99.976	53.311–818.733	2	1
GO:0006690 icosanoid metabolic process	3/48	6%	*Gstp1*; *Ephx1*; *Cyp4a2*	147.888	112.384–215.342	3	0
GO:0071385 cellular response to glucocorticoid stimulus	3/51	6%	*Hmgcs2*; *Gstp1*; *Ephx1*	147.888	112.384–215.342	3	0
GO:1901568 fatty acid derivative metabolic process	4/57	7%	*Hmgcs2*; *Gstp1*; *Ephx1*; *Cyp4a2*	220.130	150.351–433.756	4	0
GO:0046165 alcohol biosynthetic process	3/41	7%	*Hmgcs2*; *Ephx1*; *Cyp26b1*	238.250	181.323–370.243	3	0
GO:0045580 regulation of T cell differentiation	3/47	6%	*Vnn1*; *Lilrb4*; *Cyp26b1*	238.250	181.323–370.243	3	0

In Vivo Repeat Dose Biological Potency Study of
1,1,2,2-Tetrahydroperfluoro-1-dodecanol in Sprague Dawley Rats

Category Name	No. of Active Genes/Platform Genes in Gene Set	% Gene Set Coverage	Active Genes	BMD_{1std} Median of Gene Set Transcripts (mg/kg)	Median BMD_{L1Std}–BMD_{U1Std} (mg/kg)	Genes with Changed Direction Up	Genes with Changed Direction Down
GO:0021700 developmental maturation	3/51	6%	*Sez6*; *Fgg*; *C3*	251.984	163.812–471.307	2	1

BMD_{1Std} = benchmark dose corresponding to a benchmark response set to one standard deviation from the mean; BMD_{L1Std} = benchmark dose lower confidence limit corresponding to a benchmark response set to one standard deviation from the mean; BMD_{U1Std} = benchmark dose upper confidence limit corresponding to a benchmark response set to one standard deviation from the mean; GO = Gene Ontology.

[a]Definitions of GO terms were adapted from the Gene Ontology Resource.[30] Official gene symbols from the Rat Genome Database[31] are shown in the "Active Genes" column.

GO process description version: https://doi.org/10.22427/NTP-DATA-002-00600-0002-000-0.

GO:0002886 regulation of myeloid leukocyte mediated immunity: Any process that modulates the frequency, rate, or extent of myeloid leukocyte mediated immunity.

GO:0032570 response to progesterone: Any process that results in a change in state or activity of a cell or an organism (in terms of movement, secretion, enzyme production, gene expression, etc.) as a result of a progesterone stimulus.

GO:0002703 regulation of leukocyte mediated immunity: Any process that modulates the frequency, rate, or extent of leukocyte mediated immunity.

GO:0002675 positive regulation of acute inflammatory response: Any process that activates or increases the frequency, rate, or extent of an acute inflammatory response.

GO:0072347 response to anesthetic: Any process that results in a change in state or activity of a cell or an organism (in terms of movement, secretion, enzyme production, gene expression, etc.) as a result of an anesthetic stimulus. An anesthetic is a substance that causes loss of feeling, awareness, or sensation.

GO:1903531 negative regulation of secretion by cell: Any process that stops, prevents, or reduces the frequency, rate, or extent of secretion by cell.

GO:0009408 response to heat: Any process that results in a change in state or activity of a cell or an organism (in terms of movement, secretion, enzyme production, gene expression, etc.) as a result of a heat stimulus, a temperature stimulus above the optimal temperature for that organism.

GO:0050766 positive regulation of phagocytosis: Any process that activates or increases the frequency, rate, or extent of phagocytosis.

GO:0002718 regulation of cytokine production involved in immune response: Any process that modulates the frequency, rate, or extent of cytokine production that contributes to an immune response.

GO:0045665 negative regulation of neuron differentiation: Any process that stops, prevents, or reduces the frequency, rate, or extent of neuron differentiation.

GO:0045087 innate immune response: Innate immune responses are defense responses mediated by germline encoded components that directly recognize components of potential pathogens.

GO:0002253 activation of immune response: Any process that initiates an immune response.

GO:0002250 adaptive immune response: An immune response mediated by cells expressing specific receptors for antigen produced through a somatic diversification process and allowing for an enhanced secondary response to subsequent exposures to the same antigen (immunological memory).

GO:0050729 positive regulation of inflammatory response: Any process that activates or increases the frequency, rate, or extent of the inflammatory response.

GO:0006690 icosanoid metabolic process: The chemical reactions and pathways involving icosanoids, any of a group of C20 polyunsaturated fatty acids.

GO:0071385 cellular response to glucocorticoid stimulus: Any process that results in a change in state or activity of a cell (in terms of movement, secretion, enzyme production, gene expression, etc.) as a result of a glucocorticoid stimulus. Glucocorticoids are hormonal C21 corticosteroids synthesized from cholesterol with the ability to bind with the cortisol receptor and trigger similar effects. Glucocorticoids act primarily on carbohydrate and protein metabolism and have anti-inflammatory effects.

GO:1901568 fatty acid derivative metabolic process: The chemical reactions and pathways involving fatty acid derivative.

GO:0046165 alcohol biosynthetic process: The chemical reactions and pathways resulting in the formation of alcohols, any of a class of compounds containing one or more hydroxyl groups attached to a saturated carbon atom.

GO:0045580 regulation of T cell differentiation: Any process that modulates the frequency, rate, or extent of T cell differentiation.

GO:0021700 developmental maturation: A developmental process, independent of morphogenetic (shape) change that is required for an anatomical structure, cell, or cellular component to attain its fully functional state.

Gene Benchmark Dose Analysis

The top 10 genes based on BMD potency in the liver and kidney (fold change >|2|, significant Williams trend test, global goodness-of-fit p value >0.1, and $BMD_U/BMD_L \leq 40$) are shown in Table 11 and Table 12. As with the GO analysis, the biological or toxicological significance of the changes in gene expression shown in Table 11 and Table 12 should be interpreted with caution. The data primarily should be considered a metric of potency for chemical-induced transcriptional changes that could serve as a conservative surrogate of estimated biological potency, and by extension toxicological potency, when more definitive toxicological data are unavailable.

No liver genes in male or female rats had estimated BMD median values <0.023 mg/kg. In male rats, the most sensitive upregulated genes with a calculated BMD were *Akr7a3* (aldo-keto reductase family 7 member A3), *Ephx1* (epoxide hydrolase 1), *Me1* (malic enzyme 1), *Cyp4a1* (cytochrome P450, family 4, subfamily a, polypeptide 1), *Anxa7* (annexin A7), and *Slc17a3* (solute carrier family 17 member 3) with BMDs (BMD_Ls) of 2.192 (1.593), 2.467 (1.828), 3.531 (2.076), 4.588 (2.345), 4.660 (2.970), and 5.147 (3.485) mg/kg, respectively. The most sensitive genes exhibiting a decrease in expression were *Pck1* (phosphoenolpyruvate carboxykinase 1), *A2m* (alpha-2-macroglobulin), *Loc100911545/A2m* (alpha-2-macroglobulin), and *Zfp354a* (zinc finger protein 354A) with BMDs (BMD_Ls) of 1.149 (0.548), 1.733 (0.972), 1.733 (0.972), and 1.785 (0.579) mg/kg, respectively.

In female rats, all 10 of the most sensitive liver genes were upregulated. These genes were *Abcc3* (ATP-binding cassette subfamily C member 3), *Gsta2* (glutathione S-transferase alpha 2), *Gsta5* (glutathione S-transferase alpha 5), *Ephx1* (epoxide hydrolase 1), *Akr7a3* (aldo-keto reductase family 7 member A3), *Ehhadh* (enoyl-CoA hydratase and 3-hydroxyacyl CoA dehydrogenase), *Pir* (pirin), *Gclm* (glutamate-cysteine ligase, modifier subunit), *Dao* (D-amino-acid oxidase), and *Me1* (malic enzyme 1) with BMDs (BMD_Ls) of 5.019 (2.945), 5.153 (2.796), 5.153 (2.796), 5.233 (3.072), 5.348 (3.082), 5.355 (3.108), 6.124 (2.642), 8.034 (3.552), 8.071 (2.669), and 8.192 (2.618) mg/kg, respectively.

None of the top 10 most sensitive kidney genes in male rats had estimated BMD median values <0.023 mg/kg. The most sensitive upregulated genes with a calculated BMD were *Ugt2b7* (UDP-glucuronosyltransferase family 2 member B7), *Ephx1* (epoxide hydrolase 1), *Adgre1* (adhesion G protein-coupled receptor E1), *Map2* (microtubule-associated protein 2), *Slc6a1* (solute carrier family 6 member 1), *Naaa* (N-acylethanolamine acid amidase), *Il1b* (interleukin 1 beta), *Cyp24a1* (cytochrome P450, family 24, subfamily a, polypeptide 1), and *Nsg1* (neuronal vesicle trafficking associated 1) with BMDs (BMD_Ls) of 4.139 (1.398), 12.509 (3.282), 119.065 (89.170), 145.437 (104.718), 145.445 (104.722), 151.002 (107.821), 153.991 (109.464), 189.111 (127.579), and 216.472 (166.237) mg/kg, respectively. One gene, *Top2a* (DNA topoisomerase II alpha), was downregulated with a BMD (BMD_L) of 203.468 (108.442) mg/kg.

The most sensitive kidney gene in female rats, exhibiting a decrease in expression, was *Mrc1* (mannose receptor, C-type 1) with an estimated BMD median value <0.023 mg/kg. There were no other downregulated genes. The most sensitive upregulated genes with a calculated BMD were *Ckap2* (cytoskeleton associated protein 2), *Ugt2b37* (UDP-glucuronosyltransferase 2 family, member 37), *Slc51a* (solute carrier family 51 subunit alpha), *Ugt2b7* (UDP-glucuronosyltransferase family 2 member B7), *Bbox1* (gamma-butyrobetaine hydroxylase 1),

In Vivo Repeat Dose Biological Potency Study of
1,1,2,2-Tetrahydroperfluoro-1-dodecanol in Sprague Dawley Rats

Adgre1 (adhesion G protein-coupled receptor E1), *Clec4a* (C-type lectin domain family 4, member A), *Cyp26b1* (cytochrome P450, family 26, subfamily b, polypeptide 1), and *Lilrb4* (leukocyte immunoglobulin like receptor B4) with BMDs (BMD$_L$s) of 2.608 (0.997), 32.501 (7.520), 37.134 (11.007), 54.314 (15.595), 61.319 (39.473), 61.524 (39.671), 82.466 (47.872), 238.250 (181.323), and 350.991 (212.248) mg/kg, respectively.

Table 11. Top 10 Liver Genes Ranked by Potency of Perturbation, Sorted by Benchmark Dose Median[a]

Gene Symbol	Entrez Gene IDs	Probe IDs[b]	BMD$_{1Std}$ (BMD$_{L1std}$–BMD$_{U1std}$) in mg/kg	Maximum Fold Change	Direction of Expression Change
Male					
Pck1	362282	PCK1_9439	1.149 (0.548–2.562)	2.7	DOWN
A2m	24153	A2M_7932	1.733 (0.972–3.497)	3.0	DOWN
Loc100911545/A2m	100911545	A2M_7932	1.733 (0.972–3.497)	3.0	DOWN
Zfp354a	24522	ZFP354A_10203	1.785 (0.579–5.737)	3.6	DOWN
Akr7a3	26760	AKR7A3_8015	2.192 (1.593–3.715)	9.5	UP
Ephx1	25315	EPHX1_8567	2.467 (1.828–4.041)	5.6	UP
Me1	24552	ME1_9215	3.531 (2.076–6.794)	3.4	UP
Cyp4a1	50549	CYP4A1_33111	4.588 (2.345–9.587)	2.6	UP
Anxa7	155423	ANXA7_8051	4.660 (2.970–7.797)	3.8	UP
Slc17a3	266730	SLC17A3_9840	5.147 (3.485–8.103)	3.1	UP
Female					
Abcc3	140668	ABCC3_7941	5.019 (2.945–9.451)	3.5	UP
Gsta2	24422	GSTA2_8756	5.153 (2.796–10.815)	2.8	UP
Gsta5	494499	GSTA2_8756	5.153 (2.796–10.815)	2.8	UP
Ephx1	25315	EPHX1_8567	5.233 (3.072–9.586)	3.8	UP
Akr7a3	26760	AKR7A3_8015	5.348 (3.082–10.631)	5.7	UP
Ehhadh	171142	EHHADH_8534	5.355 (3.108–9.861)	2.2	UP
Pir	363465	PIR_9487	6.124 (2.642–15.294)	2.8	UP
Gclm	29739	GCLM_8700	8.034 (3.552–19.773)	2.1	UP
Dao	114027	DAO_8437	8.071 (2.669–26.141)	2.1	UP
Me1	24552	ME1_9215	8.192 (2.618–30.949)	2.3	UP

BMD$_{1Std}$ = benchmark dose corresponding to a benchmark response set to one standard deviation from the mean; BMD$_{L1Std}$ = benchmark dose lower confidence limit corresponding to a benchmark response set to one standard deviation from the mean; BMD$_{U1Std}$ = benchmark dose upper confidence limit corresponding to a benchmark response set to one standard deviation from the mean.

[a]Descriptions of orthologous human genes are shown due to the increased detail available in public resources such as UniprotKB[32] and Entrez Gene.[33] Gene definitions adapted from Human UniprotKB were used as the primary resource due to the greater breadth of annotation and depth of functional detail provided. Gene definitions adapted from Rat UniprotKB were used as the secondary resource if the primary source did not provide a detailed description of function. Human Entrez Gene was used as the third resource. Rat Entrez Gene was used as the fourth resource.

[b]In some cases, a probe may map to more than one gene, resulting in duplicate reporting of that probe mapped to different genes.
Gene definition version: https://doi.org/10.22427/NTP-DATA-002-00600-0002-000-0.

In Vivo Repeat Dose Biological Potency Study of
1,1,2,2-Tetrahydroperfluoro-1-dodecanol in Sprague Dawley Rats

Pck1: Human Uniprot function (Human *PCK1*): Cytosolic phosphoenolpyruvate carboxykinase that catalyzes the reversible decarboxylation and phosphorylation of oxaloacetate (OAA) and acts as the rate-limiting enzyme in gluconeogenesis (PubMed30193097, PubMed24863970, PubMed26971250, PubMed28216384). Regulates cataplerosis and anaplerosis, the processes that control the levels of metabolic intermediates in the citric acid cycle (PubMed30193097, PubMed24863970, PubMed26971250, PubMed28216384). At low glucose levels, it catalyzes the cataplerotic conversion of oxaloacetate to phosphoenolpyruvate (PEP), the rate-limiting step in the metabolic pathway that produces glucose from lactate and other precursors derived from the citric acid cycle (PubMed30193097). At high glucose levels, it catalyzes the anaplerotic conversion of phosphoenolpyruvate to oxaloacetate (PubMed30193097). Acts as a regulator of formation and maintenance of memory CD8(+) T-cells upregulated in these cells, where it generates phosphoenolpyruvate, via gluconeogenesis (by similarity). The resultant phosphoenolpyruvate flows to glycogen and pentose phosphate pathway, which is essential for memory CD8(+) T-cells homeostasis (by similarity). In addition to the phosphoenolpyruvate carboxykinase activity, also acts as a protein kinase when phosphorylated at Ser-90 phosphorylation at Ser-90 by AKT1 reduces the binding affinity to oxaloacetate and promotes an atypical serine protein kinase activity using GTP as donor (PubMed32322062). The protein kinase activity regulates lipogenesis upon phosphorylation at Ser-90, translocates to the endoplasmic reticulum and catalyzes phosphorylation of INSIG proteins (INSIG1 and INSIG2), thereby disrupting the interaction between INSIG proteins and SCAP and promoting nuclear translocation of SREBP proteins (SREBF1/SREBP1 or SREBF2/SREBP2) and subsequent transcription of downstream lipogenesis-related genes (PubMed32322062). {ECO0000250|UniProtKBQ9Z2V4, ECO0000269|PubMed24863970, ECO0000269|PubMed26971250, ECO0000269|PubMed28216384, ECO0000269|PubMed30193097, ECO0000269|PubMed32322062}.

A2m: Human Uniprot function (Human *A2M*): Is able to inhibit all four classes of proteinases by a unique 'trapping' mechanism. This protein has a peptide stretch, called the 'bait region' which contains specific cleavage sites for different proteinases. When a proteinase cleaves the bait region, a conformational change is induced in the protein which traps the proteinase. The entrapped enzyme remains active against low molecular weight substrates (activity against high molecular weight substrates is greatly reduced). Following cleavage in the bait region, a thioester bond is hydrolyzed and mediates the covalent binding of the protein to the proteinase.

LOC100911545/A2m: Human Uniprot function (Human *A2M*): Is able to inhibit all four classes of proteinases by a unique 'trapping' mechanism. This protein has a peptide stretch, called the 'bait region' which contains specific cleavage sites for different proteinases. When a proteinase cleaves the bait region, a conformational change is induced in the protein which traps the proteinase. The entrapped enzyme remains active against low molecular weight substrates (activity against high molecular weight substrates is greatly reduced). Following cleavage in the bait region, a thioester bond is hydrolyzed and mediates the covalent binding of the protein to the proteinase.

Zfp354a: Rat Uniprot function (Human *ZNF354A*): It may play a role in renal development and may also be involved in the repair of the kidney after ischemia-reperfusion or folic acid administration.

Akr7a3: Human Uniprot function (Human *AKR7A3*): Can reduce the dialdehyde protein-binding form of aflatoxin B1 (AFB1) to the nonbinding AFB1 dialcohol. May be involved in protection of liver against the toxic and carcinogenic effects of AFB1, a potent hepatocarcinogen. {ECO0000269|PubMed18416522}.

Ephx1: Human Uniprot function (Human *EPHX1*): Biotransformation enzyme that catalyzes the hydrolysis of arene and aliphatic epoxides to less reactive and more water soluble dihydrodiols by the trans addition of water (by similarity). Plays a role in the metabolism of endogenous lipids such as epoxide-containing fatty acids (PubMed22798687). Metabolizes the abundant endocannabinoid 2-arachidonoylglycerol (2-AG) to free arachidonic acid (AA) and glycerol (PubMed24958911). {ECO0000250|UniProtKBP07687, ECO0000269|PubMed22798687, ECO0000269|PubMed24958911}.

Me1: Human Entrez Gene Summary (Human *ME1*): This gene encodes a cytosolic, NADP-dependent enzyme that generates NADPH for fatty acid biosynthesis. The activity of this enzyme, the reversible oxidative decarboxylation of malate, links the glycolytic and citric acid cycles. The regulation of expression for this gene is complex. Increased expression can result from elevated levels of thyroid hormones or by higher proportions of carbohydrates in the diet. [provided by RefSeq, Jul 2008]

Cyp4a1: Human Uniprot function (Human *CYP4A22*): Catalyzes the omega- and (omega-1)-hydroxylation of various fatty acids such as laurate and palmitate. Shows no activity toward arachidonic acid and prostaglandin A1. Lacks functional activity in the kidney and does not contribute to renal 20-hydroxyeicosatetraenoic acid (20-HETE) biosynthesis. {ECO0000269|PubMed10860550, ECO0000269|PubMed15611369}.

Anxa7: Human Uniprot function (Human *ANXA7*): Calcium/phospholipid-binding protein that promotes membrane fusion and is involved in exocytosis.

Slc17a3: Human Uniprot function (Human *SLC17A3*): [Isoform 2] voltage-driven, multispecific, organic anion transporter able to transport para-aminohippurate (PAH), estrone sulfate, estradiol-17-beta-glucuronide, bumetanide, and ochratoxin A. Isoform 2 functions as urate efflux transporter on the apical side of renal proximal tubule and is likely to act as an exit path for organic anionic drugs as well as urate in vivo. May be involved in actively transporting phosphate into cells via Na(+) cotransport.

Abcc3: Human Uniprot function (Human *ABCC3*): ATP-dependent transporter of the ATP-binding cassette (ABC) family that binds and hydrolyzes ATP to enable active transport of various substrates, including many drugs, toxicants, and endogenous compounds across cell membranes (PubMed11581266, PubMed15083066, PubMed10359813). Transports glucuronide conjugates such as bilirubin diglucuronide, estradiol-17-beta-o-glucuronide, and GSH conjugates such as leukotriene C4 (LTC4) (PubMed15083066, PubMed11581266). Transports also various bile salts (taurocholate, glycocholate, taurochenodeoxycholate-3-sulfate, taurolithocholate- 3-sulfate) (by similarity). Does not contribute substantially to bile salt physiology but provides an alternative route for the export of bile acids and glucuronides from cholestatic hepatocytes (by similarity). Can confer resistance

to various anticancer drugs, methotrexate, tenoposide, and etoposide by decreasing accumulation of these drugs in cells (PubMed11581266, PubMed10359813).

***Gsta2*:** Human Uniprot function (Human *GSTA2*): Conjugation of reduced glutathione to a wide number of exogenous and endogenous hydrophobic electrophiles.

***Gsta5*:** Rat Uniprot function (Human *GSTA5*): Conjugation of reduced glutathione to a wide number of exogenous and endogenous hydrophobic electrophiles. Has substantial activity toward aflatoxin B1-8,9-epoxide.

***Ehhadh*:** Human Uniprot function (Human *EHHADH*): Peroxisomal trifunctional enzyme possessing 2-enoyl-CoA hydratase, 3-hydroxyacyl-CoA dehydrogenase, and delta 3, delta 2-enoyl-CoA isomerase activities. Catalyzes two of the four reactions of the long straight chain fatty acids peroxisomal beta-oxidation pathway. Optimal isomerase for 2,5 double bonds into 3,5 form isomerization in a range of enoyl-CoA species (Probable). Also able to isomerize both 3-*cis* and 3-*trans* double bonds into the 2-*trans* form in a range of enoyl-CoA species (by similarity). With HSD17B4, catalyzes the hydration of *trans*-2-enoyl-CoA and the dehydrogenation of 3-hydroxyacyl-CoA, but with opposite chiral specificity (PubMed15060085). Regulates the amount of medium-chain dicarboxylic fatty acids which are essential regulators of all fatty acid oxidation pathways (by similarity). Also involved in the degradation of long-chain dicarboxylic acids through peroxisomal beta-oxidation (PubMed15060085). {ECO0000250|UniProtKBP07896, ECO0000250|UniProtKBQ9DBM2, ECO0000269|PubMed15060085, ECO0000305|PubMed15060085}.

***Pir*:** Human Uniprot function (Human *PIR*): Transcriptional coregulator of NF-kappa-B which facilitates binding of NF-kappa-B proteins to target kappa-B genes in a redox-state-dependent manner. May be required for efficient terminal myeloid maturation of hematopoietic cells. Has quercetin 2,3-dioxygenase activity (in vitro). {ECO0000269|PubMed17288615, ECO0000269|PubMed20010624, ECO0000269|PubMed20711196, ECO0000269|PubMed23716661}.

***Gclm*:** Human Entrez Gene Summary (Human *GCLM*): Glutamate-cysteine ligase, also known as gamma-glutamylcysteine synthetase, is the first rate-limiting enzyme of glutathione synthesis. The enzyme consists of two subunits, a heavy catalytic subunit and a light regulatory subunit. Gamma-glutamylcysteine synthetase deficiency has been implicated in some forms of hemolytic anemia. Alternative splicing results in multiple transcript variants encoding different isoforms. [provided by RefSeq, Apr 2015]

***Dao*:** Human Uniprot function (Human *DAO*): Regulates the level of the neuromodulator D-serine in the brain. Has high activity toward D-DOPA and contributes to dopamine synthesis. Could act as a detoxifying agent which removes D-amino acids accumulated during aging. Acts on a variety of D-amino acids with a preference for those having small hydrophobic side chains followed by those bearing polar, aromatic, and basic groups. Does not act on acidic amino acids. {ECO0000269|PubMed17303072}.

Table 12. Top 10 Kidney Genes Ranked by Potency of Perturbation, Sorted by Benchmark Dose Median[a]

Gene Symbol	Entrez Gene IDs	Probe IDs	BMD_{1Std} (BMD_{L1std}–BMD_{U1std}) in mg/kg	Maximum Fold Change	Direction of Expression Change
Male					
Ugt2b7	286989	UGT2B7_33032	4.139 (1.398–16.569)	3.6	UP
Ephx1	25315	EPHX1_8567	12.509 (3.282–61.397)	2.1	UP
Adgre1	316137	EMR1_8558	119.065 (89.170–178.281)	3.1	UP
Map2	25595	MAP2_32650	145.437 (104.718–237.081)	2.1	UP
Slc6a1	79212	SLC6A1_32594	145.445 (104.722–237.101)	2.0	UP
Naaa	497009	NAAA_32484	151.002 (107.821–250.969)	2.2	UP
Il1b	24494	IL1B_8892	153.991 (109.464–258.668)	2.9	UP
Cyp24a1	25279	CYP24A1_32574	189.111 (127.579–364.247)	2.2	UP
Top2a	360243	TOP2A_10059	203.468 (108.442–572.253)	2.1	DOWN
Nsg1	25247	NSG1_32675	216.472 (166.237–342.576)	3.4	UP
Female					
Mrc1	291327	MRC1_33067	<0.023[b] (NR)	2.1	DOWN
Ckap2	306575	CKAP2_8324	2.608 (0.997–6.811)	2.3	UP
Ugt2b37	29623	UGT2B15_33121	32.501 (7.520–103.327)	3.3	UP
Slc51a	303879	SLC51A_33157	37.134 (11.007–108.745)	2.2	UP

In Vivo Repeat Dose Biological Potency Study of 1,1,2,2-Tetrahydroperfluoro-1-dodecanol in Sprague Dawley Rats

Gene Symbol	Entrez Gene IDs	Probe IDs	BMD$_{1Std}$ (BMD$_{L1std}$–BMD$_{U1std}$) in mg/kg	Maximum Fold Change	Direction of Expression Change
Ugt2b7	286989	UGT2B7_33032	54.314 (15.595–186.641)	4.8	UP
Bbox1	64564	BBOX1_8133	61.319 (39.473–135.622)	2.0	UP
Adgre1	316137	EMR1_8558	61.524 (39.671–132.174)	2.4	UP
Clec4a	474143	CLEC4A_32636	82.466 (47.872–265.955)	2.2	UP
Cyp26b1	312495	CYP26B1_8418	238.250 (181.323–370.243)	2.8	UP
Lilrb4	292594	LILRB4_9000	350.991 (212.248–1011.690)	2.3	UP

BMD$_{1Std}$ = benchmark dose corresponding to a benchmark response set to one standard deviation from the mean; BMD$_{L1Std}$ = benchmark dose lower confidence limit corresponding to a benchmark response set to one standard deviation from the mean; BMD$_{U1Std}$ = benchmark dose upper confidence limit corresponding to a benchmark response set to one standard deviation from the mean; NR = the BMD$_{L1Std}$–BMD$_{U1Std}$ range is not reportable because the BMD$_{1Std}$ median is below the lower limit of extrapolation (<1/3 of the lowest nonzero dose tested).

[a]Descriptions of orthologous human genes are shown due to the increased detail available in public resources such as UniprotKB[32] and Entrez Gene.[33] Gene definitions adapted from Human UniprotKB were used as the primary resource due to the greater breadth of annotation and depth of functional detail provided. Gene definitions adapted from Rat UniprotKB were used as the secondary resource if the primary source did not provide a detailed description of function. Human Entrez Gene was used as the third resource. Rat Entrez Gene was used as the fourth resource.

[b]<0.023 = a best-fit model was identified and a BMD$_{1Std}$ was estimated that was <1/3 of the lowest nonzero dose tested.

Gene definition version: https://doi.org/10.22427/NTP-DATA-002-00600-0002-000-0.

Ugt2b7: Human Uniprot function (Human *UGT2B7*): UDP-glucuronosyltransferase (UGT) that catalyzes phase II biotransformation reactions in which lipophilic substrates are conjugated with glucuronic acid to increase the metabolite's water solubility, thereby facilitating excretion into either the urine or bile (PubMed10702251, PubMed15472229, PubMed15470161, PubMed18674515, PubMed18719240, PubMed19022937, PubMed23288867, PubMed23756265, PubMed26220143, PubMed17442341). Essential for the elimination and detoxification of drugs, xenobiotics, and endogenous compounds (PubMed15470161, PubMed18674515, PubMed23756265). Catalyzes the glucuronidation of endogenous steroid hormones such as androgens (epitestosterone, androsterone) and estrogens (estradiol, epiestradiol, estriol, catechol estrogens) (PubMed2159463, PubMed15472229, PubMed18719240, PubMed19022937, PubMed23288867, PubMed26220143, PubMed17442341). Also regulates the levels of retinoic acid, a major metabolite of vitamin A involved in apoptosis, cellular growth and differentiation, and embryonic development (PubMed10702251). Contributes to bile acid (BA) detoxification by catalyzing the glucuronidation of BA substrates, which are natural detergents for dietary lipids absorption (PubMed23756265). Involved in the glucuronidation of the AGTR1 angiotensin receptor antagonist losartan, caderastan, and zolarsatan, drugs that can inhibit the effect of angiotensin II (PubMed18674515). Also metabolizes mycophenolate, an immunosuppressive agent (PubMed15470161). {ECO0000269|PubMed10702251, ECO0000269|PubMed15470161, ECO0000269|PubMed15472229, ECO0000269|PubMed17442341, ECO0000269|PubMed18674515, ECO0000269|PubMed18719240, ECO0000269|PubMed19022937, ECO0000269|PubMed2159463, ECO0000269|PubMed23288867, ECO0000269|PubMed23756265, ECO0000269|PubMed26220143}.

Ephx1: Human Uniprot function (Human *EPHX1*): Biotransformation enzyme that catalyzes the hydrolysis of arene and aliphatic epoxides to less reactive and more water soluble dihydrodiols by the trans addition of water (by similarity). Plays a role in the metabolism of endogenous lipids such as epoxide-containing fatty acids (PubMed22798687). Metabolizes the abundant endocannabinoid 2-arachidonoylglycerol (2-AG) to free arachidonic acid (AA) and glycerol (PubMed24958911). {ECO0000250|UniProtKBP07687, ECO0000269|PubMed22798687, ECO0000269|PubMed24958911}.

Adgre1: Human Uniprot function (Human *ADGRE1*): Orphan receptor involved in cell adhesion and probably in cell-cell interactions specifically involving cells of the immune system. May play a role in regulatory T-cells (Treg) development. {ECO0000250|UniProtKBQ61549}.

Map2: Human Uniprot function (Human *MAP2*): The exact function of MAP2 is unknown but MAPs may stabilize the microtubules against depolymerization. They also seem to have a stiffening effect on microtubules.

Slc6a1: Human Uniprot function (Human *SLC6A1*): Terminates the action of GABA by its high affinity sodium-dependent reuptake into presynaptic terminals.

Naaa: Human Uniprot function (Human *NAAA*): Degrades bioactive fatty acid amides to their corresponding acids with the following preference: N-palmitoylethanolamine > N-myristoylethanolamine > N-lauroylethanolamine = N-stearoylethanolamine > N-arachidonoylethanolamine > N-oleoylethanolamine (PubMed15655246, PubMed17980170, PubMed18793752, PubMed30301806, PubMed22825852). Also exhibits weak hydrolytic activity against the ceramides N-lauroylsphingosine and N-palmitoylsphingosine (PubMed15655246). {ECO0000269|PubMed15655246, ECO0000269|PubMed17980170, ECO0000269|PubMed18793752, ECO0000269|PubMed22825852, ECO0000269|PubMed30301806}.

Il1b: Human Uniprot function (Human *IL1B*): Potent proinflammatory cytokine. Initially discovered as the major endogenous pyrogen, induces prostaglandin synthesis, neutrophil influx and activation, T cell activation and cytokine production, B-cell

activation and antibody production, and fibroblast proliferation and collagen production. Promotes Th17 differentiation of T-cells. Synergizes with IL12/interleukin-12 to induce IFNG synthesis from T-helper 1 (Th1) cells (PubMed10653850). Plays a role in angiogenesis by inducing VEGF production synergistically with TNF and IL6 (PubMed12794819). {ECO0000269|PubMed10653850, ECO0000269|PubMed12794819, ECO0000269|PubMed3920526}.

Cyp24a1: Human Uniprot function (Human *CYP24A1*): A cytochrome P450 monooxygenase with a key role in vitamin D catabolism and calcium homeostasis. Via C24- and C23-oxidation pathways, catalyzes the inactivation of both the vitamin D precursor calcidiol (25-hydroxyvitamin D(3)) and the active hormone calcitriol (1-alpha,25-dihydroxyvitamin D(3)) (PubMed24893882, PubMed15574355, PubMed8679605, PubMed11012668, PubMed16617161). With initial hydroxylation at C-24 (via C24-oxidation pathway), performs a sequential 6-step oxidation of calcitriol leading to the formation of the biliary metabolite calcitroic acid (PubMed24893882, PubMed15574355). With initial hydroxylation at C-23 (via C23-oxidation pathway), catalyzes sequential oxidation of calcidiol leading to the formation of 25(OH)D3-26,23-lactone as end product (PubMed11012668, PubMed8679605). Preferentially hydroxylates at C-25 other vitamin D active metabolites, such as CYP11A1-derived secosteroids 20S-hydroxycholecalciferol and 20S,23-dihydroxycholecalciferol (PubMed25727742). Mechanistically, uses molecular oxygen inserting one oxygen atom into a substrate and reducing the second into a water molecule with two electrons provided by NADPH via FDXR/adrenodoxin reductase and FDX1/adrenodoxin (PubMed8679605). {ECO0000269|PubMed11012668, ECO0000269|PubMed15574355, ECO0000269|PubMed16617161, ECO0000269|PubMed24893882, ECO0000269|PubMed25727742, ECO0000269|PubMed8679605}.

Top2a: Human Uniprot function (Human *TOP2A*): Key decatenating enzyme that alters DNA topology by binding to two double-stranded DNA molecules, generating a double-stranded break in one of the strands, passing the intact strand through the broken strand, and religating the broken strand (PubMed17567603, PubMed18790802, PubMed22013166, PubMed22323612). May play a role in regulating the period length of ARNTL/BMAL1 transcriptional oscillation (by similarity). {ECO0000250|UniProtKBQ01320, ECO0000269|PubMed17567603, ECO0000269|PubMed18790802, ECO0000269|PubMed22013166, ECO0000269|PubMed22323612}.

Nsg1: Human Uniprot function (Human *NSG1*): Plays a role in the recycling mechanism in neurons of multiple receptors, including AMPAR, APP, and L1CAM, and acts at the level of early endosomes to promote sorting of receptors toward a recycling pathway. Regulates sorting and recycling of GRIA2 through interaction with GRIP1 and then contributes to the regulation of synaptic transmission and plasticity by affecting the recycling and targeting of AMPA receptors to the synapse (by similarity). Is required for faithful sorting of L1CAM to axons by facilitating trafficking from somatodendritic early endosome or the recycling endosome (by similarity). On the other hand, induces apoptosis via the activation of CASP3 in response to DNA damage (PubMed20599942, PubMed20878061). {ECO0000250|UniProtKBP02683, ECO0000250|UniProtKBQ62092, ECO0000269|PubMed20599942, ECO0000269|PubMed20878061}.

Mrc1: Human Uniprot function (Human *MRC1*): Mediates the endocytosis of glycoproteins by macrophages. Binds both sulfated and nonsulfated polysaccharide chains. FUNCTION (Microbial infection) Acts as phagocytic receptor for bacteria, fungi, and other pathogens. FUNCTION (Microbial infection) Acts as a receptor for Dengue virus envelope protein E. {ECO0000269|PubMed18266465}. FUNCTION (Microbial infection) Interacts with Hepatitis B virus envelope protein. {ECO0000269|PubMed19683778}.

Ckap2: Human Uniprot function (Human *CKAP2*): Possesses microtubule stabilizing properties. Involved in regulating aneuploidy, cell cycling, and cell death in a p53/TP53-dependent manner (by similarity). {ECO0000250}.

Ugt2b37: Human Uniprot function (Human *UGT2B10*): UDPGT is of major importance in the conjugation and subsequent elimination of potentially toxic xenobiotics and endogenous compounds.

Slc51a: Human Uniprot function (Human *SLC51A*): Essential component of the Ost-alpha/Ost-beta complex, a heterodimer that acts as the intestinal basolateral transporter responsible for bile acid export from enterocytes into portal blood. Efficiently transports the major species of bile acids. {ECO0000269|PubMed16317684}.

Bbox1: Human Uniprot function (Human *BBOX1*): Catalyzes the formation of L-carnitine from gamma-butyrobetaine.

Clec4a: Human Uniprot function (Human *CLEC4A*): C-type lectin receptor that binds carbohydrates mannose and fucose but also weakly interacts with N-acetylglucosamine (GlcNAc) in a Ca2+-dependent manner (PubMed27015765). Involved in regulating immune reactivity (PubMed18258799, PubMed10438934). Once triggered by an antigen, it is internalized by clathrin-dependent endocytosis and delivers its antigenic cargo into the antigen presentation pathway resulting in cross-priming of CD8+ T-cells. This cross-presentation and cross-priming are enhanced by TLR7 and TLR8 agonists with increased expansion of the CD8+ T-cells, high production of IFNG and TNF with reduced levels of IL4, IL5, and IL13 (PubMed18258799, PubMed20530286). In plasmacytoid dendritic cells, inhibits TLR9-mediated IFNA and TNF production (PubMed18258799). May be involved via its ITIM motif (immunoreceptor tyrosine-based inhibitory motifs) in the inhibition of B-cell-receptor-mediated calcium mobilization and protein tyrosine phosphorylation (PubMed10438934). {ECO0000269|PubMed10438934, ECO0000269|PubMed18258799, ECO0000269|PubMed20530286, ECO0000269|PubMed27015765} FUNCTION (Microbial infection) Involved in the interaction between HIV-1 virus and dendritic cells. Enhances HIV-1 binding/entry and virus infection. Requires ITIM motif-associated signal transduction pathway involving phosphatases PTPN6 and PTPN11, SYK, Src kinases and MAP kinases.{ECO0000269|PubMed21536857}.

Cyp26b1: Human Uniprot function (Human *CYP26B1*): Involved in the metabolism of retinoic acid (RA), rendering this classical morphogen inactive through oxidation (PubMed10823918, PubMed22020119). Involved in the specific inactivation of all-*trans*-retinoic acid (all-*trans*-RA) with a preference for the following substrates all-*trans*-RA > 9-*cis*-RA > 13-*cis*-RA (PubMed10823918, PubMed22020119). Generates several hydroxylated forms of RA, including 4-OH-RA, 4-oxo-RA, and 18-OH-RA (PubMed10823918). Catalyzes the hydroxylation of carbon hydrogen bonds of at RA primarily at C-4

(PubMed10823918, PubMed22020119). Essential for postnatal survival (by similarity). Plays a central role in germ cell development acts by degrading RA in the developing testis, preventing STRA8 expression, thereby leading to delay of meiosis (by similarity). Required for the maintenance of the undifferentiated state of male germ cells during embryonic development in Sertoli cells, inducing arrest in G0 phase of the cell cycle and preventing meiotic entry (by similarity). Plays a role in skeletal development, both at the level of patterning and in the ossification of bone and the establishment of some synovial joints (PubMed22019272). {ECO0000250|UniProtKBQ811W2, ECO0000269|PubMed10823918, ECO0000269|PubMed22019272, ECO0000269|PubMed22020119}. FUNCTION Has also a significant activity in oxidation of tazarotenic acid and may therefore metabolize that xenobiotic in vivo. {ECO0000269|PubMed26937021}.

Lilrb4: Human Uniprot function (Human *LILRB4*): Receptor for class I MHC antigens. Recognizes a broad spectrum of HLA-A, HLA-B, HLA-C, and HLA-G alleles. Involved in the downregulation of the immune response and the development of tolerance, e.g., toward transplants. Interferes with TNFRSF5-signaling and NF-kappa-B upregulation. Inhibits receptor-mediated phosphorylation of cellular proteins and mobilization of intracellular calcium ions. {ECO0000269|PubMed11875462, ECO0000269|PubMed9151699}.

Summary

1,1,2,2-Tetrahydroperfluoro-1-dodecanol (10:2 fluorotelomer alcohol) is a member of the per-
and polyfluoroalkyl class of compounds to which humans are widely exposed. A review of the
literature did not identify toxicological data for estimating the potential adverse health effects of
1,1,2,2-tetrahydroperfluoro-1-dodecanol. This study used a transcriptomic approach and standard
toxicological endpoints to estimate the in vivo biological potency of 1,1,2,2-tetrahydroperfluoro-
1-dodecanol.

A subset of standard toxicological endpoints (cholesterol concentration in male rats; neutrophil
count in female rats) exhibited benchmark dose (BMD) values much lower than would be
expected given the endpoint-specific no-observed-effect level and lowest-observed-effect level
values. Expert review of the data suggests that the BMD estimates do not accurately reflect the
true potency of the effect of these endpoints and were likely an anomalous product of the BMD
modeling approach.

Taking this into account, the most sensitive apical endpoint in male rats was an increase in
relative liver weight with an estimated BMD and benchmark dose lower confidence limit
(BMD$_L$) of 8.087 (4.336) mg/kg. An increase in absolute liver weight and a decrease in
reticulocyte count were the next most sensitive apical endpoint changes observed in male rats
with BMDs (BMD$_L$s) of 21.893 (10.337) and 54.227 (30.205) mg/kg, respectively. In female
rats, the most sensitive apical endpoint was an increase in relative liver weight with a BMD
(BMD$_L$) of 5.372 (2.294) mg/kg. The next most sensitive apical endpoints observed were an
increase in alkaline phosphatase activity and an increase in absolute liver weight with BMDs
(BMD$_L$s) of 6.461 (6.003) and 8.801 (3.465) mg/kg, respectively.

Gene set-level transcriptional changes in the liver following 1,1,2,2-tetrahydroperfluoro-1-
dodecanol exposure were estimated to occur at a BMD (BMD$_L$) as low as 5.235 (2.666) mg/kg in
male rats, corresponding to nucleotide biosynthetic process (GO:0009165), and as low as 5.355
(3.108) mg/kg in female rats, corresponding to internal protein amino acid acetylation
(GO:0006475). The most sensitive liver gene for which a reliable BMD could be determined was
Pck1, with a BMD (BMD$_L$) of 1.149 (0.548) mg/kg, in male rats, and *Abcc3*, with a BMD
(BMD$_L$) of 5.019 (2.945) mg/kg, in female rats.

Gene set-level transcriptional changes in the kidney were estimated to occur at a BMD (BMD$_L$)
as low as 144.319 (57.694) mg/kg in male rats, corresponding to regulation of myeloid leukocyte
mediated immunity (GO:0002886), and as low as 57.313 (37.882) mg/kg in female rats,
corresponding to innate immune response (GO:0045087). The most sensitive kidney gene in
male rats for which a reliable BMD could be determined was *Ugt2b7* with a BMD (BMD$_L$) of
4.139 (1.398) mg/kg. In female rats, one kidney gene exhibited changes in expression at dose
levels below which a reliable estimate of potency could be achieved (<0.023 mg/kg). The most
sensitive gene in female rats for which a reliable BMD could be determined was *Ckap2* with a
BMD (BMD$_L$) of 2.608 (0.997) mg/kg.

Under the conditions of this short-duration transcriptomic study in Sprague Dawley
(Hsd:Sprague Dawley® SD®) rats, the most sensitive point of departure with a reliable estimate
in male rats was a transcriptional change in a gene, *Pck1*, with a BMD (BMD$_L$) of 1.149
(0.548) mg/kg. Gene set transcriptional changes and apical endpoints provided potency estimates

slightly higher than *Pck1*. In female rats, the most sensitive point of departure with a reliable estimate was a transcriptional change in a gene, *Ckap2*, with a BMD (BMD$_L$) of 2.608 (0.997) mg/kg. Gene set transcriptional changes and apical endpoints provided potency estimates slightly higher than *Ckap2*.

References

1. U.S. Environmental Protection Agency (USEPA). CompTox Chemicals Dashboard: 10:2 Fluorotelomer alcohol 865-86-1 | DTXSID2029905. 2021. https://comptox.epa.gov/dashboard/chemical/details/DTXSID2029905

2. National Center for Biotechnology Information (NCBI). PubChem Compound Summary for CID 70083, 2-(Perfluorodecyl)ethanol. 2021. https://pubchem.ncbi.nlm.nih.gov/compound/70083

3. European Chemicals Agency (ECHA). Substance Infocard: 3,3,4,4,5,5,6,6,7,7,8,8,9,9,10,10,11,11,12,12,12-Henicosafluorododecanol. 2021. https://echa.europa.eu/substance-information/-/substanceinfo/100.011.590

4. Fenton SE, Ducatman A, Boobis A, DeWitt JC, Lau C, Ng C, Smith JS, Roberts SM. Per- and polyfluoroalkyl substance toxicity and human health review: Current state of knowledge and strategies for informing future research. Environ Toxicol Chem. 2021; 40(3):606-630. https://doi.org/10.1002/etc.4890

5. Domingo JL, Nadal M. Human exposure to per- and polyfluoroalkyl substances (PFAS) through drinking water: A review of the recent scientific literature. Environ Res. 2019; 177:108648. https://doi.org/10.1016/j.envres.2019.108648

6. Domingo JL, Nadal M. Per- and polyfluoroalkyl substances (PFASs) in food and human dietary intake: A review of the recent scientific literature. J Agric Food Chem. 2017; 65(3):533-543. https://doi.org/10.1021/acs.jafc.6b04683

7. U.S. Environmental Protection Agency (USEPA). CompTox Chemicals Dashboard: 10:2 Fluorotelomer alcohol 865-86-1 | DTXSID2029905: Exposure Predictions. 2021. https://comptox.epa.gov/dashboard/chemical/exposure-predictions/DTXSID2029905

8. U.S. Environmental Protection Agency (USEPA). CompTox Chemicals Dashboard: 10:2 Fluorotelomer alcohol 865-86-1 | DTXSID2029905: Executive Summary. 2021. https://comptox.epa.gov/dashboard/chemical/executive-summary/DTXSID2029905

9. Gwinn WM, Auerbach SS, Parham F, Stout MD, Waidyanatha S, Mutlu E, Collins B, Paules RS, Merrick BA, Ferguson S et al. Evaluation of 5-day in vivo rat liver and kidney with high-throughput transcriptomics for estimating benchmark doses of apical outcomes. Toxicol Sci. 2020; 176(2):343-354. https://doi.org/10.1093/toxsci/kfaa081

10. Mansouri K, Karmaus AL, Fitzpatrick J, Patlewicz G, Pradeep P, Alberga D, Alepee N, Allen TEH, Allen D, Alves VM et al. CATMoS: Collaborative Acute Toxicity Modeling Suite. Environ Health Perspect. 2021; 129(4):47013. https://doi.org/10.1289/EHP8495

11. Mansouri K, Grulke CM, Judson RS, Williams AJ. OPERA models for predicting physicochemical properties and environmental fate endpoints. J Cheminform. 2018; 10(1):10. https://doi.org/10.1186/s13321-018-0263-1

12. Patlewitz G. Personal Communication: EPA Point of Departure Estimate. 2021.

13. Waidyanatha S, Fletcher BL, Fernando RA, Cora MC, Silinski MAR. Development and validation of an ultraperformance liquid chromatography-tandem mass spectrometry method for quantitation of total 3,3',5-triiodo-L-thyronine and 3,3',5,5'-tetraiodo-L-thyronine in rodent serum. Anal Lett. 2021; 55(5):796-811. https://doi.org/10.1080/00032719.2021.1967969

14. Langmead B, Trapnell C, Pop M, Salzberg SL. Ultrafast and memory-efficient alignment of short DNA sequences to the human genome. Genome Biol. 2009; 10(3):R25. https://doi.org/10.1186/gb-2009-10-3-r25

15. Williams DA. A test for differences between treatment means when several dose levels are compared with a zero dose control. Biometrics. 1971; 27(1):103-117. http://dx.doi.org/10.2307/2528930

16. Williams DA. The comparison of several dose levels with a zero dose control. Biometrics. 1972; 28(2):519-531. http://dx.doi.org/10.2307/2556164

17. Dunnett CW. A multiple comparison procedure for comparing several treatments with a control. J Am Stat Assoc. 1955; 50(272):1096-1121. http://dx.doi.org/10.1080/01621459.1955.10501294

18. Shirley E. A non-parametric equivalent of Williams' test for contrasting increasing dose levels of a treatment. Biometrics. 1977; 33(2):386-389. http://dx.doi.org/10.2307/2529789

19. Dunn OJ. Multiple comparisons using rank sums. Technometrics. 1964; 6(3):241-252. http://dx.doi.org/10.1080/00401706.1964.10490181

20. Jonckheere AR. A distribution-free k-sample test against ordered alternatives. Biometrika. 1954; 41(1/2):133-145. http://dx.doi.org/10.2307/2333011

21. Dixon WJ, Massey FJ. Introduction to Statistical Analysis. New York,: McGraw-Hill; 1951.

22. U.S. Environmental Protection Agency (USEPA). Benchmark dose technical guidance. Washington, DC: U.S. Environmental Protection Agency, Risk Assessment Forum; 2012. https://www.epa.gov/sites/production/files/2015-01/documents/benchmark_dose_guidance.pdf

23. Wignall JA, Shapiro AJ, Wright FA, Woodruff TJ, Chiu WA, Guyton KZ, Rusyn I. Standardizing benchmark dose calculations to improve science-based decisions in human health assessments. Environ Health Perspect. 2014; 122(5):499-505. http://dx.doi.org/10.1289/ehp.1307539

24. National Toxicology Program (NTP). NTP research report on National Toxicology Program approach to genomic dose-response modeling. Research Triangle Park, NC: U.S. Department of Health and Human Services, National Institute of Environmental Health Sciences, National Toxicology Program; 2018. NTP Research Report No. 5.

25. Shi L, Jones WD, Jensen RV, Harris SC, Perkins RG, Goodsaid FM, Guo L, Croner LJ, Boysen C, Fang H et al. The balance of reproducibility, sensitivity, and specificity of lists of differentially expressed genes in microarray studies. BMC Bioinformatics. 2008; 9:S10. https://doi.org/10.1186/1471-2105-9-s9-s10

26. Auerbach SS, Ballin JD, Blake JC, Browning DB, Collins BJ, Cora MC, Fernando RA, Fostel JM, Liu YF, Luh J et al. NIEHS report on the in vivo repeat dose biological potency study of perfluorohexanesulfonamide (CASRN 41997-13-1) in Sprague Dawley (Hsd:Sprague Dawley® SD®) rats (gavage studies). Research Triangle Park, NC: U.S. Department of Health and Human Services, Public Health Service, National Institute of Environmental Health Sciences; 2023. NIEHS Report 10. https://doi.org/10.22427/NIEHS-10

27. Auerbach SS, Aillon KL, Ballin JD, Collins BJ, Cora MC, Duncan NS, Fostel JM, Liu YF, Luh J, Machesky NJ et al. NIEHS report on the in vivo repeat dose biological potency study of 6:1 fluorotelomer alcohol (CASRN 375-82-6) in Sprague Dawley (Hsd:Sprague Dawley® SD®) rats (gavage studies). Research Triangle Park, NC: U.S. Department of Health and Human Services, Public Health Service, National Institute of Environmental Health Sciences; 2023. NIEHS Report 07. https://doi.org/10.22427/NIEHS-07

28. Auerbach SS, Aillon KL, Ballin JD, Collins BJ, Cora MC, Duncan NS, Fostel JM, Kerns SP, Liu YF, Luh J et al. NIEHS report on the in vivo repeat dose biological potency study of 2,3-benzofluorene (CASRN 243-17-4) in Sprague Dawley (Hsd:Sprague Dawley® SD®) rats (gavage studies). Research Triangle Park, NC: U.S. Department of Health and Human Services, Public Health Service, National Institute of Environmental Health Sciences; 2023. NIEHS Report 09. https://doi.org/10.22427/NIEHS-09

29. National Toxicology Program (NTP). NIEHS 08: Chemical Effects in Biological Systems (CEBS) data repository. Research Triangle Park, NC: U.S. Department of Health and Human Services, National Institute of Environmental Health Sciences, National Toxicology Program; 2023. https://doi.org/10.22427/NIEHS-DATA-NIEHS-08

30. Geneontology. The gene ontology resource. 2021. http://geneontology.org/

31. Medical College of Wisconsin. Rat Genome Database. 2021. https://rgd.mcw.edu/

32. UniProt. UniProtKB results. 2021. https://www.uniprot.org/uniprot/

33. Entrez Gene. Gene. 2021. https://www.ncbi.nlm.nih.gov/gene/

34. Thomas RS, Allen BC, Nong A, Yang L, Bermudez E, Clewell HJ, III, Andersen ME. A method to integrate benchmark dose estimates with genomic data to assess the functional effects of chemical exposure. Toxicol Sci. 2007; 98(1):240-248. http://dx.doi.org/10.1093/toxsci/kfm092

Appendix A. Internal Dose Assessment

Table of Contents

A.1. Quantitation of 1,1,2,2-Tetrahydroperfluoro-1-dodecanol in Plasma

Quantification of 1,1,2,2-tetrahydroperfluoro-1-dodecanol (10:2 fluorotelomer alcohol) in plasma samples was completed by RTI International (Research Triangle Park, NC). A gas chromatography with mass spectrometry detection (GC/MS) method was developed to determine 1,1,2,2-tetrahydroperfluoro-1-dodecanol concentrations in rat plasma. A six-point matrix calibration curve, in the range of 10–1,000 ng/mL, was prepared by adding 10 µL of an appropriate spiking solution (1,1,2,2-tetrahydroperfluoro-1-dodecanol in ethyl acetate) and 20 µL of an internal standard solution (2-perfluorodecyl-[1,1-2H2]-[1,2-13e2]-ethanol in methanol) to 100 µL of control matrix (adult male Sprague Dawley rat plasma). Quality control (QC) samples were prepared similarly at a target concentration of 100 ng/mL in plasma. Blanks and study samples were prepared like calibration standards, except 10 µL of ethyl acetate was used in place of spiking solution. All samples were then extracted by adding 300 µL of ethyl acetate, vortex mixing, and centrifuging for 5 minutes. The organic layer of each sample was collected for analysis.

All samples were analyzed using an Agilent 7890A GC with an Agilent 5975C mass selective detector (Santa Clara, CA). A J&W DB-WAX column (30 m × 0.32 mm inner diameter) with a 0.50 µm film was used with a Helium carrier gas. A flow rate of 2.0 mL/min was run with a temperature program starting at 50°C for 2 minutes, a linear ramp at 15°C/min to 230°C, and held at 230°C for 2 minutes. Electron impact ionization was used with an ionization voltage of 70 eV and a source temperature of 230°C. Single ion monitoring was used at m/z 95 (1,1,2,2-tetrahydroperfluoro-1-dodecanol quantitation ion) and m/z 509 (internal standard).

A linear regression with $1/X^2$ weighting was used to relate peak area ratios of analyte to internal standard and analyte concentrations. Calibration curves were linear (r > 0.99). The lower limit of quantitation (LOQ) for 1,1,2,2-tetrahydroperfluoro-1-dodecanol in rat plasma was 10.0 ng/mL. For QC samples, the accuracy measured as percent relative error was within ±16.7% of the nominal concentration. The concentrations (ng/mL) of 1,1,2,2-tetrahydroperfluoro-1-dodecanol in study samples were calculated using peak area ratios and the regression equation. All values above LOQ were reported.

Appendix B. Animal Identifiers

Tables

In Vivo Repeat Dose Biological Potency Study of
1,1,2,2-Tetrahydroperfluoro-1-dodecanol in Sprague Dawley Rats

Table B-1. Animal Numbers and FASTQ Data File Names

Animal Number	Sex	Group	Dose (mg/kg)	Survived to Study Termination	Tissue	FASTQ File ID
211	Male	Vehicle control	0	Yes	Kidney	Plate10-211
211	Male	Vehicle control	0	Yes	Liver	Plate11-211
212	Male	Vehicle control	0	Yes	Kidney	Plate10-212
212	Male	Vehicle control	0	Yes	Liver	Plate11-212
213	Male	Vehicle control	0	Yes	Kidney	Plate10-213
213	Male	Vehicle control	0	Yes	Liver	Plate9-213
214	Male	Vehicle control	0	Yes	Kidney	Plate12-214[a]
214	Male	Vehicle control	0	Yes	Liver	Plate11-214
215	Male	Vehicle control	0	Yes	Kidney	Plate10-215
215	Male	Vehicle control	0	Yes	Liver	Plate9-215
216	Male	Vehicle control	0	Yes	Kidney	Plate10-216
216	Male	Vehicle control	0	Yes	Liver	Plate9-216
217	Male	Vehicle control	0	Yes	Kidney	Plate10-217
217	Male	Vehicle control	0	Yes	Liver	Plate11-217
218	Male	Vehicle control	0	Yes	Kidney	Plate10-218
218	Male	Vehicle control	0	Yes	Liver	Plate9-218
219	Male	Vehicle control	0	Yes	Kidney	Plate10-219
219	Male	Vehicle control	0	Yes	Liver	Plate9-219
220	Male	Vehicle control	0	Yes	Kidney	Plate10-220
220	Male	Vehicle control	0	Yes	Liver	Plate9-220
221	Female	Vehicle control	0	Yes	Kidney	Plate10-221
221	Female	Vehicle control	0	Yes	Liver	Plate9-221
222	Female	Vehicle control	0	Yes	Kidney	Plate10-222
222	Female	Vehicle control	0	Yes	Liver	Plate9-222
223	Female	Vehicle control	0	Yes	Kidney	Plate10-223
223	Female	Vehicle control	0	Yes	Liver	Plate9-223
224	Female	Vehicle control	0	Yes	Kidney	Plate10-224
224	Female	Vehicle control	0	Yes	Liver	Plate9-224
225	Female	Vehicle control	0	Yes	Kidney	Plate10-225
225	Female	Vehicle control	0	Yes	Liver	Plate9-225
226	Female	Vehicle control	0	Yes	Kidney	Plate10-226
226	Female	Vehicle control	0	Yes	Liver	Plate9-226
227	Female	Vehicle control	0	Yes	Kidney	Plate10-227
227	Female	Vehicle control	0	Yes	Liver	Plate9-227

In Vivo Repeat Dose Biological Potency Study of
1,1,2,2-Tetrahydroperfluoro-1-dodecanol in Sprague Dawley Rats

Animal Number	Sex	Group	Dose (mg/kg)	Survived to Study Termination	Tissue	FASTQ File ID
228	Female	Vehicle control	0	Yes	Kidney	Plate10-228
228	Female	Vehicle control	0	Yes	Liver	Plate9-228
229	Female	Vehicle control	0	Yes	Kidney	Plate10-229
229	Female	Vehicle control	0	Yes	Liver	Plate9-229
230	Female	Vehicle control	0	Yes	Kidney	Plate10-230
230	Female	Vehicle control	0	Yes	Liver	Plate9-230
231	Male	1,1,2,2-Tetrahydroperfluoro-1-dodecanol	0.07	Yes	Kidney	Plate10-231
231	Male	1,1,2,2-Tetrahydroperfluoro-1-dodecanol	0.07	Yes	Liver	Plate9-231
232	Male	1,1,2,2-Tetrahydroperfluoro-1-dodecanol	0.07	Yes	Kidney	Plate10-232
232	Male	1,1,2,2-Tetrahydroperfluoro-1-dodecanol	0.07	Yes	Liver	Plate9-232
233	Male	1,1,2,2-Tetrahydroperfluoro-1-dodecanol	0.07	Yes	Kidney	Plate10-233
233	Male	1,1,2,2-Tetrahydroperfluoro-1-dodecanol	0.07	Yes	Liver	Plate9-233
234	Male	1,1,2,2-Tetrahydroperfluoro-1-dodecanol	0.07	Yes	Kidney	Plate10-234
234	Male	1,1,2,2-Tetrahydroperfluoro-1-dodecanol	0.07	Yes	Liver	Plate9-234
235	Male	1,1,2,2-Tetrahydroperfluoro-1-dodecanol	0.07	Yes	Kidney	Plate10-235
235	Male	1,1,2,2-Tetrahydroperfluoro-1-dodecanol	0.07	Yes	Liver	Plate11-235
236	Female	1,1,2,2-Tetrahydroperfluoro-1-dodecanol	0.07	Yes	Kidney	Plate10-236
236	Female	1,1,2,2-Tetrahydroperfluoro-1-dodecanol	0.07	Yes	Liver	Plate9-236
237	Female	1,1,2,2-Tetrahydroperfluoro-1-dodecanol	0.07	Yes	Kidney	Plate12-237[a]
237	Female	1,1,2,2-Tetrahydroperfluoro-1-dodecanol	0.07	Yes	Liver	Plate9-237
238	Female	1,1,2,2-Tetrahydroperfluoro-1-dodecanol	0.07	Yes	Kidney	Plate12-238[a]
238	Female	1,1,2,2-Tetrahydroperfluoro-1-dodecanol	0.07	Yes	Liver	Plate11-238
239	Female	1,1,2,2-Tetrahydroperfluoro-1-dodecanol	0.07	Yes	Kidney	Plate10-239
239	Female	1,1,2,2-Tetrahydroperfluoro-1-dodecanol	0.07	Yes	Liver	Plate9-239
240	Female	1,1,2,2-Tetrahydroperfluoro-1-dodecanol	0.07	Yes	Kidney	Plate10-240
240	Female	1,1,2,2-Tetrahydroperfluoro-1-dodecanol	0.07	Yes	Liver	Plate9-240
241	Male	1,1,2,2-Tetrahydroperfluoro-1-dodecanol	0.2	Yes	Kidney	Plate10-241
241	Male	1,1,2,2-Tetrahydroperfluoro-1-dodecanol	0.2	Yes	Liver	Plate9-241
242	Male	1,1,2,2-Tetrahydroperfluoro-1-dodecanol	0.2	Yes	Kidney	Plate10-242
242	Male	1,1,2,2-Tetrahydroperfluoro-1-dodecanol	0.2	Yes	Liver	Plate11-242
243	Male	1,1,2,2-Tetrahydroperfluoro-1-dodecanol	0.2	Yes	Kidney	Plate10-243
243	Male	1,1,2,2-Tetrahydroperfluoro-1-dodecanol	0.2	Yes	Liver	Plate9-243
244	Male	1,1,2,2-Tetrahydroperfluoro-1-dodecanol	0.2	Yes	Kidney	Plate10-244
244	Male	1,1,2,2-Tetrahydroperfluoro-1-dodecanol	0.2	Yes	Liver	Plate9-244
245	Male	1,1,2,2-Tetrahydroperfluoro-1-dodecanol	0.2	Yes	Kidney	Plate10-245

In Vivo Repeat Dose Biological Potency Study of
1,1,2,2-Tetrahydroperfluoro-1-dodecanol in Sprague Dawley Rats

Animal Number	Sex	Group	Dose (mg/kg)	Survived to Study Termination	Tissue	FASTQ File ID
245	Male	1,1,2,2-Tetrahydroperfluoro-1-dodecanol	0.2	Yes	Liver	Plate9-245
246	Female	1,1,2,2-Tetrahydroperfluoro-1-dodecanol	0.2	Yes	Kidney	Plate10-246
246	Female	1,1,2,2-Tetrahydroperfluoro-1-dodecanol	0.2	Yes	Liver	Plate9-246[b]
247	Female	1,1,2,2-Tetrahydroperfluoro-1-dodecanol	0.2	Yes	Kidney	Plate10-247
247	Female	1,1,2,2-Tetrahydroperfluoro-1-dodecanol	0.2	Yes	Liver	Plate9-247
248	Female	1,1,2,2-Tetrahydroperfluoro-1-dodecanol	0.2	Yes	Kidney	Plate10-248
248	Female	1,1,2,2-Tetrahydroperfluoro-1-dodecanol	0.2	Yes	Liver	Plate9-248
249	Female	1,1,2,2-Tetrahydroperfluoro-1-dodecanol	0.2	Yes	Kidney	Plate10-249
249	Female	1,1,2,2-Tetrahydroperfluoro-1-dodecanol	0.2	Yes	Liver	Plate9-249
250	Female	1,1,2,2-Tetrahydroperfluoro-1-dodecanol	0.2	Yes	Kidney	Plate10-250
250	Female	1,1,2,2-Tetrahydroperfluoro-1-dodecanol	0.2	Yes	Liver	Plate9-250
251	Male	1,1,2,2-Tetrahydroperfluoro-1-dodecanol	0.7	Yes	Kidney	Plate10-251
251	Male	1,1,2,2-Tetrahydroperfluoro-1-dodecanol	0.7	Yes	Liver	Plate9-251
252	Male	1,1,2,2-Tetrahydroperfluoro-1-dodecanol	0.7	Yes	Kidney	Plate10-252
252	Male	1,1,2,2-Tetrahydroperfluoro-1-dodecanol	0.7	Yes	Liver	Plate9-252
253	Male	1,1,2,2-Tetrahydroperfluoro-1-dodecanol	0.7	Yes	Kidney	Plate10-253
253	Male	1,1,2,2-Tetrahydroperfluoro-1-dodecanol	0.7	Yes	Liver	Plate11-253
254	Male	1,1,2,2-Tetrahydroperfluoro-1-dodecanol	0.7	Yes	Kidney	Plate10-254
254	Male	1,1,2,2-Tetrahydroperfluoro-1-dodecanol	0.7	Yes	Liver	Plate9-254
255	Male	1,1,2,2-Tetrahydroperfluoro-1-dodecanol	0.7	Yes	Kidney	Plate12-255[a]
255	Male	1,1,2,2-Tetrahydroperfluoro-1-dodecanol	0.7	Yes	Liver	Plate9-255
256	Female	1,1,2,2-Tetrahydroperfluoro-1-dodecanol	0.7	Yes	Kidney	Plate10-256
256	Female	1,1,2,2-Tetrahydroperfluoro-1-dodecanol	0.7	Yes	Liver	Plate9-256
257	Female	1,1,2,2-Tetrahydroperfluoro-1-dodecanol	0.7	Yes	Kidney	Plate12-257[a]
257	Female	1,1,2,2-Tetrahydroperfluoro-1-dodecanol	0.7	Yes	Liver	Plate9-257
258	Female	1,1,2,2-Tetrahydroperfluoro-1-dodecanol	0.7	Yes	Kidney	Plate10-258
258	Female	1,1,2,2-Tetrahydroperfluoro-1-dodecanol	0.7	Yes	Liver	Plate9-258
259	Female	1,1,2,2-Tetrahydroperfluoro-1-dodecanol	0.7	Yes	Kidney	Plate10-259
259	Female	1,1,2,2-Tetrahydroperfluoro-1-dodecanol	0.7	Yes	Liver	Plate9-259
260	Female	1,1,2,2-Tetrahydroperfluoro-1-dodecanol	0.7	Yes	Kidney	Plate10-260
260	Female	1,1,2,2-Tetrahydroperfluoro-1-dodecanol	0.7	Yes	Liver	Plate9-260
261	Male	1,1,2,2-Tetrahydroperfluoro-1-dodecanol	2.0	Yes	Kidney	Plate10-261
261	Male	1,1,2,2-Tetrahydroperfluoro-1-dodecanol	2.0	Yes	Liver	Plate11-261
262	Male	1,1,2,2-Tetrahydroperfluoro-1-dodecanol	2.0	Yes	Kidney	Plate10-262
262	Male	1,1,2,2-Tetrahydroperfluoro-1-dodecanol	2.0	Yes	Liver	Plate9-262

In Vivo Repeat Dose Biological Potency Study of
1,1,2,2-Tetrahydroperfluoro-1-dodecanol in Sprague Dawley Rats

Animal Number	Sex	Group	Dose (mg/kg)	Survived to Study Termination	Tissue	FASTQ File ID
263	Male	1,1,2,2-Tetrahydroperfluoro-1-dodecanol	2.0	Yes	Kidney	Plate10-263
263	Male	1,1,2,2-Tetrahydroperfluoro-1-dodecanol	2.0	Yes	Liver	Plate9-263
264	Male	1,1,2,2-Tetrahydroperfluoro-1-dodecanol	2.0	Yes	Kidney	Plate12-264[a]
264	Male	1,1,2,2-Tetrahydroperfluoro-1-dodecanol	2.0	Yes	Liver	Plate9-264
265	Male	1,1,2,2-Tetrahydroperfluoro-1-dodecanol	2.0	Yes	Kidney	Plate10-265
265	Male	1,1,2,2-Tetrahydroperfluoro-1-dodecanol	2.0	Yes	Liver	Plate9-265
266	Female	1,1,2,2-Tetrahydroperfluoro-1-dodecanol	2.0	Yes	Kidney	Plate10-266
266	Female	1,1,2,2-Tetrahydroperfluoro-1-dodecanol	2.0	Yes	Liver	Plate9-266
267	Female	1,1,2,2-Tetrahydroperfluoro-1-dodecanol	2.0	Yes	Kidney	Plate10-267
267	Female	1,1,2,2-Tetrahydroperfluoro-1-dodecanol	2.0	Yes	Liver	Plate9-267
268	Female	1,1,2,2-Tetrahydroperfluoro-1-dodecanol	2.0	Yes	Kidney	Plate10-268
268	Female	1,1,2,2-Tetrahydroperfluoro-1-dodecanol	2.0	Yes	Liver	Plate11-268
269	Female	1,1,2,2-Tetrahydroperfluoro-1-dodecanol	2.0	Yes	Kidney	Plate10-269
269	Female	1,1,2,2-Tetrahydroperfluoro-1-dodecanol	2.0	Yes	Liver	Plate9-269
270	Female	1,1,2,2-Tetrahydroperfluoro-1-dodecanol	2.0	Yes	Kidney	Plate10-270
270	Female	1,1,2,2-Tetrahydroperfluoro-1-dodecanol	2.0	Yes	Liver	Plate9-270
271	Male	1,1,2,2-Tetrahydroperfluoro-1-dodecanol	6.0	Yes	Kidney	Plate10-271
271	Male	1,1,2,2-Tetrahydroperfluoro-1-dodecanol	6.0	Yes	Liver	Plate9-271
272	Male	1,1,2,2-Tetrahydroperfluoro-1-dodecanol	6.0	Yes	Kidney	Plate10-272
272	Male	1,1,2,2-Tetrahydroperfluoro-1-dodecanol	6.0	Yes	Liver	Plate9-272
273	Male	1,1,2,2-Tetrahydroperfluoro-1-dodecanol	6.0	Yes	Kidney	Plate12-273[a]
273	Male	1,1,2,2-Tetrahydroperfluoro-1-dodecanol	6.0	Yes	Liver	Plate9-273
274	Male	1,1,2,2-Tetrahydroperfluoro-1-dodecanol	6.0	Yes	Kidney	Plate10-274
274	Male	1,1,2,2-Tetrahydroperfluoro-1-dodecanol	6.0	Yes	Liver	Plate11-274
275	Male	1,1,2,2-Tetrahydroperfluoro-1-dodecanol	6.0	Yes	Kidney	Plate10-275
275	Male	1,1,2,2-Tetrahydroperfluoro-1-dodecanol	6.0	Yes	Liver	Plate9-275
276	Female	1,1,2,2-Tetrahydroperfluoro-1-dodecanol	6.0	Yes	Kidney	Plate10-276
276	Female	1,1,2,2-Tetrahydroperfluoro-1-dodecanol	6.0	Yes	Liver	Plate9-276
277	Female	1,1,2,2-Tetrahydroperfluoro-1-dodecanol	6.0	Yes	Kidney	Plate10-277
277	Female	1,1,2,2-Tetrahydroperfluoro-1-dodecanol	6.0	Yes	Liver	Plate9-277
278	Female	1,1,2,2-Tetrahydroperfluoro-1-dodecanol	6.0	Yes	Kidney	Plate10-278
278	Female	1,1,2,2-Tetrahydroperfluoro-1-dodecanol	6.0	Yes	Liver	Plate9-278
279	Female	1,1,2,2-Tetrahydroperfluoro-1-dodecanol	6.0	Yes	Kidney	Plate10-279
279	Female	1,1,2,2-Tetrahydroperfluoro-1-dodecanol	6.0	Yes	Liver	Plate9-279
280	Female	1,1,2,2-Tetrahydroperfluoro-1-dodecanol	6.0	Yes	Kidney	Plate10-280

In Vivo Repeat Dose Biological Potency Study of
1,1,2,2-Tetrahydroperfluoro-1-dodecanol in Sprague Dawley Rats

Animal Number	Sex	Group	Dose (mg/kg)	Survived to Study Termination	Tissue	FASTQ File ID
280	Female	1,1,2,2-Tetrahydroperfluoro-1-dodecanol	6.0	Yes	Liver	Plate9-280
281	Male	1,1,2,2-Tetrahydroperfluoro-1-dodecanol	18.0	Yes	Kidney	Plate12-281[a]
281	Male	1,1,2,2-Tetrahydroperfluoro-1-dodecanol	18.0	Yes	Liver	Plate9-281
282	Male	1,1,2,2-Tetrahydroperfluoro-1-dodecanol	18.0	Yes	Kidney	Plate10-282
282	Male	1,1,2,2-Tetrahydroperfluoro-1-dodecanol	18.0	Yes	Liver	Plate9-282
283	Male	1,1,2,2-Tetrahydroperfluoro-1-dodecanol	18.0	Yes	Kidney	Plate12-283[a]
283	Male	1,1,2,2-Tetrahydroperfluoro-1-dodecanol	18.0	Yes	Liver	Plate9-283
284	Male	1,1,2,2-Tetrahydroperfluoro-1-dodecanol	18.0	Yes	Kidney	Plate10-284
284	Male	1,1,2,2-Tetrahydroperfluoro-1-dodecanol	18.0	Yes	Liver	Plate9-284
285	Male	1,1,2,2-Tetrahydroperfluoro-1-dodecanol	18.0	Yes	Kidney	Plate10-285
285	Male	1,1,2,2-Tetrahydroperfluoro-1-dodecanol	18.0	Yes	Liver	Plate11-285
286	Female	1,1,2,2-Tetrahydroperfluoro-1-dodecanol	18.0	Yes	Kidney	Plate10-286
286	Female	1,1,2,2-Tetrahydroperfluoro-1-dodecanol	18.0	Yes	Liver	Plate9-286
287	Female	1,1,2,2-Tetrahydroperfluoro-1-dodecanol	18.0	Yes	Kidney	Plate10-287
287	Female	1,1,2,2-Tetrahydroperfluoro-1-dodecanol	18.0	Yes	Liver	Plate9-287
288	Female	1,1,2,2-Tetrahydroperfluoro-1-dodecanol	18.0	Yes	Kidney	Plate10-288
288	Female	1,1,2,2-Tetrahydroperfluoro-1-dodecanol	18.0	Yes	Liver	Plate9-288
289	Female	1,1,2,2-Tetrahydroperfluoro-1-dodecanol	18.0	Yes	Kidney	Plate12-289[a]
289	Female	1,1,2,2-Tetrahydroperfluoro-1-dodecanol	18.0	Yes	Liver	Plate9-289
290	Female	1,1,2,2-Tetrahydroperfluoro-1-dodecanol	18.0	Yes	Kidney	Plate10-290
290	Female	1,1,2,2-Tetrahydroperfluoro-1-dodecanol	18.0	Yes	Liver	Plate9-290
291	Male	1,1,2,2-Tetrahydroperfluoro-1-dodecanol	55.0	Yes	Kidney	Plate12-291[a]
291	Male	1,1,2,2-Tetrahydroperfluoro-1-dodecanol	55.0	Yes	Liver	Plate9-291
292	Male	1,1,2,2-Tetrahydroperfluoro-1-dodecanol	55.0	Yes	Kidney	Plate12-292[a]
292	Male	1,1,2,2-Tetrahydroperfluoro-1-dodecanol	55.0	Yes	Liver	Plate9-292
293	Male	1,1,2,2-Tetrahydroperfluoro-1-dodecanol	55.0	Yes	Kidney	Plate12-293[a]
293	Male	1,1,2,2-Tetrahydroperfluoro-1-dodecanol	55.0	Yes	Liver	Plate11-293
294	Male	1,1,2,2-Tetrahydroperfluoro-1-dodecanol	55.0	Yes	Kidney	Plate10-294
294	Male	1,1,2,2-Tetrahydroperfluoro-1-dodecanol	55.0	Yes	Liver	Plate9-294
295	Male	1,1,2,2-Tetrahydroperfluoro-1-dodecanol	55.0	Yes	Kidney	Plate10-295
295	Male	1,1,2,2-Tetrahydroperfluoro-1-dodecanol	55.0	Yes	Liver	Plate9-295
296	Female	1,1,2,2-Tetrahydroperfluoro-1-dodecanol	55.0	Yes	Kidney	Plate10-296
296	Female	1,1,2,2-Tetrahydroperfluoro-1-dodecanol	55.0	Yes	Liver	Plate11-296
297	Female	1,1,2,2-Tetrahydroperfluoro-1-dodecanol	55.0	Yes	Kidney	Plate10-297
297	Female	1,1,2,2-Tetrahydroperfluoro-1-dodecanol	55.0	Yes	Liver	Plate9-297

In Vivo Repeat Dose Biological Potency Study of
1,1,2,2-Tetrahydroperfluoro-1-dodecanol in Sprague Dawley Rats

Animal Number	Sex	Group	Dose (mg/kg)	Survived to Study Termination	Tissue	FASTQ File ID
298	Female	1,1,2,2-Tetrahydroperfluoro-1-dodecanol	55.0	Yes	Kidney	Plate10-298
298	Female	1,1,2,2-Tetrahydroperfluoro-1-dodecanol	55.0	Yes	Liver	Plate9-298
299	Female	1,1,2,2-Tetrahydroperfluoro-1-dodecanol	55.0	Yes	Kidney	Plate10-299
299	Female	1,1,2,2-Tetrahydroperfluoro-1-dodecanol	55.0	Yes	Liver	Plate9-299
300	Female	1,1,2,2-Tetrahydroperfluoro-1-dodecanol	55.0	Yes	Kidney	Plate10-300
300	Female	1,1,2,2-Tetrahydroperfluoro-1-dodecanol	55.0	Yes	Liver	Plate9-300
301	Male	1,1,2,2-Tetrahydroperfluoro-1-dodecanol	160.0	Yes	Kidney	Plate10-301
301	Male	1,1,2,2-Tetrahydroperfluoro-1-dodecanol	160.0	Yes	Liver	Plate11-301
302	Male	1,1,2,2-Tetrahydroperfluoro-1-dodecanol	160.0	Yes	Kidney	Plate10-302
302	Male	1,1,2,2-Tetrahydroperfluoro-1-dodecanol	160.0	Yes	Liver	Plate9-302
303	Male	1,1,2,2-Tetrahydroperfluoro-1-dodecanol	160.0	Yes	Kidney	Plate10-303
303	Male	1,1,2,2-Tetrahydroperfluoro-1-dodecanol	160.0	Yes	Liver	Plate11-303
304	Male	1,1,2,2-Tetrahydroperfluoro-1-dodecanol	160.0	Yes	Kidney	Plate10-304
304	Male	1,1,2,2-Tetrahydroperfluoro-1-dodecanol	160.0	Yes	Liver	Plate9-304
305	Male	1,1,2,2-Tetrahydroperfluoro-1-dodecanol	160.0	Yes	Kidney	Plate12-305[a]
305	Male	1,1,2,2-Tetrahydroperfluoro-1-dodecanol	160.0	Yes	Liver	Plate9-305
306	Female	1,1,2,2-Tetrahydroperfluoro-1-dodecanol	160.0	Yes	Kidney	Plate12-306[a]
306	Female	1,1,2,2-Tetrahydroperfluoro-1-dodecanol	160.0	Yes	Liver	Plate9-306
307	Female	1,1,2,2-Tetrahydroperfluoro-1-dodecanol	160.0	Yes	Kidney	Plate12-307[a]
307	Female	1,1,2,2-Tetrahydroperfluoro-1-dodecanol	160.0	Yes	Liver	Plate9-307
308	Female	1,1,2,2-Tetrahydroperfluoro-1-dodecanol	160.0	Yes	Kidney	Plate10-308
308	Female	1,1,2,2-Tetrahydroperfluoro-1-dodecanol	160.0	Yes	Liver	Plate9-308
309	Female	1,1,2,2-Tetrahydroperfluoro-1-dodecanol	160.0	Yes	Kidney	Plate10-309
309	Female	1,1,2,2-Tetrahydroperfluoro-1-dodecanol	160.0	Yes	Liver	Plate9-309
310	Female	1,1,2,2-Tetrahydroperfluoro-1-dodecanol	160.0	Yes	Kidney	Plate10-310
310	Female	1,1,2,2-Tetrahydroperfluoro-1-dodecanol	160.0	Yes	Liver	Plate9-310
311	Male	1,1,2,2-Tetrahydroperfluoro-1-dodecanol	475.0	Yes	Kidney	Plate10-311
311	Male	1,1,2,2-Tetrahydroperfluoro-1-dodecanol	475.0	Yes	Liver	Plate9-311
312	Male	1,1,2,2-Tetrahydroperfluoro-1-dodecanol	475.0	Yes	Kidney	Plate12-312[a]
312	Male	1,1,2,2-Tetrahydroperfluoro-1-dodecanol	475.0	Yes	Liver	Plate9-312
313	Male	1,1,2,2-Tetrahydroperfluoro-1-dodecanol	475.0	Yes	Kidney	Plate10-313
313	Male	1,1,2,2-Tetrahydroperfluoro-1-dodecanol	475.0	Yes	Liver	Plate11-313
314	Male	1,1,2,2-Tetrahydroperfluoro-1-dodecanol	475.0	Yes	Kidney	Plate12-314[a]
314	Male	1,1,2,2-Tetrahydroperfluoro-1-dodecanol	475.0	Yes	Liver	Plate11-314
315	Male	1,1,2,2-Tetrahydroperfluoro-1-dodecanol	475.0	Yes	Kidney	Plate12-315[a]

In Vivo Repeat Dose Biological Potency Study of
1,1,2,2-Tetrahydroperfluoro-1-dodecanol in Sprague Dawley Rats

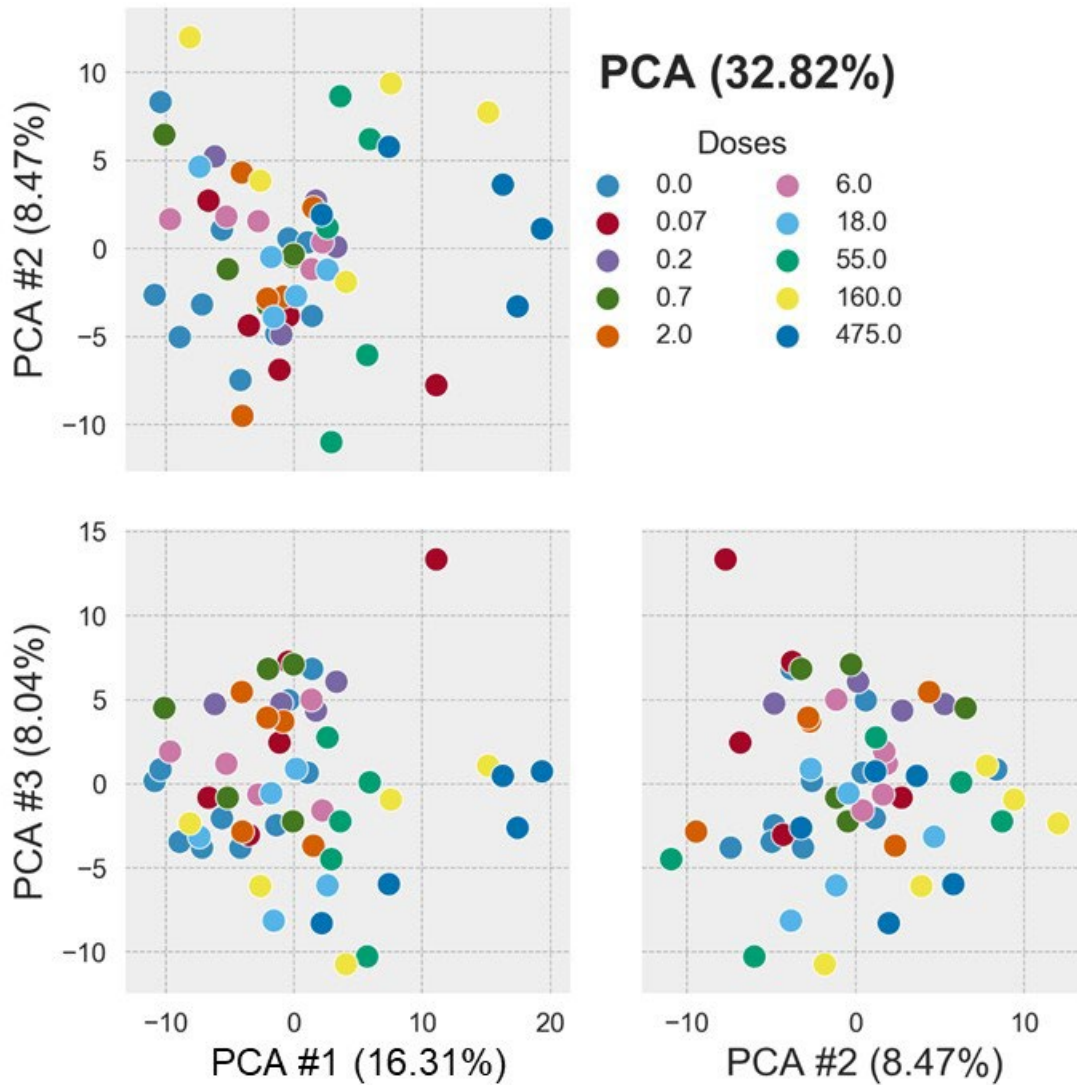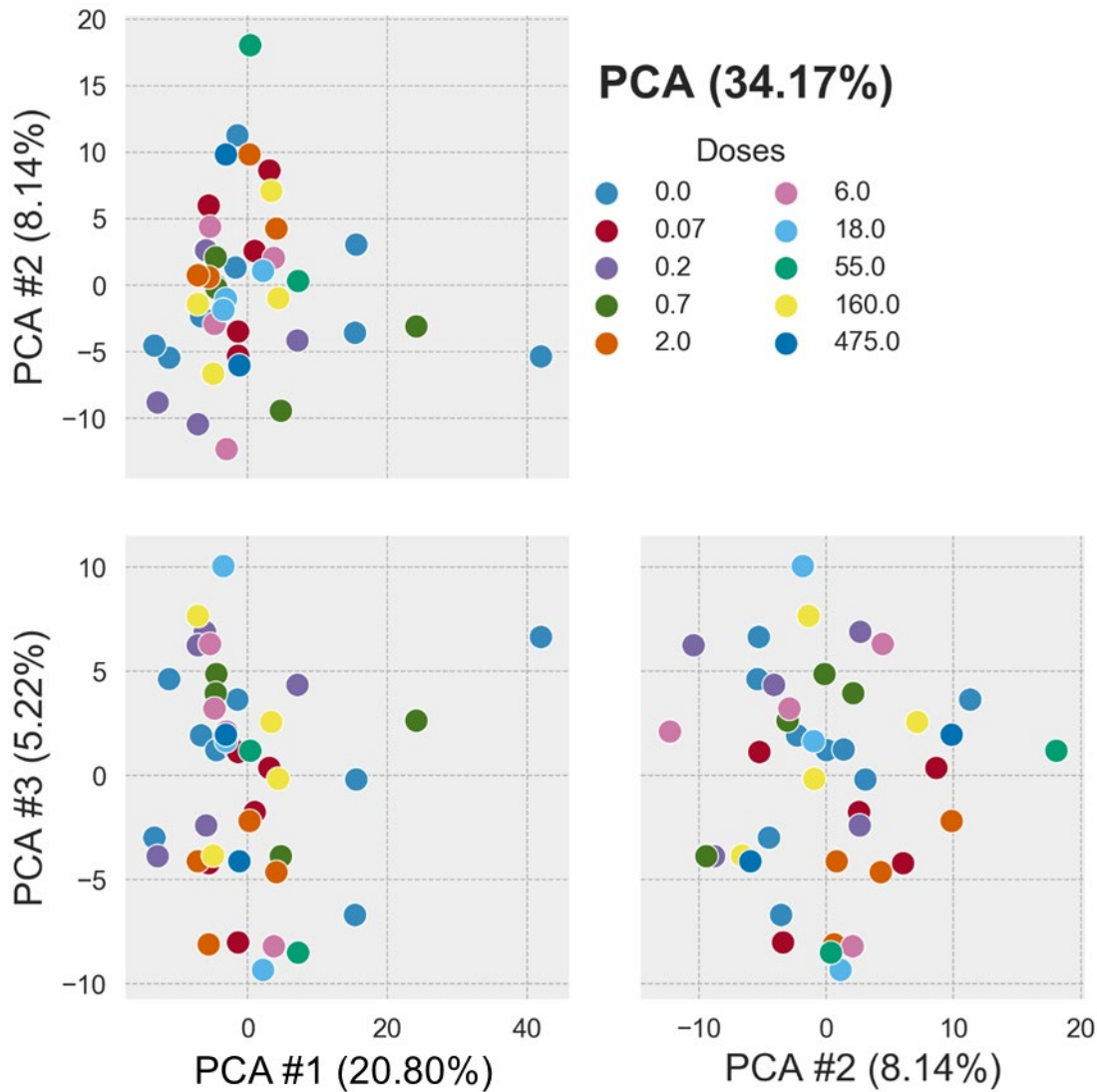| Animal Number	Sex	Group	Dose (mg/kg)	Survived to Study Termination	Tissue	FASTQ File ID
315	Male	1,1,2,2-Tetrahydroperfluoro-1-dodecanol	475.0	Yes	Liver	Plate9-315
316	Female	1,1,2,2-Tetrahydroperfluoro-1-dodecanol	475.0	Yes	Kidney	Plate10-316
316	Female	1,1,2,2-Tetrahydroperfluoro-1-dodecanol	475.0	Yes	Liver	Plate9-316
317	Female	1,1,2,2-Tetrahydroperfluoro-1-dodecanol	475.0	Yes	Kidney	Plate12-317[a]
317	Female	1,1,2,2-Tetrahydroperfluoro-1-dodecanol	475.0	Yes	Liver	Plate11-317
318	Female	1,1,2,2-Tetrahydroperfluoro-1-dodecanol	475.0	Yes	Kidney	Plate10-318
318	Female	1,1,2,2-Tetrahydroperfluoro-1-dodecanol	475.0	Yes	Liver	Plate9-318
319	Female	1,1,2,2-Tetrahydroperfluoro-1-dodecanol	475.0	Yes	Kidney	Plate10-319
319	Female	1,1,2,2-Tetrahydroperfluoro-1-dodecanol	475.0	Yes	Liver	Plate9-319
320	Female	1,1,2,2-Tetrahydroperfluoro-1-dodecanol	475.0	Yes	Kidney	Plate10-320
320	Female	1,1,2,2-Tetrahydroperfluoro-1-dodecanol	475.0	Yes	Liver	Plate11-320

[a]Removed due to plate/batch effect.
[b]Removed due to principal component analysis/hierarchical cluster analysis outlier.

Appendix C. Transcriptomic Quality Control and Empirical False Discovery Rate

Table of Contents

Tables
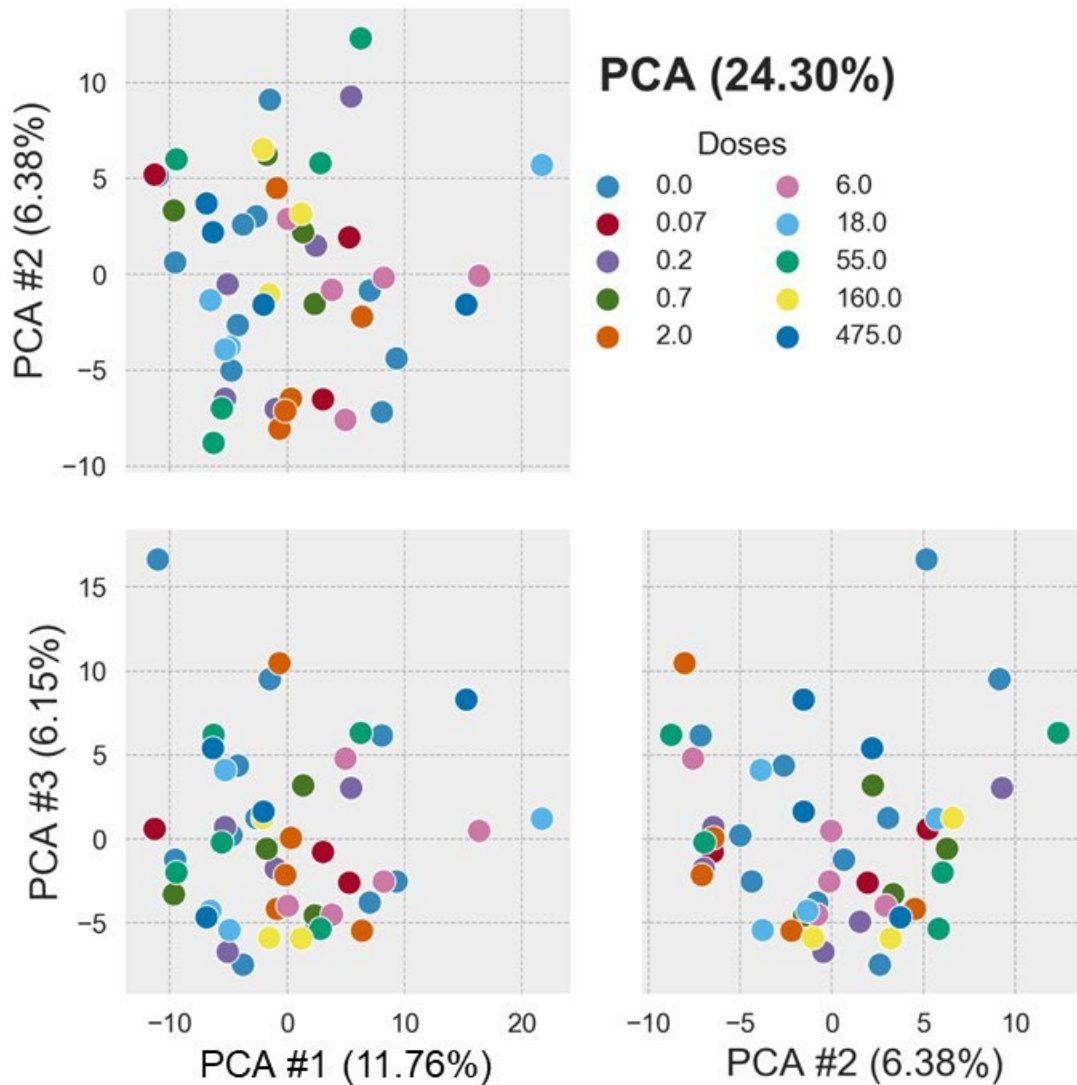
Figures

C.1. Gene Expression Quality Control

Figure C-1. A Principal Component Analysis of the Normalized Data from the Liver of Male Rats

A principal component analysis (PCA) plot enables visualization of global transcriptional changes in two dimensions, with each plot showing a different angle on the basis of the principal components plotted. Global transcript data are shown for individual animals (dots) within each dose group (designated by color). Dots that are spatially closer to each other indicate more similarity in global expression profiles; dots that are farther apart indicate dissimilarity in global expression profiles for those animals. The data represented in the plot are those employed in dose response modeling (i.e., if outliers were identified in the quality control process, they were removed from the data set and are not present in the plot). Visual inspection does not suggest subgrouping of the data other than dose-related changes, which indicates any technical batch-related effects are minimal.

Figure C-2. A Principal Component Analysis of the Normalized Data from the Liver of Female Rats

A principal component analysis (PCA) plot enables visualization of global transcriptional changes in two dimensions, with each plot showing a different angle on the basis of the principal components plotted. Global transcript data are shown for individual animals (dots) within each dose group (designated by color). Dots that are spatially closer to each other indicate more similarity in global expression profiles; dots that are farther apart indicate dissimilarity in global expression profiles for those animals. The data represented in the plot are those employed in dose response modeling (i.e., if outliers were identified in the quality control process, they were removed from the data set and are not present in the plot). Visual inspection does not suggest subgrouping of the data other than dose-related changes, which indicates any technical batch-related effects are minimal.

Figure C-3. A Principal Component Analysis of the Normalized Data from the Kidney of Male Rats

A principal component analysis (PCA) plot enables visualization of global transcriptional changes in two dimensions, with each plot showing a different angle on the basis of the principal components plotted. Global transcript data are shown for individual animals (dots) within each dose group (designated by color). Dots that are spatially closer to each other indicate more similarity in global expression profiles; dots that are farther apart indicate dissimilarity in global expression profiles for those animals. The data represented in the plot are those employed in dose response modeling (i.e., if outliers were identified in the quality control process, they were removed from the data set and are not present in the plot). Visual inspection does not suggest subgrouping of the data other than some minimal dose-related changes, which indicates any technical batch-related effects are minimal.

Figure C-4. A Principal Component Analysis of the Normalized Data from the Kidney of Female Rats

A principal component analysis (PCA) plot enables visualization of global transcriptional changes in two dimensions, with each plot showing a different angle on the basis of the principal components plotted. Global transcript data are shown for individual animals (dots) within each dose group (designated by color). Dots that are spatially closer to each other indicate more similarity in global expression profiles; dots that are farther apart indicate dissimilarity in global expression profiles for those animals. The data represented in the plot are those employed in dose response modeling (i.e., if outliers were identified in the quality control process, they were removed from the data set and are not present in the plot). Visual inspection does not suggest subgrouping of the data other than minimal dose-related changes, which indicates any technical batch-related effects are minimal.

C.2. Empirical False Discovery Rate

C.2.1. Methods

Empirical false discovery assessment was performed to evaluate the performance of the benchmark dose (BMD) analysis technique and underlining probe/pathway filtering criteria. Toward this goal, 20 computationally generated data sets were used with this study design (each data set containing 10 vehicle control replicates and 5 replicates per dose), and equivalent BMD analysis was performed using the same parameter configurations. The 20 data sets were generated from the original 1,1,2,2-tetrahydroperfluoro-1-dodecanol (10:2 fluorotelomer alcohol) study data, along with data from three other chemicals that were studied in parallel under a similar protocol.[26-28]

For a given group (tissue per sex combination), up to 40 vehicle control samples from the original studies (10 replicates × 4 chemicals) were used for this analysis. The previously identified outlier vehicle control samples and overflow plate control samples exhibiting a batch effect were excluded from this analysis.

Each computationally generated sample was created by randomly mixing the normalized expression signal from two randomly selected vehicle control samples using a weighted average approach. The weights utilized during per-probe mixing were randomly simulated from uniform (0,1) distribution. A total of 55 samples (10 vehicle control samples + 45 dosed samples [9 doses × 5 replicates]) were computationally generated per data set and assigned to either vehicle control or 1 of the 9 dosed groups that were separated by approximately half-log spacing, consistent with the dose spacing used in the original studies. For each group, 20 such data sets were generated. Because each of the 20 generated data sets used in the empirical false discovery analysis was derived from actual vehicle control samples, none of the data sets should have any true dose-responsive genes.

Each data set was then analyzed using the same parameter settings and significance criteria that were implemented in the original study. At the gene level, genes that passed the following criteria were considered false positive discoveries: fold change $\geq|2|$, Williams's trend p value ≤ 0.05, global goodness-of-fit p value >0.1, BMD upper confidence limit/BMD lower confidence limit (BMD_U/BMD_L) ≤ 40, and BMD <highest dose tested. Categorical analysis on Gene Ontology (GO) gene sets was performed using the genes that passed the gene-level criteria with maximum absolute fold change ≥ 1.5. At the gene set GO level, GO biological processes that passed the following criteria were considered false positive discoveries: ≥ 3 genes that pass all filters, totaling at least 5% of the genes in a gene set.

False positive discovery rates were assessed for each computationally generated data set using the following equations:

$$\text{False Positive Gene Rate} = \frac{\text{\# False Positive Entrez Gene IDs}}{2{,}680} \times 100 \tag{1}$$

$$\text{False Positive GO Biological Process Rate} = \frac{\text{\# False Positive GO Biological Processes}}{5{,}667} \times 100 \tag{2}$$

where 2,680 is the number of unique Entrez Gene IDs on the rat S1500+ platform and 5,667 is the number of GO biological processes that have at least three genes in rat S1500+.

Mean and median false discovery rates across all 20 computationally generated data sets were calculated for each tissue per sex in the study.

C.2.2. Results

The number of false positives for genes and GO biological processes are given in Table C-1. Mean and median false positive rates were <0.1% for genes and <0.5% for GO biological processes for all tissue per sex group (Figure C-5 and Figure C-6). The maximum false positive rates for any of the 80 computationally generated control data sets were 0.3% (gene) and 4.4% (GO biological process).
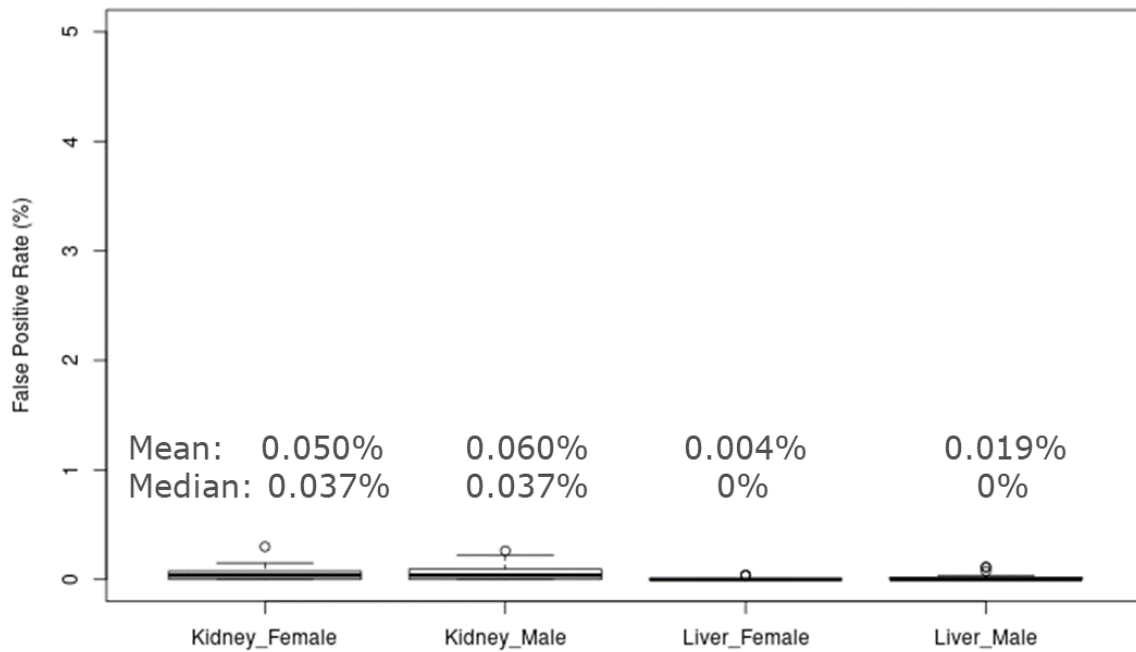
Figure C-5. Boxplots of the False Positive Gene Rate for Each Tissue per Sex Combination

Each boxplot displays the distribution of the false positive rates for 20 computationally generated data sets.

In Vivo Repeat Dose Biological Potency Study of
1,1,2,2-Tetrahydroperfluoro-1-dodecanol in Sprague Dawley Rats
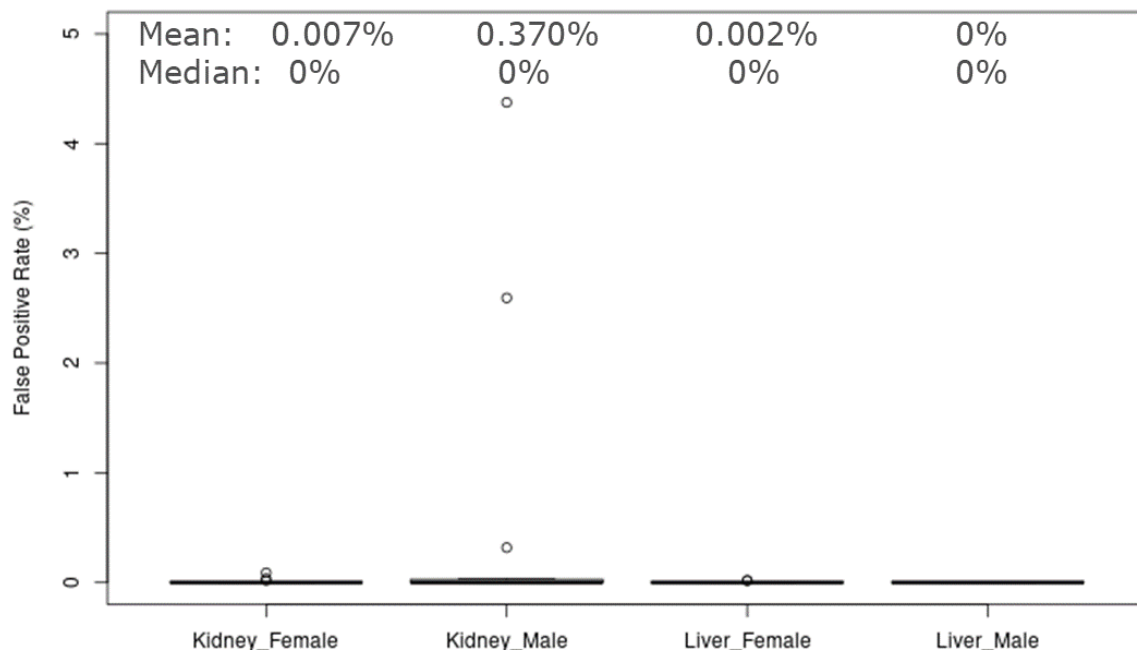
Figure C-6. Boxplots of the False Positive Gene Ontology Biological Process Rate for Each Tissue per Sex Combination

Each boxplot displays the distribution of the false positive rates for 20 computationally generated data sets.

Table C-1. Number of False Positives

Generated Data Set	# False Positive Genes				# False Positive GO Biological Process			
	Kidney Female	Kidney Male	Liver Female	Liver Male	Kidney Female	Kidney Male	Liver Female	Liver Male
01	3	0	0	0	0	0	0	0
02	4	0	0	0	2	1	0	0
03	0	2	0	0	0	1	1	0
04	2	1	0	0	0	0	0	0
05	2	3	0	0	0	0	0	0
06	1	0	0	3	0	0	1	0
07	1	6	0	0	0	18	0	0
08	0	0	0	0	0	0	0	0
09	3	0	0	0	0	0	0	0
10	0	0	0	0	0	0	0	0
11	0	1	0	1	0	0	0	0
12	1	4	0	3	1	147	0	0
13	0	2	0	0	0	2	0	0
14	1	0	0	2	0	0	0	0
15	0	3	0	0	0	2	0	0
16	0	1	1	0	0	0	0	0
17	0	0	1	0	0	0	0	0
18	0	2	0	0	0	0	0	0
19	1	0	0	1	0	0	0	0
20	8	7	0	0	5	248	0	0

GO = Gene Ontology.

Appendix D. Benchmark Dose Model Recommendation and Selection Methodologies
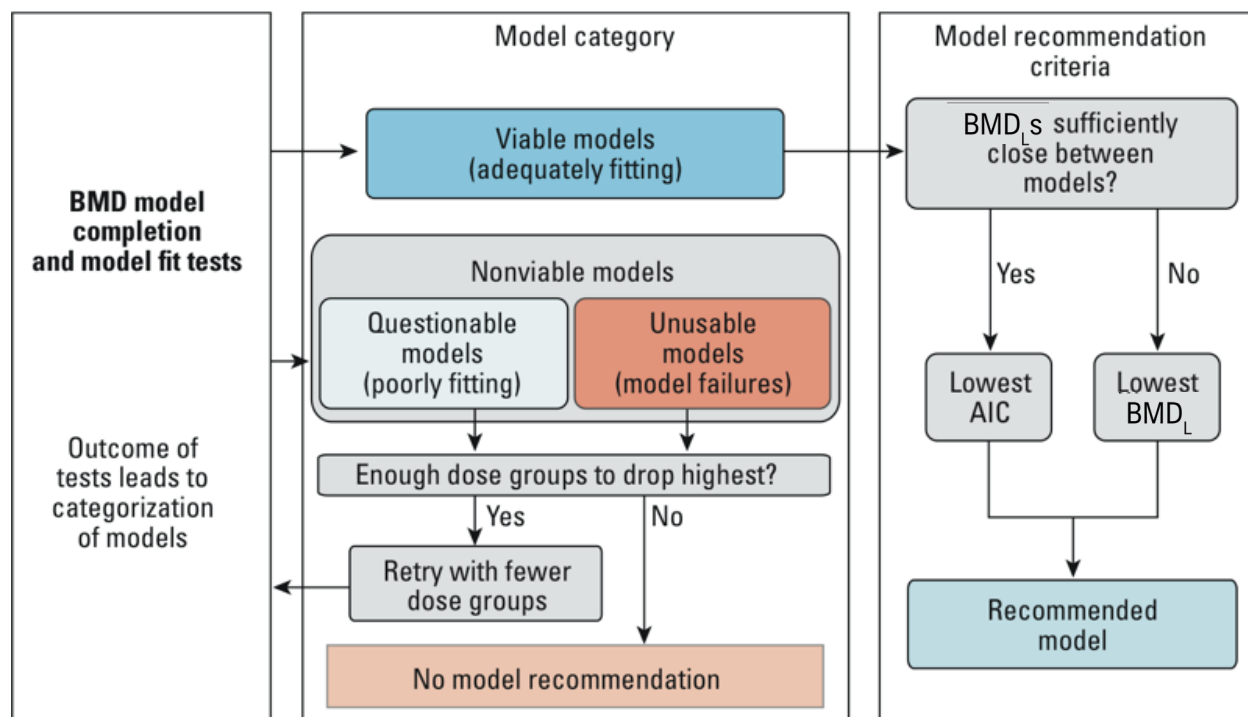
Tables

Figures

In Vivo Repeat Dose Biological Potency Study of
1,1,2,2-Tetrahydroperfluoro-1-dodecanol in Sprague Dawley Rats

Table D-1. Benchmark Dose Model Recommendation/Selection Rules for Apical Endpoints

Rule	Criteria for "Viable"	Numerical Threshold	Bin Placement for Rule Failure
BMD Existence	A BMD exists.	NA	Failure
BMD$_L$ Existence	A BMD$_L$ exists.	NA	Failure
AIC Existence	An AIC exists.	NA	Failure
Residual of Interest Existence	The residual at the dose group closest to the BMD (i.e., the residual of interest) exists.	NA	Failure
Variance Model Fit	The variance model used fits the data.	NA	Nonviable
Variance Model Selection	The variance model is appropriate.	NA	Nonviable
Global Goodness of Fit	The mean model fits the data means sufficiently well (BMDS 2.7.0 Test 4 p value >N).	0.1	Nonviable
Degrees of Freedom	There is at least 1 degree of freedom (i.e., more dose groups than model parameters).	NA	Nonviable
BMD-to-BMD$_L$ Ratio	The ratio of BMD to BMD$_L$ is not large (BMD/BMD$_L$ <N).	20	Viable
High BMD$_L$	The BMD$_L$ is <N times higher than the maximum dose.	1	Viable
High BMD	The BMD is <N times higher than the maximum dose.	1	Viable
Low BMD	The BMD is <N times lower than the minimum nonzero dose.	3	Nonreportable
Control Residual	The residual at control is small (residual <N).	2	Nonviable
Control Standard Deviation	The modeled standard deviation is similar to the actual (<N times different).	1.5	Nonviable
Residual of Interest	The residual at the dose group closest to the BMD (i.e., the residual of interest) is small (residual <N).	2	Nonviable
No Warnings Reported	No warnings in the BMD model system were reported.	NA	Viable

BMD = benchmark dose; NA = not applicable; BMD$_L$ = benchmark dose lower confidence limit; AIC = Akaike information criterion; BMDS = Benchmark Dose Software; N = numerical threshold.
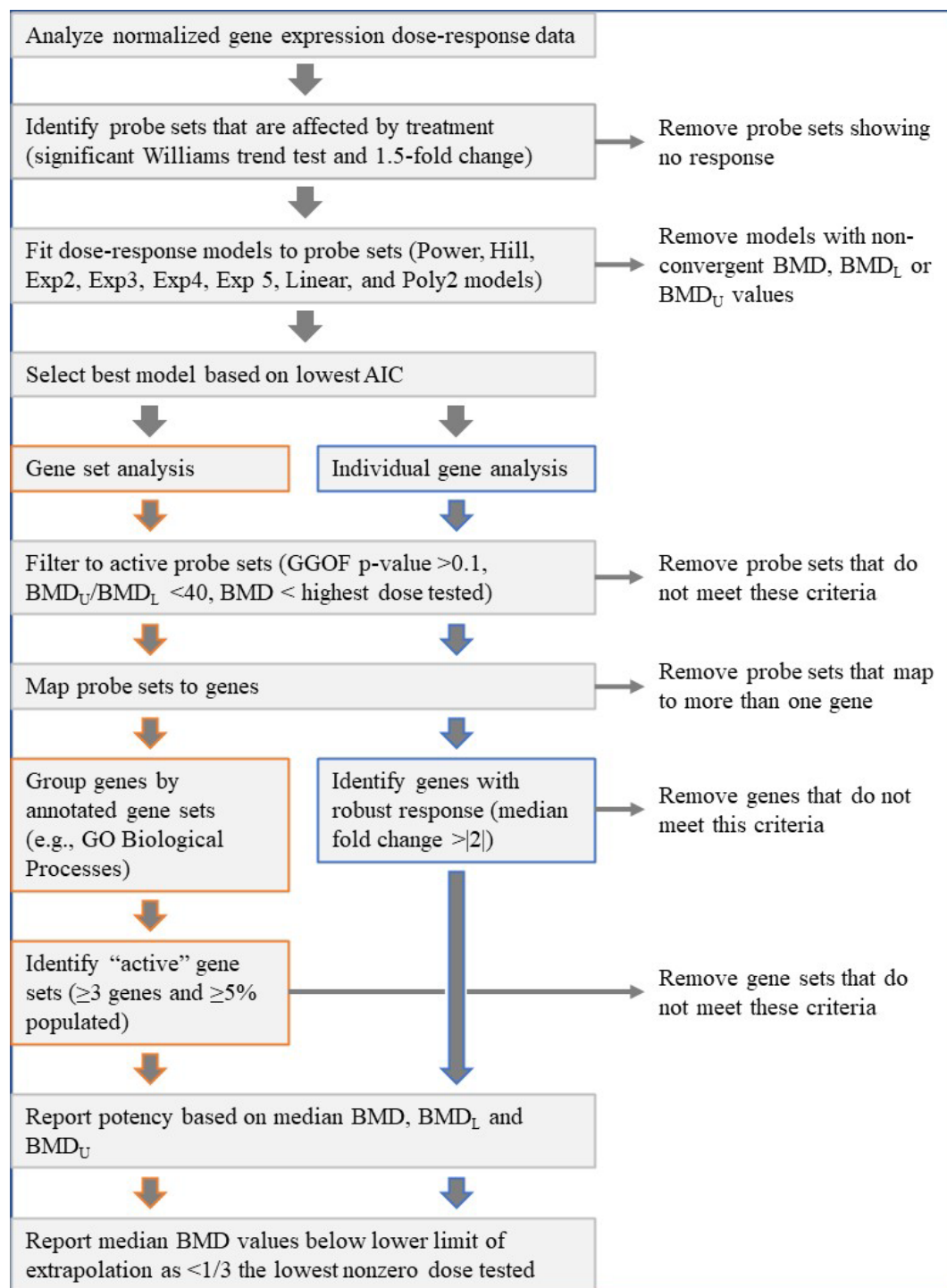
Figure D-1. Benchmark Dose Model Recommendation/Selection Methodology for Automated Benchmark Dose Execution of Apical Endpoints

Source: Figure adapted from Wignall et al. (2014)[23]
BMD = benchmark dose; BMD_L = benchmark dose lower confidence limit; AIC = Akaike information criterion.

Figure D-2. Benchmark Dose Model Recommendation/Selection Methodology for Benchmark Dose Execution of Gene Sets with Expression Changes Enacted by Chemical Exposure

Adapted from Thomas et al. (2007)[34]
Exp = exponential; Poly = polynomial; BMD = benchmark dose; BMD_L = benchmark dose lower confidence limit; BMD_U = benchmark dose upper confidence limit; AIC = Akaike information criterion; GGOF = global goodness of fit; GO = Gene Ontology.

Appendix E. Organ Weight Descriptions

Table of Contents

E.1. Organ Weight Descriptions

Liver: The liver carries out biotransformation and excretion of endogenous and xenobiotic substances, regulation of blood sugar, enzymatic transformation of essential nutrients, generation of blood proteins involved in fluid balance and clotting, and bile production for digestion and absorption of fats. Liver weight changes can be an indication of chemical-induced stress. Specifically, in subacute studies, increases in liver weight in response to low doses of toxicants typically stem from increases in xenobiotic metabolizing enzymes and associated hepatocyte hypertrophy or peroxisome proliferation. Increased liver weight, particularly when accompanied by evidence of leakage of liver-specific enzymes into blood, likely reflects hemodynamic changes related to severe hepatotoxicity. Higher liver weight relative to body weight may also occur at any dose level that causes a slowed rate of body growth and does not necessarily indicate liver toxicity. Decreased liver weight in subacute studies is typically of unknown toxicological significance but in rare cases may be related to glycogen depletion.

Kidney: The kidneys remove waste products and xenobiotics from the body, balance blood electrolytes, regulate blood pressure through the release of hormones, synthesize the active form of vitamin D, and control the production of erythropoiesis. In subacute studies, changes in kidney weight may reflect renal toxicity (particularly if accompanied by increases in other markers of kidney toxicity, e.g., increased Kim-1) and/or tubular hypertrophy. Decreased kidney weights in subacute studies are typically of unknown toxicological significance.

Heart: The heart drives the circulatory system, supplying oxygen and essential macro- and micronutrients to the tissues. Increased heart weight in subacute studies would indicate severe cardiotoxicity, compensatory myocardial hypertrophy, and/or pulmonary injury. Decreased heart weight in subacute studies is often of unknown toxicological significance; however, it may be caused by decreased load on the heart from dehydration or modulation of contractility.

Appendix F. Supplemental Data

The following supplemental files are available at https://doi.org/10.22427/NIEHS-DATA-NIEHS-08.[29]

F.1. Apical Benchmark Dose Analysis

Mean Body Weight Summary
C04051-01_Mean_Body_Weight_Summary.docx

Organ Weights Summary
C04051-01_Organ_Weights_Summary.docx

Clinical Chemistry Summary
C04051-01_Clinical_Chemistry_Summary.docx

Hematology Summary
C04051-01_Hematology_Data_Summary.docx

Hormone and Enzymes Summary
C04051-01_Hormone_Summary.docx

BMD, NOEL and LOEL Summary for Apical Endpoints
C04051-01_BMD_BMDL_LOEL_and_NOEL_Summary_for_Apical_Endpoints_Sorted_by_BMD_LOEL_from_Low_to_High.docx

Male BMD Apical Endpoints Model Fits
C04051-01_Appendix_Male_07282021.docx

Female BMD Apical Endpoints Model Fits
C04051-01_Appendix_Female_07282021.docx

BMD Model Recommendation Selection Rules
C04051-01_Benchmark_Dose_Model_Recommendation_Selection_Rules_for_Apical_Endpoints.docx

Read Me
C04051-01_ReadME.docx

Male Model Parameters
C04051-01_Parameter_Male_07282021.xlsx

Female Model Parameters
C04051-01_Parameter_Female_07282021.xlsx

BMDs code package
C04051-01_bmds.zip

F.2. Genomic Benchmark Dose Analysis

BMDExpress Project File (bm2 format)
C04051-
01_EPA_PFAS_Kidney_Overflow_plate_removed_S1500_Plus_Analysis_Traditional.bm2

Top 10 Genes Ranked by Potency of Perturbation_Kidney
C04051-
01_Kidney_Top_10_Genes_Ranked_by_Potency_of_Perturbation_Sorted_by_BMD_Median.do
cx

Top 10 GO Biological Process Gene Sets_Kidney
C04051-
01_Kidney_Top_10_GO_Biological_Process_Gene_Sets_Ranked_by_Potency_of_Perturbation
_Sorted_by_BMD_Median.docx

Top 10 Genes Ranked by Potency of Perturbation_Liver
C04051-
01_Liver_Top_10_Genes_Ranked_by_Potency_of_Perturbation_Sorted_by_BMD_Median.docx

Top 10 GO Biological Process Gene Sets_Liver
C04051-
01_Liver_Top_10_GO_Biological_Process_Gene_Sets_Ranked_by_Potency_of_Perturbation_S
orted_by_BMD_Median.docx

BMDExpress Expression Data_Kidney_Female
C04051-01_Kidney_10-2_FTOH_Female.txt

BMDExpress Expression Data_Kidney_Male
C04051-01_Kidney_10-2_FTOH_Male.txt

BMDExpress Expression Data_Liver_Female
C04051-01_Liver_10-2_FTOH_Female.txt

BMDExpress Expression Data_Liver_Male
C04051-01_Liver_10-2_FTOH_Male.txt

BMDExpress Individual Gene BMD Results_Kidney_Male
C04051-01_Kidney_10-
2_FTOH_Male_williams_0.05_NOMTC_foldfilter1.5_BMD_S1500_Plus_Rat_GENE_true_true
_pval0.1_ratio40_foldchange2_conf0.5.txt

BMDExpress GO Biological Process Deduplicated BMD Results_Kidney_Male
C04051-01_Kidney_10-
2_FTOH_Male_williams_0.05_NOMTC_foldfilter1.5_BMD_S1500_Plus_Rat_GO_BP_true_tr
ue_pval0.1_ratio40_conf0.5_deduplicate.txt

BMDExpress Individual Gene BMD Results_Kidney_Female

C04051-01_Kidney_10-
2_FTOH_Female_williams_0.05_NOMTC_foldfilter1.5_BMD_S1500_Plus_Rat_GENE_true_tr
ue_pval0.1_ratio40_foldchange2_conf0.5.txt

BMDExpress GO Biological Process Deduplicated BMD Results_Kidney_Female
C04051-01_Kidney_10-
2_FTOH_Female_williams_0.05_NOMTC_foldfilter1.5_BMD_S1500_Plus_Rat_GO_BP_true_
true_pval0.1_ratio40_conf0.5_deduplicate.txt

BMDExpress Individual Gene BMD Results_Liver_Male
C04051-01_Liver_10-
2_FTOH_Male_williams_0.05_NOMTC_foldfilter1.5_BMD_S1500_Plus_Rat_GENE_true_true
_pval0.1_ratio40_foldchange2_conf0.5.txt

BMDExpress GO Biological Process Deduplicated BMD Results_Liver_Male
C04051-01_Liver_10-
2_FTOH_Male_williams_0.05_NOMTC_foldfilter1.5_BMD_S1500_Plus_Rat_GO_BP_true_tr
ue_pval0.1_ratio40_conf0.5_deduplicate.txt

BMDExpress Individual Gene BMD Results_Liver_Female
C04051-01_Liver_10-
2_FTOH_Female_williams_0.05_NOMTC_foldfilter1.5_BMD_S1500_Plus_Rat_GENE_true_tr
ue_pval0.1_ratio40_foldchange2_conf0.5.txt

BMDExpress GO Biological Process Deduplicated BMD Results_Liver_Female
C04051-01_Liver_10-
2_FTOH_Female_williams_0.05_NOMTC_foldfilter1.5_BMD_S1500_Plus_Rat_GO_BP_true_
true_pval0.1_ratio40_conf0.5_deduplicate.txt

BMDExpress Prefilter Results_ Kidney _Female
C04051-01_BMDExpress_Prefilter_Results_Kidney_Female.txt

BMDExpress Prefilter Results_ Kidney _Male
C04051-01_BMDExpress_Prefilter_Results_Kidney_Male.txt

BMDExpress Prefilter Results_ Liver _Female
C04051-01_BMDExpress_Prefilter_Results_Liver_Female.txt

BMDExpress Prefilter Results_ Liver _Male
C04051-01_BMDExpress_Prefilter_Results_Liver_Male.txt

Animal and Fastaq Metadata
C04051-01_Animal_and_FASTQ_Metadata.zip

Kidney Principal Components Analysis Files
C04051-01_Kidney_PCA.zip

Liver Principal Components Analysis Files
C04051-01_Liver_PCA.zip

Individual Gene BMD Analysis Results File

C04051-01_Individual_Gene_Defined_Category_Files_for_Gene_Level_BMD_Analysis_of_Array_Platform_GPL1355.zip

BMDExpress Software
C04051-01_Software.zip

BMDExpress Project File (JSON format)
C04051-01_EPA_PFAS_Kidney_Overflow_plate_removed_S1500_Plus_Analysis_Traditional_JSON.zip

GO Biological Process BMD Analysis Results
C04051-01_Functional_Classification_Annotation_Files_for_GO_Biological_Process_Analysis_of_Array_Platform_GPL1355.zip

F.3. Study Tables

I04 – Mean_Body_Weight_Summary
C04051-01_I04_–_Mean_Body_Weight_Summary.pdf

I05 – Clinical_Observations_Summary
C04051-01_I05_–_Clinical_Observations_Summary.pdf

PA06 – Organ_Weights_Summary
C04051-01_PA06_–_Organ_Weights_Summary.pdf

PA41 – Clinical_Chemistry_Summary
C04051-01_PA41_–_Clinical_Chemistry_Summary.pdf

PA43 - Hematology Summary
C04051-01_PA43_-_Hematology_Summary.pdf

PA48 - Summary of Tissue Concentration
C04051-01_PA48_-_Summary_of_Tissue_Concentration.pdf

R07 – Hormone_Summary
C04051-01_R07_–_Hormone_Summary.pdf

F.4. Individual Animal Data

Individual Animal Body Weight Data
C04051-01_Individual_Animal_Body_Weight_Data.xlsx

Individual Animal Clinical Chemistry Data
C04051-01_Individual_Animal_Clinical_Chemistry_Data.xlsx

Individual Animal Clinical Observations Data
C04051-01_Individual_Animal_Clinical_Observations_Data.xlsx

Individual Animal Hormone Data
C04051-01_Individual_Animal_Hormone_Data.xlsx

Individual Animal Organ Weight Data
C04051-01_Individual_Animal_Organ_Weight_Data.xlsx

Individual Animal Hematology Data
C04051-01_Individual_Animal_Hematology_Data.xlsx

Individual Animal Tissue Concentration Data
C04051-01_Individual_Animal_Tissue_Concentration_Data.xlsx